SURFACTANT-ENHANCED ELECTROKINETIC REMEDIATION OF HYDROCARBON-CONTAMINATED SOILS

By

STEVEN P. THOMAS

A Thesis
Submitted to the Faculty of Graduate Studies
in Partial Fulfilment of the Requirements
for the Degree of

MASTER OF SCIENCE

Department of Biosystems Engineering
University of Manitoba
Winnipeg, Manitoba

April, 1996

ISBN 0-612-16332-6

Canada

THE UNIVERSITY OF MANITOBA

FACUTY OF GRADUATE STUDIES

COPYRIGHT PERMISSION

SURFACTANT-ENHANCED ELECTROKINETIC REMEDIATION OF HYDROCARBON-CONTAMINATED SOILS

BY

STEVEN P. THOMAS

A Thesis/Practicum submitted to the Faculty of Graduate Studies of the University of Manitoba in partial fulfillment of the requirements for the degree of

MASTER OF SCIENCE

Abstract

Concern over soil and groundwater contamination has created a demand for new and efficient remediation technologies. Surfactant-enhanced electrokinetic remediation is an innovative technique which has the potential to remove hydrocarbons from contaminated clay soils faster and more efficiently than conventional remediation methods. The main objectives of this research were to (1) evaluate the efficiency of using surfactant-enhanced electrokinetic remediation to remove hydrocarbons from contaminated soil columns in the laboratory; (2) identify the effect of various physical and chemical factors on the performance of electrokinetic remediation; and (3) develop equations to model surfactant-enhanced electrokinetic remediation. Research was also conducted on expanding and improving the analytical methods using the relatively new solid-phase microextraction technique for the determination of hydrocarbon concentration in water.

The soil column experiments indicate surfactant-enhanced electrokinetic remediation with sodium dodecylsulfate (SDS) is dominated by electrophoretic transport of micelles. The application of a surfactant increased the current through the soil which led to increased electrolysis of water. Pore fluid flow was also significantly greater in clay columns with an applied voltage potential gradient.

Values for SDS micelle-water partition coefficients were determined as 3.19, 3.42, 3.45, 3.39, and 3.36 for toluene, ethylbenzene, *p*-xylene, *m*-xylene, and *o*-xylene respectively. A new relationship between the SDS micelle-water partition coefficient and the octanol-water partition coefficient was determined to allow prediction of surfactant effects for other hydrocarbons. The optimum SDS concentration during surfactant-enhanced electrokinetic remediation should be less than 2% (w/w).

Surfactant-enhanced electrokinetic remediation was modelled by adapting the classical advection-dispersion-retardation equation to include a modified retardation factor and electrokinetic effects. The model results were highly dependent on the input parameters chosen. Modelling results indicate that electrophoretic transport of hydrocarbons in SDS micelles is the dominant factor influencing transport during surfactant-enhanced electrokinetic remediation. In order to utilize electroosmotic flow, the voltage potential gradient should be greater than 1 V/cm.

Surfactant-enhanced electrokinetic remediation is still an emerging technology and a greater understanding of the factors involved is necessary before decontamination can be confidently applied in the field. However, this research significantly adds to the knowledge of surfactant-enhanced electrokinetic remediation.

"I have yet to see any problem, however complicated, which, when you looked at it in the right way, did not become more complicated."

Anderson's Law,

Ground Water Monitoring and Review,

Fall 1994 p.148-158

Acknowledgements

The completion of this research would not be possible without the guidance and support from a number of people. I wish to express my gratitude to Dr. Sri Ranjan for his assistance, financial support, and counsel during my Masters program. Specials thanks to Dr. Webster for his advice, support, and encouragement. Thank-you to Dr. Shields for his constructive comments.

Financial support for research and equipment was provided by Manitoba Hydro and Imperial Oil Research Foundation/ESTAC. Thanks to Varian Canada Inc. for the use of the autosampler modified for SPME. The consultation with Mr. Paul Janzen of Manitoba Hydro is appreciated.

I would also like to thank the following people for their contributions. Thank-you Messrs. Leonard Sarna, Matt McDonald, Dale Bourns, Jack Putnam, Rob Ataman, and Thayalan Karthigesu for their excellent technical support. Thanks to Mr. David Hay, Ms. Kristina Grahmn, the staff from the Department of Soil Science, and the faculty and staff from the Department of Biosystems Engineering for their active support and help.

I am also indebted to my family and friends who provided essential moral support during my university career. Finally, I wish to express my thanks to Shannon whose love and companionship makes everyday more enjoyable.

Table of Contents

List of Tables

Page

List of Figures

List of Symbols

A = cross sectional area

B = Thomas ratio factor

C = hydrocarbon concentration in the solution phase

C_{cmc} = apparent hydrocarbon solubility at the CMC

C_{mic} = concentration of hydrocarbon in surfactant micelles expressed as amount per volume of solution

CMC = critical micelle concentration

C_{sat} = apparent hydrocarbon solubility in solution at a particular surfactant concentration greater than the CMC

C_{soil} = concentration of hydrocarbon sorbed onto the soil

C_{surf} = surfactant concentration

C_w = concentration of hydrocarbon in the aqueous phase expressed as amount per volume of solution

dE/dx = voltage potential gradient

dh/dx = hydraulic gradient

D^* = coefficient of molecular diffusion for the solute in the porous medium

D_o = permittivity of the pore fluid

DS_{mic} = moles of surfactant in micellar form per volume of solution, i.e., (C_{surf}-CMC)

D_x = hydrodynamic dispersion coefficient in the x direction

EC = electrical conductivity

f_{HCmic} = fraction of hydrocarbon in surfactant micelles

f_{oc} = weight fraction of organic carbon

I = current

J_x = the mass of solute per cross-section area transported in the x direction per unit time

K = the distribution constant of the analyte on the SPME fibre

K_d = distribution coefficient

K_{eo} = coefficient of electroosmotic permeability

K_h = hydraulic conductivity

K_i = coefficient of water-transport efficiency

K_{mc} = micelle-water partition coefficient expressed in concentration-based units

K_{mm} = micelle-water partition coefficient expressed as a dimensionless mole fraction ratio

K_{oc} = partition coefficient of a compound between organic carbon and the aqueous phase

$K_{oc,\ cmc}$ = modified partition coefficient of a compound between organic carbon and the aqueous phase taking into account surfactant effects

K_{ow} = octanol-water partition coefficient

LOD = limit of detection

M_o = mass of contaminant added to the system

MSR = molar solubilization ratio

n = porosity

n_{mol} = number of moles sorbed by the SPME fibre

N = the mean occupancy number of the organic molecules in SDS micelles at saturation

%RSD = percent relative standard deviation

Q = the volume flow rate

Q_{eo} = electroosmotic flow rate

R = retardation factor

R_f = modified retardation factor

R_p = radius of the charged particle

S = hydrocarbon solubility in the aqueous phase

SDS = sodium dodecylsulfate

S_i = the aqueous solubility of a compound in a complex mixture

S_{wi} = individual aqueous solubility of a compound

t = elapsed time

T_e = Thomas ratio

u_{ep} = electrophoretic mobility of the micelle

v_{eo} = electroosmotic flux

v_{ep} = electrophoretic flux or the flux of the micelles

v_h = hydraulic flux

V_{mol} = the molar volume of water (0.01805 L/mol at 25°C)

v_w = average linear groundwater velocity

V_s = volume of the stationary phase of the SPME fibre

x = distance travelled in the x direction

X_a = mole fraction of a compound in the aqueous phase

X_i = mole fraction of a compound in a complex mixture

X_m = mole fraction of compound in the micellar pseudo-phase

α = confidence limit

α_l = dispersivity

κ = diffuse double layer thickness

η = viscosity of the pore fluid

ρ_b = dry bulk density

σ = electrical conductivity of the pore fluid

ζ_{soil} = zeta potential of the soil

ζ_{mic} = zeta potential of the micelles

1.0 Introduction

1.1 Scope

Hydrocarbon contamination of soil and groundwater has become a major environmental concern in recent years due to increased environmental awareness and knowledge of the widespread occurrence of hydrocarbon contamination. Contamination by organic liquids originates from many sources ranging from leaking underground storage tanks at gasoline service stations to accidental spills at large industrial facilities. It has been estimated that hundreds of thousands of gasoline leaks to the subsurface may be presently occurring from the seven to eight million underground storage tanks found in the United States (Hoag and Marley 1986). With over half of the U.S. population depending on groundwater as a potable water supply (Putnam 1988) and the high demand for clean groundwater in Canada, the potential impact of hydrocarbon contamination is enormous.

Concern over soil and groundwater contamination along with the cost and limitations of current remediation methods has created a demand for new and efficient remediation technologies. Electrokinetic remediation with a surfactant is an innovative technique which has the potential to remove hydrocarbons from contaminated clay soils faster and more

efficiently than other techniques. However, limited research has been done in using electrokinetic remediation with a surfactant and the complicated chemical and physical interactions involved have not been adequately understood. The scope of this research is to evaluate the performance of using surfactant-enhanced electrokinetic remediation to remove hydrocarbons from contaminated soil columns in the laboratory and to identify the effect of various physical and chemical factors on the performance of surfactant-enhanced electrokinetic remediation. In addition, equations which combine electrokinetic and surfactant effects are to be developed to model contaminant transport during surfactant-enhanced electrokinetic remediation.

1.2 Surfactant-Enhanced Electrokinetic Remediation

Electrokinetic remediation is an innovative *in situ* remediation technique which promotes the movement of contaminants through soil by applying a low-level voltage potential gradient. The application of an electrical gradient causes the movement of cations (positively charged particles) which drag the pore fluid toward the negatively

charged cathode (Fig. 1.1). This bulk flow of pore fluid, referred to as electroosmotic flow, can significantly increase flow through low permeability soils. Electroosmotic flow transports the contaminants toward the cathode within the aqueous phase.

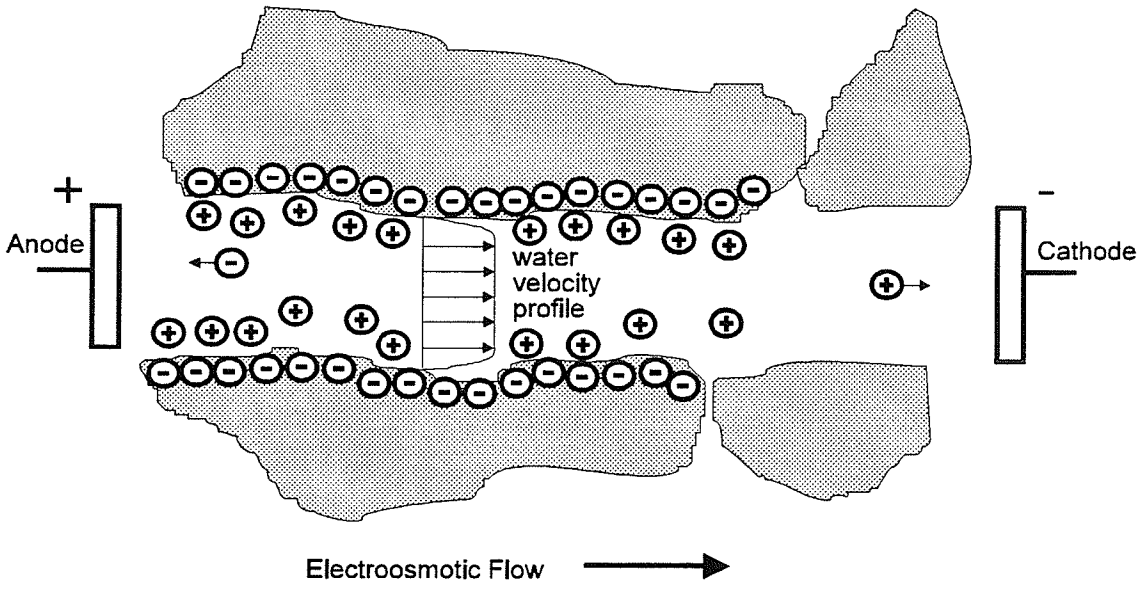

Figure 1.1 Schematic of electroosmotic flow in a charge porous media (adapted from Shapiro et al. 1989).

Another transport phenomena called electrophoretic flow occurs when combining electrokinetics with a processing fluid consisting of an ionic surfactant (enhanced electrokinetic remediation). Electrophoretic flow is the movement of charged particles toward the oppositely charged electrode with the application of a voltage potential

gradient. Above a certain surfactant concentration called the critical micelle concentration, surfactant molecules combine together to form charged particles called micelles. These charged particles form an organic pseudo-phase which attracts hydrophobic compounds and increases their aqueous solubilities. By using an anionic surfactant, the surfactant micelles will have a negative charge and will be repelled by the negatively charged clay particles. This repulsion minimizes surfactant loss due to sorption. The applied electrical potential gradient moves the negatively charged micelles and attached hydrocarbons toward the anode. The relative dominance of electroosmosis and electrophoresis is complex and depends upon the chemistry of the soil/water system which changes over time.

In a field situation, electrokinetic remediation with a surfactant removes hydrocarbons by placing electrodes within boreholes surrounding the contaminated soil (Fig. 1.2). Hydrocarbons are transported toward the electrodes by electroosmotic and electrophoretic flow. The contaminants can then be removed from the boreholes by pumping continuously or periodically and treated above ground. Once the hydrocarbons are removed from the soil, the soil can be flushed with water to remove the surfactant leaving a clean soil behind. Since the surfactant is biodegradable and non-toxic, any remaining surfactant in the soil system would pose no environmental threat.

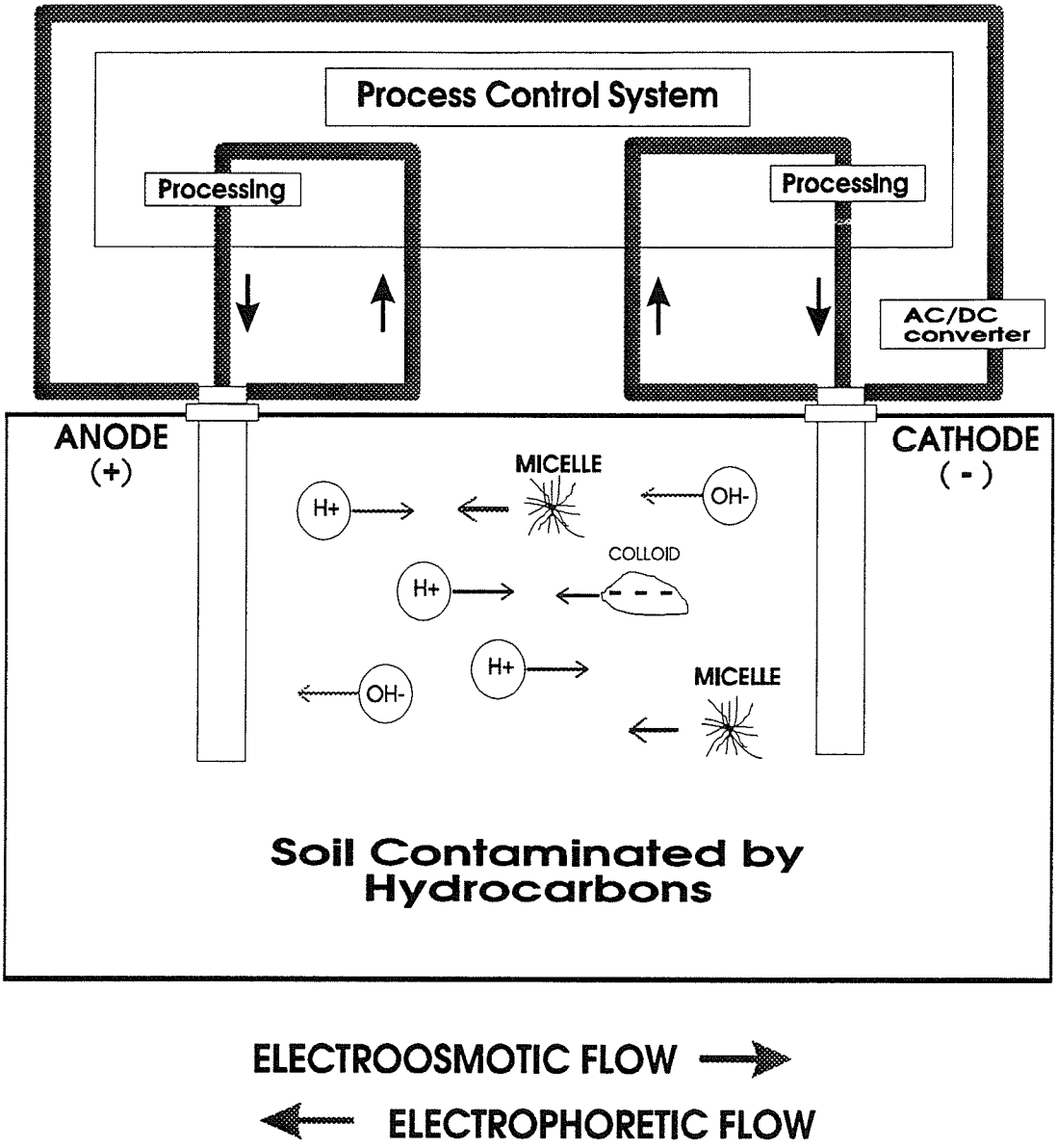

Figure 1.2 Schematic of surfactant-enhanced electrokinetic remediation in a field situation showing electroosmotic and electrophoretic transport phenomena.

1.3 Limits of Conventional Remediation Methods

There are many conventional remediation techniques such as excavation with disposal, pump-and-treat, vapour extraction, *in situ* biorestoration, and surfactant-enhanced aquifer remediation (SEAR) which can successfully remove hydrocarbons from contaminated soils. However, each technique has limitations which prevent successful remediation of clay soils contaminated with heavier-weight organics such as diesel fuel.

Excavation with disposal at a regulated landfill has been the most common remediation alternative for diesel-contaminated soil over the past 10-15 years (Dineen 1991). The main problem of excavation with landfill disposal is cost, landfill access, and impracticality with large areas of contamination. There is also a desire today to have an *in situ* treatment of the contaminated soil to prevent spreading the contamination to another area (Pamucku and Wittle 1992). In addition to cost and the potential for further contamination, excavation and disposal of contaminated soil at a regulated landfill can create problems with long-term liability (Dineen 1991).

Pump-and-treat is a widely used remediation technique which uses hydraulic control to move contaminants toward extraction wells where contaminants are removed and treated

above ground. Pump-and-treat strategy is often unsuccessful in heterogeneous soils because of difficulties encountered in recovering the contaminants from relatively immobile zones in the porous medium. These regions of undissolved hydrocarbons bypassed using the pump-and-treat method can form long term sources of *in situ* contamination. In addition, since contaminant transport is restricted to the aqueous phase, low aqueous solubilities and slow desorption processes can increase the duration of the pump-and-treat method and limit the efficiency of clean-up. Therefore, heavier weight hydrocarbons such as diesel fuel cannot be easily remediated by the pump-and-treat method. Another limitation of the pump-and-treat technique is the restriction to soils of relatively high hydraulic conductivities because of prolonged remediation times in low permeability soils. Pump-and-treat can be effective for containment but complete aquifer restoration may take many decades (Wunderlich et al. 1992).

Soil vapour extraction has been proven to be a cost-effective remediation alternative in removing volatile organic chemicals from soil in the unsaturated zone. However, vapour extraction has little use for the remediation of low permeability clay soils contaminated with heavier weight organics.

Biorestoration is another technique which is widely applied to remediate hydrocarbon-contaminated soils. Biorestoration cleans a soil by using microorganisms to break down the contaminant into non-toxic products. Biorestoration is generally cost-effective and can be used for large areas of contamination. However, biorestoration is limited to acting on the dissolved phase or at the aqueous/hydrocarbon interface (Aronstein et al. 1991; Wunderlich et al. 1992). Therefore, organic compounds sorbed onto clay particles are not (bio)available for breakdown by microorganisms. The slow mass transfer rate for the sorbed compounds to the aqueous phase is a limiting process in biorestoration which leads to long treatment times (Volkering et al. 1995). In addition, the effectiveness of *in situ* biorestoration is reduced in the presence of various organic compounds such as toluene which inhibit microbial growth, especially at high concentrations (Frankenburger 1992). The main disadvantage of biorestoration is the relatively long treatment time (Dineen 1991).

Surfactant-enhanced aquifer remediation (SEAR) is a remediation method that uses a biodegradable, non-toxic surfactant to wash hydrocarbons from soil. Interest in SEAR has grown in recent years but SEAR is still an emerging

remediation technique with problems which need to be addressed before successful field application. One disadvantage of SEAR is the need to collect and dispose of or treat the surfactant hydrocarbon effluent mixture after soil washing. SEAR is also inefficient in low permeability and heterogeneous soils where the surfactant cannot infiltrate into the entire soil.

The cost and limitations of current conventional remediation methods restrict the restoration of hydrocarbon-contaminated clay soils. Problems such as soil heterogeneity, low soil permeability, low compound aqueous solubility, and prolonged remediation time cannot all be handled with current conventional remediation technologies.

1.4 Advantages of Surfactant-Enhanced Electrokinetic Remediation

Surfactant-enhanced electrokinetic remediation has the potential to overcome the limitations of conventional remediation techniques by combining the advantages of electrokinetic remediation with surfactant-enhanced aquifer remediation. Electrokinetic remediation with a surfactant is a promising method that can efficiently remove both the light weight and the heavier weight organics, such as polyaromatic hydrocarbons found in diesel fuel, from low permeability soils.

By using an electrical potential gradient, flow through fine-grained soils can be dramatically increased compared to flow caused by a hydraulic gradient. For example, with the application of similar hydraulic and electrical gradients to a clay soil with a typical hydraulic conductivity and coefficient of electroosmotic conductivity of 1×10^{-8} cm/sec and 5×10^{-5} (cm/sec)/(V/cm) respectively, the flow caused by the electrical gradient will be 5000 times greater than the hydraulic flow. The increase in pore fluid flow with an electrical gradient leads to an increase in the efficiency of soil decontamination, especially in low permeability soils.

The widely accepted electrokinetic theory of Helmholtz and Smoluchowski shows that electroosmosis is not a function of pore size. Therefore, a heterogeneous soil mass with varying hydraulic conductivity and pore size will have the same flow rate throughout the entire soil mass. The uniform flow distribution can lead to high contaminant recoveries even in heterogeneous soils.

By incorporating a surfactant into the pore fluid, hydrocarbon solubilities are increased leading to a further reduction in remediation time and number of pore volumes required to clean the soil. Residual hydrocarbons absorbed onto the soil can also be removed with a surfactant which leads to enhanced aquifer clean-up. Electrokinetic

remediation with a surfactant is more advantageous in clayey soils contaminated with heavier weight organics over a relatively small volume. Electrokinetics can also be used to remediate contaminated soils under buildings which are inaccessible to other remediation methods. Electrokinetic remediation will improve soil strength by stabilizing the soil with dewatering and consolidation (Lo and Ho 1991; Morris and Caldwell 1985). Wide applicability, relatively smaller pore volumes, increase in pore fluid flux, uniform flow distribution, higher recoveries, and reduced clean-up time makes surfactant-enhanced electrokinetic remediation a cost-effective and promising remediation alternative.

1.5 Goals of the Research

The main objective of the research was to evaluate the performance of surfactant-enhanced electrokinetic remediation in removing hydrocarbons from contaminated soils. To meet this objective, laboratory equipment was designed and constructed. An extensive literature review was carried out and an annotated bibliography was completed. The research also developed analytical methods using the relatively new solid-phase microextraction (SPME) technique to allow the determination of a wide range of hydrocarbon concentrations and to improve the efficiency of conventional

SPME. The development of analytical techniques was required to use SPME for evaluation of contaminant removal for individual hydrocarbon compounds. These analytical methods allow the simple, fast, and cost-effective SPME technique to be used to determine hydrocarbon concentrations in other environmental investigations. The three goals of the research were the following:

1) to evaluate the performance of surfactant-enhanced electrokinetic remediation in removing hydrocarbons from contaminated soil columns in the laboratory.

2) to identify the effect of various physical and chemical factors on the performance of surfactant-enhanced electrokinetic remediation.

3) to develop equations that can be used to model contaminant transport during surfactant-enhanced electrokinetic remediation.

2.0 Literature Review

2.1 Introduction

A literature review of the processes involved in applying surfactant-enhanced electrokinetic remediation was separated into the two remediation methods, surfactant-enhanced aquifer remediation and electrokinetic remediation, which combine to form the surfactant-enhanced electrokinetic remediation method. The review of surfactant-enhanced aquifer remediation includes the effects of a surfactant in removing hydrocarbons from contaminanted soil and the review of electrokinetic remediation comprises the processes invoked during the application of a voltage potential gradient to a soil. A summary of the processes encountered in applying analytical methods using solid-phase microextraction (SPME) to determine hydrocarbon concentration is presented in chapter 4.0 along with the experimental research on SPME.

2.2 Surfactant-Enhanced Aquifer Remediation

2.2.1 Introduction

Surfactant-enhanced aquifer remediation (SEAR) has recently received increased attention as an alternative method for remediating hydrocarbon-contaminated soils (Abdul et al. 1992; Abdul et al. 1990; Abdul and Gibson 1991; Brown

and Pope 1994; Clarke et al. 1991; Fountain et al. 1991; Kan and Tomson 1986; Pennel et al. 1994; Rixey et al. 1991; Sale and Pitts 1989; Vigon and Rubin 1989; West and Harwell 1992; Wunderlich et al. 1992). Although SEAR is primarily in the developmental stage (Peters et al. 1992), it has been used to remove automatic transmission fluid (Abdul et al. 1990), polychlorinated biphenyls (PCBs) (Abdul et al. 1992; Abdul and Gibson 1991; Clarke et al. 1991), anthracene (Roy et al. 1994), naphthalene (Kan and Tomson 1986), residual tetrachloroethylene (Pennel et al. 1994), and BTEX (Rixey et al. 1991) from sandy soils in the laboratory.

There are two general ways in which surfactants can enhance remediation of hydrocarbon-contaminated soils. One is micellar solubilization which refers to the increase in hydrocarbon solubility due to micelles and the other is the mobilization of the hydrocarbon by lowering the interfacial tension (Sale and Pitts 1989; West and Harwell 1992). In enhanced oil recovery with surfactants, the mechanism of lowering of interfacial tension is more important (Vigon and Rubin 1989). However, in SEAR, surfactants are selected to increase solubility while minimizing the reduction in interfacial tension (Wunderlich et al. 1992). This allows for maintaining hydraulic control and prevents mobilization of contaminants to uncontaminated areas (Wunderlich et al. 1992). Micellar solubilization is the main mechanism by

which hydrophobic organic compounds have been removed from contaminated sand (Pennel et al. 1994; Roy et al. 1994). Therefore, the success of SEAR is directly attributed to the capacity of surfactants to increase the solubilities of hydrophobic compounds (Pennel et al. 1994).

2.2.2 Surfactant Theory

A surfactant is a surface active agent consisting of a hydrophilic head group and a hydrophobic hydrocarbon tail (Myers 1992). Surfactants are classified according to the properties of the hydrophilic head group (West and Harwell 1992). The head group can carry a negative charge (anionic), a positive charge (cationic), both negative and positive charges (zwitterionic), or no charge (nonionic) (West and Harwell 1992).

At a specific concentration known as the critical micelle concentration (CMC), the hydrophobic tail groups of excess surfactant molecules are attracted to each other in solution forming micelles (Edwards et al. 1991a). A micelle is a conglomerate of surfactant molecules consisting of a hydrocarbon core, an outer layer with the ionic head groups along with their counter ions, and an intermediate area termed the palisade layer (Valsaraj and Thibodeaux 1989). The CMC is a function of the surfactant structure and

composition, temperature, ionic strength, and the presence and type of organic additives in solution (Myers 1992). The CMCs typically range from 0.1 to 10 mmol/L (West and Harwell 1992).

The presence of an organic solute can reduce the CMC of the surfactant (Pennel et al. 1993). The reduction in the CMC increases the amount of hydrocarbon that will partition into surfactant micelles at a given surfactant concentration above the CMC. Therefore, knowledge about the impact of hydrocarbons on the CMC is important in predicting the performance of SEAR.

The application of SEAR is influenced by temperature. At a specific temperature known as the Kraft point the solubility of an ionic surfactant becomes equal to the CMC (West and Harwell 1992). Therefore, when the temperature drops below the Kraft point, the surfactant solution loses its ability to form micelles. This is important in the field application of surfactants since the temperature of the groundwater can be lower than the Kraft temperature of some surfactants (West and Harwell 1992). However, it is possible to reduce the Kraft point by branching the hydrocarbon tail and by using a co-solvent (West and Harwell 1992).

The solubility of an organic compound may be enhanced at surfactant concentrations below the CMC. For example,

DDT has exhibited a significant increase in solubility below the CMC for several surfactants (Kile and Chiou 1989). At the CMC, the apparent solubility may increase by a factor of up to two to three for polycyclic aromatic hydrocarbons (Edwards et al. 1991a). Generally the more hydrophobic a compound the greater the increase in apparent solubility below the CMC. However, it has been reported that below the CMC a surfactant has minimal effect on the solubility of most hydrocarbons (Pennel et al. 1993).

Hydrocarbon distribution in the aqueous phase of a soil system varies in the presence of a surfactant. With no surfactant in the aqueous phase, the hydrocarbon partitioning onto organic carbon in the soil can be determined using standard equations. However, in the presence of a surfactant, the amount of hydrocarbon sorbed onto the soil is decreased and the partition coefficient of a compound between organic carbon and the aqueous phase, K_{oc}, is decreased (Fig. 2.1). A modified organic carbon-aqueous phase partition coefficient is needed in the presence of a surfactant at concentrations equal to or at the CMC to take into account the increase in hydrocarbon solubility and the decreased K_{oc} value.

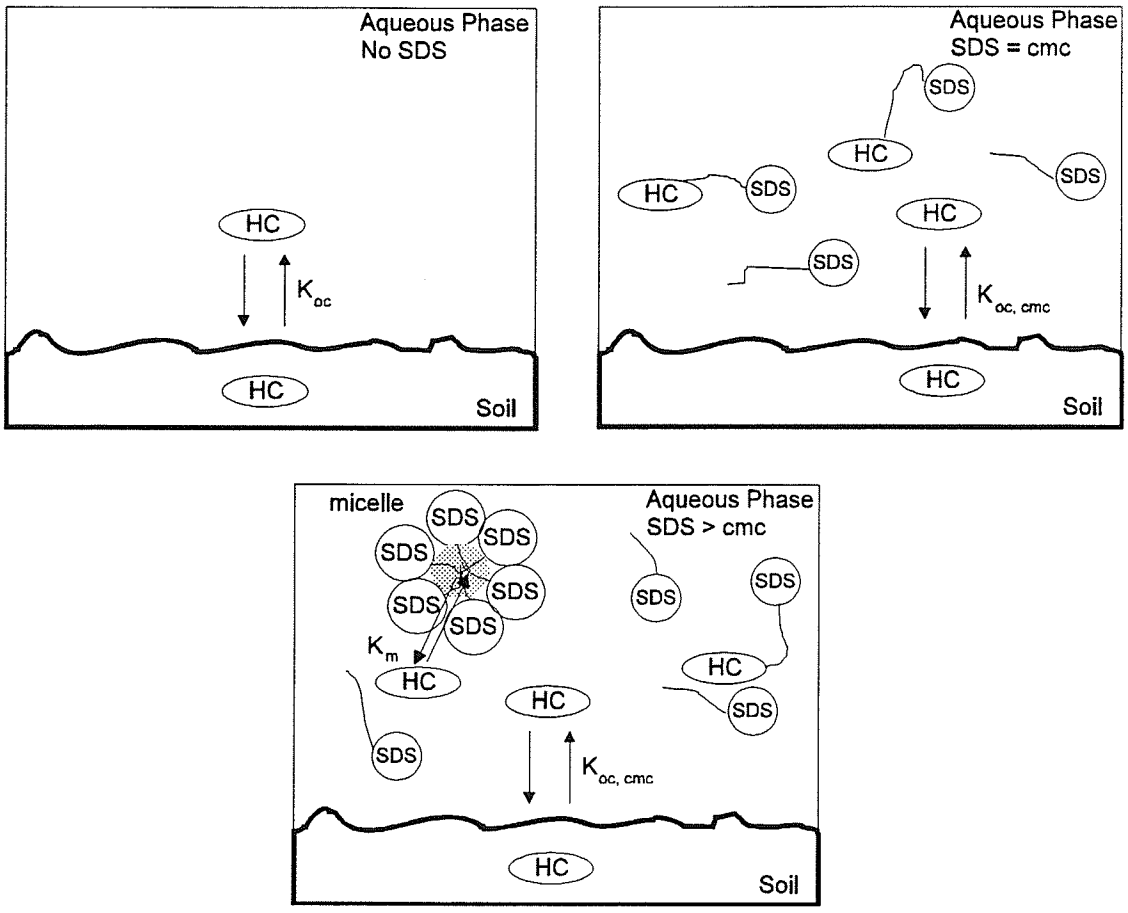

Figure 2.1 Distribution of hydrocarbons and anionic surfactant in a soil/aqueous system (adapted from Edwards et al. (1991a)): HC = hydrocarbon, SDS = sodium dodecylsulfate surfactant, $K_{oc,\ cmc}$ = modified partition coefficient of a compound between organic carbon and the aqueous phase taking into account surfactant effects.

2.2.3 Micellar Solubilization

At surfactant concentrations above the CMC, the aqueous solubilities of organic compounds are greatly increased. The increase in solubility caused by the partitioning of hydrophobic compounds within surfactant micelles is called micellar solubilization (West and Harwell 1992). Knowledge of micellar solubilization can be used to predict the electrophoretic transport of hydrocarbons in micelles during surfactant-enhanced remediation.

Micellar solubilization can be characterized by the molar solubilization ratio (MSR). The MSR is defined as the number of moles of organic compound solubilized per mole of surfactant added to solution (Edwards et al. 1991c). It has been shown that there is a linear relationship between solubility and surfactant concentration at concentrations above the CMC (Edwards et al. 1991c; Gannon et al. 1989; Rouse et al. 1993; Valsaraj et al. 1988). In the presence of excess free-phase, the MSR can be obtained from the slope of the linear line fitted through a plot of hydrocarbon concentration (mol/L) as a function of surfactant concentration (mol/L) above the CMC,

$$MSR = \frac{(C_{sat} - C_{cmc})}{DS_{mic}} = \frac{(C_{sat} - C_{cmc})}{(C_{surf} - CMC)} \quad (1)$$

where:

MSR = molar solubilization ratio (dimensionless),

C_{sat} = apparent hydrocarbon solubility in solution at a particular surfactant concentration greater than the CMC (mol/L),

C_{cmc} = apparent hydrocarbon solubility at the CMC (mol/L),

C_{surf} = surfactant concentration at which C_{sat} is evaluated (mol/L),

CMC = critical micelle concentration (mol/L),

DS_{mic} = moles of surfactant in micellar form per litre of solution, i.e., $(C_{surf} - CMC)$ (mol/L).

Another approach in reporting the amount of hydrophobic compound which partitions into surfactant micelles is the determination of the micelle-water partition coefficient. The micelle-water partition coefficient, expressed as dimensionless units on a mole fraction basis, K_{mm}, is the ratio of the mole fraction in the micellar pseudo-phase, X_m, to the mole fraction of compound in the aqueous phase, X_a (Edwards et al. 1991c).

$$K_{mm} = \frac{X_m}{X_a} \qquad (2)$$

The dimensionless micelle-water partition coefficient can be calculated using the MSR by (Edwards et al. 1991c)

$$K_{mm} = \frac{1}{C_{cmc}\, V_{mol}} \frac{MSR}{1+MSR} \qquad (3)$$

where:

K_{mm} = micelle-water partition coefficient (dimensionless),

MSR = molar solubilization ratio (dimensionless),

V_{mol} = the molar volume of water (0.01805 L/mol at 25°C),

C_{cmc} = apparent hydrocarbon solubility at the CMC (mol/L).

The value of K_{mm} is constant in the presence or absence of separate phase hydrocarbon compounds whereas the value of the MSR in the absence of separate phase hydrocarbon compounds varies with surfactant concentration as a result of changes in the aqueous pseudo-phase hydrocarbon concentration (Edwards et al. 1991c).

The choice of units to express the micelle-water partition coefficient has caused confusion in reported literature values. Since micelles are actually pseudo-phases and not isotropic liquids, the choice of units has been inconsistent (Jafvert 1991). Values of the micelle-water partition coefficient have been reported as a dimensionless mole fraction ratio as described above and in concentration-based units (L/mol). It is believed that when micelles are considered as a separate pseudo-phase, the concentration-based unit is used and when micelles are

considered as part of an isotropic solution, the dimensionless mole fraction ratio is used. Confusion may occur because octanol-water partition coefficients, K_{ow}, often used in remediation studies, are reported as a dimensionless concentration ratio (Domenico and Schwartz 1990). The dimensionless concentration ratio is used for K_{ow} since octanol is not considered as a separate pseudo-phase as are micelles. Reported micelle-water partition coefficients are more often given by the dimensionless mole fraction ratio (Edwards et al. 1991a; Edwards et al. 1991b; Edwards et al. 1991c; Jafvert 1991; Valsaraj et al. 1988) as compared to the concentration-based unit (Almgren et al. 1979; Clarke et al. 1991; Gannon et al. 1989) but the choice of units is not always indicated. Therefore, care must be taken in using micelle-water partition coefficients reported in the literature.

2.2.4 Selection of Surfactant

The selection of an optimum surfactant depends upon a number of factors such as the type of soil, type and concentration of contaminant, cost and availability of surfactant, and the method to be used to recycle the surfactant effluent. Laboratory studies have been conducted to evaluate the relative suitability of various surfactants

to wash automatic transmission fluid, diesel fuel, and other hydrocarbons from contaminated soil (Abdul et al. 1990; Abdul and Gibson 1991; Edwards et al. 1991c; Kile and Chiou 1989; Laha and Luthy 1991; Lui et al. 1991; Pennel et al. 1994; Peters et al. 1992). A comparison of individual anionic, nonionic, and cationic surfactants found that anionic surfactants result in the greatest mobilization of diesel fuel (Peters et al. 1992). Blends of surfactants have been shown to remove hydrocarbon contaminants more effectively than individual anionic and nonionic surfactants (Peters et al. 1992). Furthermore, twin head group ionic surfactants have less tendency to precipitate in solution than single head group surfactants due to increased solubility (Rouse et al. 1993). Since the economics of SEAR is affected by the loss of surfactant because of sorption and precipitation, anionic surfactants are preferred because of their resistance to sorption in clay soils.

The anionic surfactant sodium dodecylsulfate was selected because it is inexpensive, non-toxic, and readily available (Gannon et al. 1989). Sodium dodecylsulfate (SDS) is also a popular surfactant which has been widely researched (Myers 1992). Nonionic surfactants have low CMC values and increased solubilization powers (Kile and Chiou 1989). However, an anionic surfactant is preferred because of its resistance to sorption by clays. In addition,

solvent extraction, a promising effluent treatment technique, cannot be used with nonionic surfactants. The surfactant SDS has been used for *in situ* soil washing because solvent extraction can then be used to recycle the surfactant solution (Underwood et al. 1993). The advantages of using nonionic surfactants might be outweighed by the ability of using solvent extraction to handle the critical problem of treating the effluent (Gannon et al. 1989). However, an anionic surfactant can lead to dispersion of clay particles which can clog soil pores and reduce flow.

2.2.5 Properties of Sodium Dodecylsulfate

Sodium dodecylsulfate (SDS) is an anionic surfactant from the sulfate ester family of surfactants (Myers 1992). SDS is also referred to by its product name sodium lauryl sulfate (SLS) and by the abbreviations NaLS, NaDDS, DDS, and NaDS. SDS is a simple straight chain aliphatic with the molecular structure $CH_3(CH_2)_{11}\,O\,SO_3^-\,Na^+$. The dodecyl chain has a very low water solubility while the sulfate group has a very high water solubility (West and Harwell 1992). The CMC for SDS is 8 mmol/L (Almgren et al. 1979; Mukerjee and Mysels 1971; Vold and Vold 1983). SDS has a reported Kraft point of 15°C (Myers 1992).

2.2.6 Field Application of Surfactant-Enhanced Aquifer Remediation

The field application of surfactant-enhanced aquifer remediation is similar to the pump-and-treat method except a surfactant solution is used as the influent. Contaminants are pumped to boreholes and treated above ground by air stripping or other methods as in traditional pump-and-treat remediation. It is becoming apparent that the cost limiting factor in SEAR is the ability to recycle the surfactant and the technology to clean up the extracted pore fluid (Clarke et al. 1993; Clarke et al. 1991).

One advantage of the field application of SEAR is that the addition of a surfactant to a soil leads to increased biological breakdown of the contaminants (Aronstein et al. 1991; Bury and Miller 1993; Laha and Luthy 1991). The presence of a surfactant increases the amount of organic compound in the aqueous phase and, therefore, increases the amount of organic compound (bio)available to microorganisms (Lui et al. 1995). The additional decontamination by biological breakdown increases the success of SEAR.

2.3 Electrokinetic Remediation

2.3.1 Introduction

Engineers have been using electrokinetics for dewatering and stabilizing clay soils since the 1930's (Mattson and Lindgren 1994; Putnam 1988). However, interest in applying electrokinetics to remediate soil began when Segall et al. (1980) reported increased concentrations of heavy metals and organic material in electroosmotically generated leachate from dredged sludges. With the growing concern over hydrocarbon contamination of soil and groundwater in recent years, interest in electrokinetic remediation has increased but it is still considered an emerging technology (Acar et al. 1993b). Electrokinetic remediation has been used to remove inorganic and organic contaminants from soils in the laboratory by utilizing the ionic charge on the compounds and electroosmotic flow (Acar et al. 1992; Bruell et al. 1992; Hamed et al. 1991; Mattson and Lindgren 1994; Pamucku et al. 1990; Pamucku and Wittle 1992; Runnells and Larson 1986; Runnells and Wahli 1993; Shapiro and Probstein 1993; Shapiro et al. 1989). Electrokinetics has been used in many areas including remediating radio-nuclides in agricultural soil surrounding Chernobyl, Ukraine (Mattson and Lindgren 1994) and forming electrokinetic barriers to contaminant transport through

compacted clay liners (Mitchell and Yeung 1990). It is also believed that electrokinetics could be used for a number of other purposes such as (1) diversion schemes for water plumes, (2) injection of grouts, (3) injection of microorganisms and nutrients into soil (Segall and Bruell 1992), (4) dewatering and consolidation of waste water sludges, mine tailings, or dredged materials (Alshawabkeh and Acar 1992). Electrokinetic remediation is also applicable to both saturated and unsaturated porous media (Mattson and Lindgren 1994) but is more efficient in soils with high water contents (Mitchell 1976).

2.3.2 Electrokinetic Processes

Electrokinetic remediation invokes three main electrokinetic processes: electroosmosis, electrophoresis, and electrolytic migration of ionic and polar species (Pamucku and Wittle 1992). Electroosmosis involves the transport of pore fluid such as water relative to the charged soil surface; whereas, electrophoresis involves the transport of charged particles such as micelles through the pore fluid (Hachisu 1984). The third electrokinetic process, electrolytic migration, refers to the transport of ionic and polar species. This is the migration of charged ions such as hydrogen ions in the pore fluid under the influence of an electrical potential gradient. Another

electrokinetic phenomena, the streaming potential, is the formation of a potential difference across the upstream and the downstream ends of a stationary solid phase (Gopinath 1994). There is also a sedimentation potential caused by the movement of a solid phase through a stationary liquid phase induced by the gravitational field. The electrokinetic processes are summarized in Table 2.1.

2.3.2.1 Electroosmosis

In a porous medium, electroosmotic flow is caused by an electric field acting on the charged double layer at the particle surface. In clay soils, cations are attracted to the negatively charged surface of the clay particles. The diffuse layer of cations and associated anions that form at the solid-liquid interface is referred to as the "diffuse double layer". The double layer is the region near the pore wall in which the fluid possesses a charge density that balances the surface charge on the pore wall (Shapiro et al. 1989). When a direct-current (DC) is applied to a moist soil, the mobile cations associated with the diffuse double layer migrate to the cathode and the water molecules are dragged along with them (Mitchell 1976). Extraction of contaminants by electroosmosis is based on the assumption that the advection generated by electroosmotic flow carries the contaminants within the liquid phase toward the cathode.

Table 2.1 Summary of Electrokinetic Transport Processes

Electrokinetic	Description	Cause
electroosmosis	pore fluid transport relative to a charged surface	drag of cations with the application of externally applied voltage gradient
electrophoresis	charged particle transport through a fluid	application of externally applied voltage gradient
ionic migration	ionic and polar species transport	application of externally applied voltage gradient
streaming potential	formation of potential difference across the upstream and downstream sides of a stationary solid phase	movement of a liquid phase through a stationary phase induced by an externally applied hydraulic gradient*
sedimentation potential	movement of solid phase through a stationary liquid phase induced by a gravitational field	movement of a solid phase through a stationary liquid phase induced by the gravitational field*

* From: Gopinath (1994)

A number of theories have been proposed for electroosmotic flow by Schmid (1950), Spiegler (1958), Acar et al. (1990b), Pamucku et al. (1991), Shapiro and Probstein (1989), and Helmholtz-Smoluchowski. One theory by Spiegler takes into account the interactions of the mobile components of soil (water and ions) and the friction interactions of these components with the pore walls (Spiegler 1958). Spiegler (1958) measured the electroosmotic flow as the difference between the total water movement and the amount of hydrated water moving with ions (Pamucku and Wittle 1992). This is important to electrokinetic remediation with a surfactant since it suggests that water flow caused by the migration of anions in the opposite direction of electroosmotic flow can retard electroosmotic flow when the anion concentration exceeds the cationic concentration (Pamucku and Wittle 1992).

One of the earliest and widely accepted theoretical description of electroosmotic flow is the Helmholtz-Smoluchowski theory (H-S theory). The H-S theory suggests that the electroosmotic velocity depends upon the electrical potential gradient, viscosity, and permittivity of the pore fluid, and the zeta potential of the surfaced charged porous medium that the fluid passes through. The Helmholtz-Smoluchowski theory estimates that the electroosmotic flow produced by an applied electrical potential gradient is given by the expression

$$v_{eo} = \frac{D_o \zeta_{soil}}{4\pi\eta} \frac{dE}{dx} \quad (4)$$

where:

v_{eo} = electroosmotic flow velocity (m/sec),

η = viscosity of the pore fluid (Pa sec),

D_o = permittivity of the pore fluid (C/V/m or N/V^2),

ζ_{soil} = zeta potential of the soil (V),

dE/dx= voltage potential gradient (V/m).

The permittivity represents the ability of a liquid to transmit charge and the zeta potential is the potential across the diffuse double layer or the potential of the slipping plane where static forces are overcome and fluid movement starts to occur (Stumm and Morgan 1981). Due to the negatively charged zeta potential of soil, ζ_{soil}, electroosmotic flow is toward the cathode. The H-S theory does not always fit experimental results since ζ_{soil} varies with pH and ionic concentration of the pore fluid (Eykholt and Daniel 1994; Mitchell 1976). In addition, the electrical potential gradient changes over time with the changing resistivity and oxidation/reduction state of the soil (Pamucku and Wittle 1992).

An equation similar in form to Darcy's Law is used to describe the electroosmotic flow,

$$v_{eo} = \frac{Q_{eo}}{A} = K_{eo} \frac{dE}{dx} \qquad (5)$$

where:

Q_{eo} = electroosmotic flow rate (m^3/sec),

K_{eo} = coefficient of electroosmotic permeability (m^2/(V sec)),

dE/dx= voltage potential gradient (V/m),

A = cross sectional area (m^2).

Values of K_{eo} are relatively independent of soil type varying within one order of magnitude between 10^{-9} and 10^{-10} m^2/(V sec) (Bruell et al. 1992).

In electroosmosis, the electroosmotic flow rate can be related to the current (Acar et al. 1990a; Hamed et al. 1991) as

$$Q_{eo} = K_{eo} \frac{dE}{dx} A = K_i I = \frac{K_{eo}}{\sigma} I \qquad (6)$$

where:

K_i = coefficient of water-transport efficiency (m^3/amp sec),

I = current (amp),

σ = electrical conductivity of the pore fluid (mS/m).

Values for K_i range from 0 to 1.0×10^{-3} L/(amp sec) for a wide range of soils (Acar et al. 1990a).

Electroosmotic flow is a function of many variables. Comparing the Helmholtz-Smoluchowski equation (4) and equation (5) shows that K_{eo} is a function of zeta potential, viscosity of the pore fluid, and electrical permittivity of the soil medium. The coefficient of electroosmotic conductivity is also accepted as being a function of porosity (Acar et al. 1993b). It is important to note that K_{eo} is not a function of pore size as is hydraulic conductivity. Therefore, electroosmotic flow can be significant in fine-grained soils and the flow distribution will be uniform even in heterogeneous soils. In addition, electroosmotic flow increases with increasing water content but decreases with increasing ionic concentration of the pore fluid in most soils (Pamucku and Wittle 1992). When the ionic conductivity of the pore fluid is high or when the pH is low (2 to 3), very little electroosmotic flow occurs. It has been shown that the electroosmotic flow can reverse when the pH is reduced below the isoelectric point of the clay (Acar and Alshawabkeh 1993). The isoelectric point is the pH where the molecule bears no net charge so that the

zeta potential is zero and no migration is produced by the application of an electrical potential gradient (Stumm and Morgan 1981). It has been generally found that the electroosmotic flow is greater when the ratio of the current carried by the pore fluid to the electrolytic current (current by the ions in the pore fluid) is large due to reduced concentration of ions in the pore fluid (Pamucku and Wittle 1992). Therefore, surfactant addition should decrease the efficiency of electroosmotic flow.

2.3.2.2 Electrophoresis

Electrophoresis refers to the migration of charged particles such as micelles and clay particles through fluid under an electrical potential gradient. Charged particles are attracted to one electrode and repelled by the other. The mobility of clay particles which varies from 1×1^{-10} to 3×10^{-9} (m/sec)/(V/m) is less than the electroosmotic mobility (Lageman et al. 1989). Therefore, electrophoresis becomes significant in electrokinetic remediation only when surfactants at concentrations above the CMC are introduced into the pore fluid.

2.3.2.3 Electrolytic Migration

Electrolytic migration is the migration of polar and ionic species present in the pore fluid. This includes the migration of hydrogen ions and hydroxide ions which are responsible for the current in the soil water system in the absence of charged surfactant micelles. Electrolytic migration does not transport water except for the water of hydration surrounding an ion. The amount of electrolytic migration is related to the ionic concentration in the pore fluid and the charge on the ion.

Electrolytic migration is relatively more important in the removal of heavy metals such as lead and iron from soil due to their high electric charge. The average mobility of ions is approximately 5×10^{-8} (m/sec)/(V/m), which is ten times greater than that of the electroosmotic mobility (Lageman et al. 1989). However, organic compounds often have low polarity and, therefore, electrolytic migration is not expected to influence their transport.

2.3.3 Electrochemistry

During the application of an electric field to a soil, oxidation (electrons removed) and reduction (electrons gained) reactions occur at the electrodes. The electrolysis reactions of water are the principal reactions which affect

the electrokinetic remediation process. The electrolysis reactions leads to a change in the pH of the soil/water system. The importance of the effect of pH changes on electroosmosis has been reported by many researchers (Pamucku et al. 1990; Putnam 1988; Shapiro and Probstein 1993). Various models have been developed to predict the pH changes in a soil system during electrokinetic remediation (Acar et al. 1990a; Acar et al. 1990b; Alshawabkeh and Acar 1992; Datla 1994) In the electrochemical reactions, hydrogen ions and hydrogen gas are produced at the cathode and hydroxide ions and oxygen gas are produced at the anode (Acar and Alshawabkeh 1993; Acar et al. 1990a; Acar et al. 1992).

Anode

$2H_2O - 4e^- \Rightarrow O_2 \uparrow + 4H^+$

Cathode

$2H_2O + 2e^- \Rightarrow H_2 \uparrow + 2OH^-$

These reactions can be used to determine the production of hydrogen ions, hydroxide ions, and gas for a known current.

Acidic conditions are created by the hydrogen ions produced at the anode and basic conditions are created by the hydroxyl ions produced at the cathode. However, the

soil system becomes acidic over time since the ionic velocity of the hydrogen ion is approximately 1.8 times higher than that of the hydroxyl ions (Acar and Alshawabkeh 1993). In addition, electroosmotic flow transports the hydrogen ions toward the cathode. This leads to a drop in pH of the soil system with time except at the cathode. The pH can drop at the anode to below 2 and it can increase at the cathode to above 12 depending on the total current applied, the buffering capacity of the soil, the total flow rate and the presence of processing fluids (Acar and Alshawabkeh 1993; Acar et al. 1993b; Acar et al. 1990a; Acar et al. 1990b). The change in pH affects the soil surface properties such as cation exchange capacity and zeta potential (Pamucku and Wittle 1992). Reduction in the zeta potential with decreasing pH can cause electroosmotic flow to stop and possibly reverse (Shapiro and Probstein 1993).

Secondary reactions may occur depending upon the concentration of available species such as metals (Acar and Alshawabkeh 1993). Electrode reactions may be minimized by isolating the electrodes from the soil surface and/or by using inert electrodes (Pamucku and Wittle 1992). Electrode reactions should be prevented because other ions generated at the electrodes can enter the soil and interfere with the remediation process.

The minimum theoretical voltage required to cause electrolysis of chemical species in an aqueous solution is determined by the summation of the standard voltages of the appropriate anode/cathode half-reactions (Segall and Bruell 1992). However, a higher voltage is sometimes needed for electrolysis than indicated by the reduction potential voltages (Gillespie et al. 1989). This additional voltage required to cause electrolysis is called over-voltage (Gillespie et al. 1989). Over-voltages are required to overcome ion-concentration polarization occurring at the electrodes (Segall and Bruell 1992). The over-voltage leads to lower voltage application than the voltage supplied from a constant power source.

2.3.4 Field Application of Electrokinetic Remediation

Various pilot projects have been conducted using electrokinetic remediation in the field (Banjaree et al. 1991; Lageman 1993; Lageman et al. 1989; Trombly 1994). Electrodes can be installed at any depth, either horizontally or vertically in deep directionally drilled tunnels or in trenches around the contaminated soil (Lageman 1993; Lageman et al. 1989). Electrodes can also be placed within boreholes installed into the contaminated soil (Runnells and Wahli 1993). The contaminant is pumped,

either continuously or periodically, from the boreholes to the surface for treatment.

Electrokinetic remediation can also be combined with other methods such as pumping (Banjaree et al. 1991) and biorestoration (Lageman 1993). In relatively high permeability soils, a combination of hydraulic and electrokinetic techniques will lead to the most economic results (Lageman et al. 1989). Inert electrodes composed of graphite, carbon, or platinum should be used to reduce the formation of secondary corrosion products (Acar et al. 1993b). Steel reinforcing bars have been used as electrodes in field application (Banjaree et al. 1991).

Electrode spacing will depend upon the type and concentration of the contaminants (Acar et al. 1993b). Some research indicates that a voltage gradient of 1 V/cm is preferred with electrode spacing up to 3 m (Acar and Hamed 1991). However, electrode spacing between 4 and 10 m have been found to be more practical in the field (Banjaree et al. 1991). One challenge in the field application of electrokinetics is the number of electrodes and spacing required (Runnells and Wahli 1993). A current density of about 30-50 $\mu A/cm^2$ has been shown to be the most efficient (Acar et al. 1993b). A substantial decrease in efficiency may occur with the temperature increase caused by higher voltage potential gradients associated with larger electrode

spacing (Acar et al. 1993b). There should not be a depth limitation in the process beyond practical problems that may be encountered in electrode installation (Acar and Hamed 1991). The soil material should not contain any metal or isolating objects which can cause preferential flow for electrical current (Lageman 1993).

2.4 Surfactant-Enhanced Electrokinetic Remediation

Surfactant-enhanced electrokinetic remediation is a promising technique to remediate hydrocarbon-contaminated soils more efficiently than conventional remediation methods. However, limited research has been done and consequently an understanding of the complex effects of various physical and chemical factors on the performance of surfactant-enhanced electrokinetic remediation has not been achieved. Literature review indicates that no research has used surfactants to remediate clay soils and there have been no reported data on combining electrokinetics with a surfactant in remediating hydrocarbon-contaminated clay soils. The combination of two emerging remediation technologies is a major challenge and has a number of unknowns. The successful application of electrokinetic remediation with a surfactant requires integrating knowledge from many disciplines including hydrology, organic

chemistry, physical chemistry, electrical chemistry, analytical chemistry, engineering, and soil science.

Surfactant-enhanced electrokinetic remediation involves a complex interaction of many physical and chemical factors. The following factors which must be considered are hydraulic conductivity, electrolysis reactions, zeta potential of the surfactant micelles and soil, ionic mobility, electrical conductivity of the pore fluid, clay interactions with the surfactant, surfactant sorption, surfactant concentration, voltage potential gradients, pH changes, effects of organic on the CMC, retardation and sorption of the organic compounds, and micellar solubilization of the organic compounds. Sufficient information on the effects of these factors is yet to be established.

3.0 Experimental Materials and Methods

3.1 Laboratory Equipment

The laboratory set-up used for the electrokinetic remediation studies consisted of six specially designed glass columns, a constant head flow device, a flow rate measuring system, a constant voltage source, and a computer controlled data acquisition system coupled with a voltmeter and a 24-channel multiplexer (Fig. 3.1). Soil was packed into 30-cm long, 5.08-cm O.D., 4.76-cm I.D. (cross sectional area = 17.8 cm^2) glass columns (Fig. 3.2). Electrokinetic treatment was applied to three soil columns, referred to as electrical columns, and hydraulic treatment was applied to the other three soil columns, referred to as hydraulic columns. The soil was secured in place using Teflon-backed plexiglass endcaps and stainless steel tie rods. The endcaps were separated from the sandy soil by a thin nylon mesh and from the clay soils by a thin mesh and glass beads. An O-ring was used to ensure the endcaps sealed completely with the glass columns.

Specially fused ports made from 2-ml screw-cap vials were included along the length of the columns to allow for voltage drop measurements and sampling of organic compound concentrations. The sampling ports were located 2, 8.5, 15, 21.5 and 28 cm from one end of the column. The 8 voltage

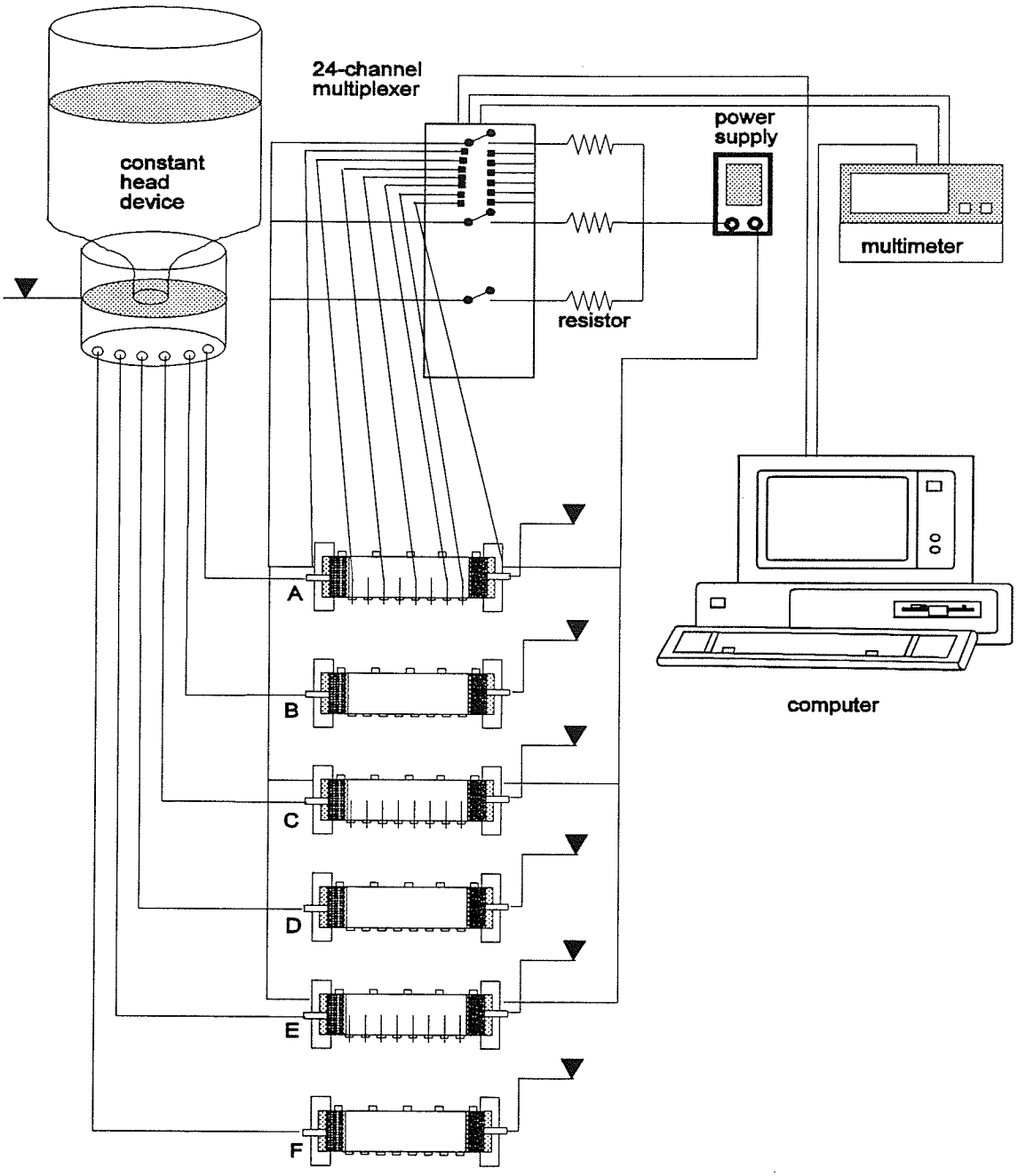

Figure 3.1 Schematic of laboratory set-up. Columns A, C, and E are electrokinetic treatment columns and columns B, D, and F are hydraulic columns. Set-up for voltage drop measurements is only shown for electrical column A.

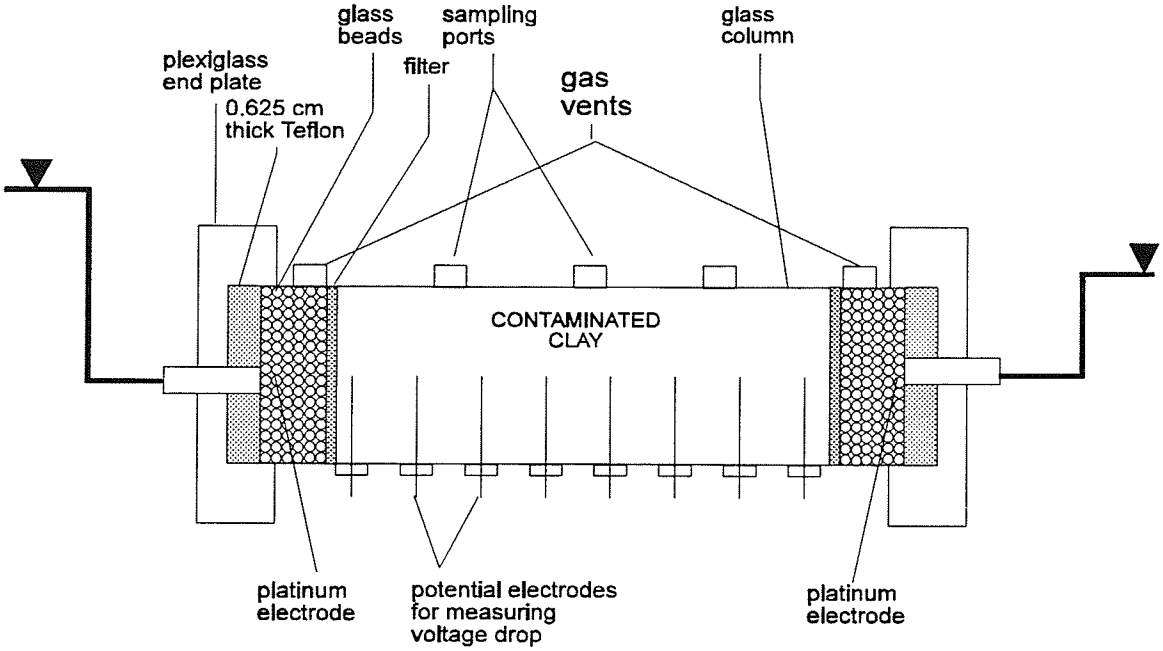

Figure 3.2 Schematic of glass column packed with clay soil as in experiment No.4.

drop measuring ports were spaced 3 cm apart starting 4.5 cm from the one end of the column. The voltage potential was applied to the electrokinetic treatment samples using active platinum electrodes consisting of a 0.51-mm diameter platinum wire. Platinum wire was also used to measure the voltage gradients in the electrical columns.

A 24-channel multiplexer coupled with a multimeter and computer controlled data acquisition system was used to measure the current and voltage drops in the samples. The computer control system can apply a DC electrical field continuously or in a cycle. The constant power supply was a

BK Precision DC Power Supply 1610. The multimeter was a Hewlett Packard 34410A. The 24-channel multiplexer is a device which controls channel switches for voltage control and for voltage drop and current measurements. Channels 1, 9, and 17 were used to control voltage on/off time. Channels 8, 16, and 24 were used to measure the voltage drop across a 1000 ohm resistor in series with each electrical column. Ohm's Law was then used to determine the current in each column. The remaining channels measured the voltage drops within the electrical columns. The C++ program "current2.c" given in Appendix A was used to control the 24-channel multiplexer and the data acquisition system.

The set-up had the capability to run six samples simultaneously. The use of six columns allowed test replicates to be completed at the same time and under similar conditions for both the electrical and hydraulic columns. Thus, experimental variability could be established with the use of six columns.

The constant head device in the first preliminary experiment and part of the second preliminary experiment with sand was a Mariotte siphon. The Mariotte siphon led to problems achieving constant flow in all six columns in the preliminary sand experiments. Therefore, a specially designed constant head device consisting of an inverted carboy over a cylinder with six independent fittings for

tubing was designed and built for use in further experiments.

Column holders were also designed and constructed to be able to run experiments with the soil column in both the horizontal and vertical positions.

3.2 Soil Column Preparation

3.2.1 Preliminary Experiments No.1 and No.2 on Sand

The glass columns were packed with a fine silica sand in the preliminary experiments No.1 and No.2. The sand columns were prepared by pouring dry fine Selkirk silica sand (60-100 mesh) through a funnel and steel mesh apparatus which allowed for uniform packing. The steel mesh apparatus consisted of a 32-cm long 3.5-cm I.D. tube with two mesh screens spaced 3 cm apart at the end of the tube. This is known as the constant kinetic energy packing method. The repeatability of parameters such as bulk density was measured using the % relative standard deviation (% RSD) computed by

$$\%\ RSD = \frac{sample\ standard\ deviation}{sample\ average} \times 100 \qquad (7).$$

After packing, the soil columns had a dry bulk density of 1.59 g/cm^3 (% RSD = 1.36%) in experiment No.1 and 1.60 g/cm^3

(% RSD = 0.75%) in experiment No.2. Using a particle density of 2.65 g/cm^3, the porosity of the sand columns was determined as 40% $(1 - \frac{1.60}{2.65} \times 100)$ which is in the typical range for sandy soils (Freeze and Cherry 1979).

The sand columns were first slowly saturated with distilled and de-aired water to minimize air entrapment before the hydraulic conductivity was measured. In experiment No.2 the sand columns were also flushed with CO_2 gas before wetting to further minimize the possibility of air entrapment. Care was taken to saturate all tubing completely. In the sand experiments, a period of approximately one month elapsed prior to the hydraulic conductivity determination to ensure saturation. In experiment No.1, the hydraulic conductivity was determined by measuring the effluent flow rate when applying a constant hydraulic gradient of 0.5 using a Mariotte siphon. Two Mariotte siphons, one for the electrical columns and one for the hydraulic columns, were used to apply a hydraulic gradient of 0.333 to measure the hydraulic conductivity in experiment No.2. The initial hydraulic conductivities of the sand columns in experiment No.1 and No.2 were determined as 1.70×10^{-5} m/sec (% RSD = 1.35%) and 3.48×10^{-5} m/sec (% RSD = 73.1%) respectively.

3.2.2 Experiment No.3 on Clay

The clay columns in experiment No.3 were prepared by packing the glass columns with a wet soil paste made from reconstituted clay core samples obtained from Manitoba Hydro. The clay core samples were placed in tared 600-mL beakers, weighed, and then oven dried at 105°C to determine their gravimetric water content by using equation (8).

$$w = \frac{(Wt.\ of\ wet\ soil + tare) - (Wt.\ of\ oven\ dry\ soil + tare)}{(Wt.\ of\ oven\ dry\ soil + tare) - (tare)} \quad (8)$$

Samples were allowed to cool in a desiccator after removing from the oven to prevent samples from absorbing moisture from the atmosphere. The volumes of the cylindrical cores were measured to calculate the dry bulk density (mass of solid/volume total). In experiment No.3, the core samples used to prepare the clay columns (Pine Falls: PF012, Sec 'A', S-1, S-3; PF011, Sec 'A', S-3, S-5, S-6, S-7, S-8, Sec 'B', S-5, S-6, S-8) had a gravimetric water content of 49% (% RSD = 19.7%) and a dry bulk density of 1.28 g/cm^3.

After the soil cores were dried, they were ground into particles which would pass through a 60-100 mesh sieve. Soil cores were combined together before a portion was taken to prepare the clay soil columns. Distilled water was mixed with the dry clay particles to make a clay paste with a

gravimetric water content of 80.0%. The clay paste was spooned into the glass columns over the anode mesh. A tamping tool was used to carefully tap the soil down throughout the column packing procedure to minimize air entrapment and allow for uniform bulk density. After packing, the columns were slowly saturated with distilled and de-aired water. Dry bulk density of the soil columns were determined by taking the amount of dry soil added to the columns and dividing by the volume of the soil within the columns. In experiment No.3 the clay columns had a bulk density of 0.84 g/cm^3 (% RSD = 3.56%). Assuming a particle density of 2.65 g/cm^3, the porosity of the clay columns was determined to be 68.3% which is in the typical range for unconsolidated clay soils (Freeze and Cherry 1979). To reduce the possibility of entrapped air, the clay columns were flushed with water for two months prior to measurements. The hydraulic conductivity was determined as 3.31×10^{-9} m/sec (% RSD = 22.0%) by measuring the outflow rate at a constant hydraulic gradient of 2.

3.2.3 Experiment No.4 on Clay

Glass columns were packed with clay similar to experiment No.3 by adding distilled water to the ground Manitoba Hydro clay core samples. However, the distilled

water was mixed with mercuric chloride at a concentration of 500 mg/L to inhibit microbial growth. This is similar to other work which used 38 and 1000 ppm $HgCl_2$ solutions to prevent microbial growth (Fletcher and Kaufman 1980; Foreman et al. 1992). Mercuric chloride was chosen as a microbial growth inhibitor because it effectively prevents microbial growth while causing no physical and chemical changes to the soil (Wolf et al. 1989). In addition, the added mercuric chloride did not lead to any analytical interferences in the determination of hydrocarbon contamination. The added mercuric chloride was equivalent to 180 mg of $HgCl_2$/g of dry soil or 663 mmol/kg of soil. The Manitoba Hydro soil cores used to prepare the clay columns (Pine Falls: PF009, Sec 'B', S-1, S-2, S-3, S-4, S-5, S-6; PF010, Sec 'A', S-1, S-2, S-3, Sec'B', S-1, S-2, S-3) had a bulk density of 1.31 g/cm^3 (% RSD = 15.0%) and a gravimetric water content of 44.4% (% RSD = 27.3%). Distilled water with mercuric chloride was added to reconstituted dry clay particles to a gravimetric water content of 70.0%. The clay paste was packed into the columns similar to experiment No.3 as described in section 3.2.3. The dry bulk densities of the experiment No.4 clay columns were 0.857 g/cm^3 (% RSD = 1.29%). With a particle density of 2.65 g/cm^3, the porosity was calculated as 67.7%. Hydraulic conductivities of the samples were determined after flushing with distilled

and de-aired water for a period of two months to reduce air entrapment. The average hydraulic conductivity of the six columns was determined to be 2.96×10^{-7} cm/sec (% RSD = 42.4%).

3.3 Model Diesel Fuel Composition

A model diesel fuel was developed to determine the efficiency of removing diesel compounds from contaminated soil using electrokinetic remediation with a surfactant. Since diesel fuel is a complex mixture of more than 200 compounds (Block et al. 1991), a simplified diesel fuel was needed to enable the analysis of individual compounds. The complex composition of diesel fuel not only changes between sources but also between shipments which makes the exact chemical description of diesel fuel impossible (Milner et al. 1992). The most abundant (65-85%) compounds found in diesel fuel are normal, branched, and cyclic alkanes (paraffins) (Block et al. 1991). Aromatic compounds represent 10 to 30% of a No.2 diesel fuel (Block et al. 1991). The individual components of diesel fuel which are of environmental and public health concern are the volatile aromatic hydrocarbons and the polycyclic aromatic hydrocarbons (PAHs). The volatile aromatic compounds, benzene, toluene, ethylbenzene, and the xylene isomers

(*para-*, *meta-*, and *ortho-*) (BTEX) have low concentrations in diesel fuel. However, the BTEX compounds are frequent target analytes in environmental investigations due to their carcinogenic or suspected carcinogenic nature (Dineen 1991; Stone 1991). The PAHs, naphthalene, 2-methylnaphthalene, and phenanthrene are most commonly found in diesel fuel and individually pose the highest calculable health risks through ingestion (Dineen 1991). The model diesel fuel was prepared with BTEX and the three common PAHs which pose the most significant environmental and health threat. The chosen compounds were at concentrations in the model diesel fuel representative of their concentrations in a typical No.2 diesel fuel (Milner et al. 1992; Stone 1991). The model diesel fuel compounds along with their concentrations and some of their physical properties are shown in Table 3.1.

The model diesel fuel was prepared by adding the above organic compounds to acetone at the given concentrations. Acetone was chosen as the base solvent because the organic compounds are soluble in acetone and acetone is miscible with water. Hexane was originally tried but hexane's low aqueous solubility (9 mg/L) (Yaws et al. 1993a) led to analysis problems with the solid-phase microextraction technique. The presence of acetone reduced the retardation of other compounds by increasing their aqueous solubilities.

Table 3.1 Composition of Model Diesel Fuel

Compound	Concentration (mg/L)	Solubility (mg/L)*	Specific Gravity*	Mol. Wt.*
benzene	50	1750	0.87	78.11
toluene	500	515	0.87	92.14
ethylbenzene	500	152	0.88	106.17
p-xylene	500	198	0.86	106.17
m-xylene	500	158	0.86	106.17
o-xylene	500	152	0.88	106.17
naphthalene	2000	30	1.15	128.18
2-methyl naphthalene	6000	25	1.01	142.20
phenanthrene	1500	1	1.18	178.24

* From: Knox et al. (1993)

3.4 Experimental Materials

All chemicals were used as received. Benzene and ethylbenzene were purchased from Caledon Laboratories, Inc., Georgetown, Ontario, Canada. Naphthalene (catalog No. 18,450-0), 2-methylnaphthalene (catalog No. M5,700-6), phenanthrene (catalog No. P1,140-9), *p*-xylene (catalog No. 29,633-3), *m*-xylene (catalog No. 29,632-5), and *o*-xylene (catalog No. 29,588-4) were obtained from Aldrich Chemical Company Inc., Milwaukee, Wisconsin, USA. HPLC grade water was purchased from Mallinckrodt, ChromAR®, Paris, Kentucky, USA. Toluene (catalog No. GD-9165) and acetone (catalog No. GD-1050) were obtained from Anachemia, Toronto, Ontario, Canada.

The fibres for the solid-phase microextraction technique were 100-µm polydimethylsiloxane autosampler fibres (catalog No. 5-7301) obtained from Supelco, Bellefonte, Pennsylvania, USA.

Disposable 1-mL syringes were obtained from B-D (Fisher Scientific Co., catalog No. 14-823-2F). Needle tips were B-D precision glide needles, 3.81-cm long, and 25-gauge (Fisher Scientific Co., catalog No. 14-826-49).

The pH 7.00 buffer solution was from Mallinckrodt Specialty Chemical Company (Lot 0098 KMDB) and the 4.63 buffer solution was from Fisher Scientific Company (Lot 704100). Lauryl Sulfate (sodium dodecylsulfate) or sodium salt was from Sigma Chemical Co. (L-5750, Lot 49F0849).

3.5 Micellar Solubilization Experiments

3.5.1 Determination of SDS Micelle-Water Partition Coefficients

The effectiveness of sodium dodecylsulfate in solubilizing toluene, ethylbenzene, and the three xylene isomers can be determined by measuring the SDS micelle-water partition coefficients of the compounds. The SDS micelle-water partition coefficients were measured by adding the hydrocarbon compounds individually to SDS solutions with concentrations ranging from 0, 0.1, 0.23, 0.5, 1.0, 1.5, and

2.0% (w/w) in separatory funnels. The surfactant solutions were prepared by adding 0, 0.25, 0.575, 1.25, 2.5, 3.75, and 5 g of SDS to distilled water in 250-mL volumetrics. The SDS solutions were stirred to obtain a homogeneous solution prior to pouring into the separatory funnels.

In the experiments, 4 mL of each compound was individually added to each of the 250-mL separatory funnels to ensure the formation of free-phase and saturation of the SDS solutions. A separatory funnel containing only distilled water (0% (w/w) SDS) was used to compare determined concentrations to the reported aqueous solubilities of the compounds. After the compound injection, the separatory funnels were shaken occasionally over a period of at least three days and then left without agitation to allow the separation of free-phase from the solution. After equilibration between the hydrocarbon compounds and the SDS solutions was attained, an aliquot of 2.5 mL was taken from the bottom of the separatory funnels and diluted by a factor of 100 and 1000 for analysis. Since the densities of the compounds were all less than that of water, free-phase accumulated at the top of the separatory funnels leaving a saturated solution below. Sample aliquots of 1.4 mL were placed within 2-mL screw-cap vials for SPME-GC-FID analysis to determine the solubility of the organic compounds at the various surfactant concentrations.

The relationship between compound solubility and SDS concentration can be used to determine the MSR and the SDS micelle-water partition coefficients.

3.5.2 Determination of the Effect of Organic Compounds on the Critical Micelle Concentration

The effect of organic compounds on the critical micelle concentration can be determined by measuring the electrical conductivity of different surfactant solutions saturated with organics. The CMC can also be defined as the concentration of micelle at which the rate of increase of electrical conductance with an increase in concentration stabilizes or proceeds at a much lower rate (Peters et al. 1992). Therefore, plotting electrical conductivity against concentration gives two straight lines whose intersection is the CMC (Mukerjee and Mysels 1971). By measuring the electrical conductivity of the solutions saturated with the organic compounds in the micellar solubilization experiments, the effect of organic compounds on the CMC of SDS can be determined.

3.6 Preliminary Experiment No.1 - BTEX in Sand

3.6.1 Experimental Methodology

The first experiment evaluating the efficiency of electrokinetic remediation with a surfactant was conducted using a BTEX-contaminated sand. The experiment applied surfactant flushing to three hydraulic columns and combined surfactant flushing with an electrical potential gradient to three electrical columns. A constant voltage potential of 20 V was supplied to the electrical columns. All columns were flushed with a SDS solution at a concentration of 0.26% (w/w) or 9.0 mmol/L over a period of 15 days. The glass columns were completely filled with sand and no glass beads were placed near the electrodes.

In experiment No.1, the cathode was located at the inflow end of the column causing the electroosmotic flow to counter the hydraulic flow. This set-up was chosen to allow the electrophoretic flow of micelles to move toward the outflow end. A summary of the test conditions for all experiments are given in Table 3.2.

3.6.2 Flow Rate Determination

A constant hydraulic gradient of 0.077 was applied using a single Mariotte siphon. This hydraulic gradient was chosen to allow the slow development of hydrocarbon

Table 3.2 Summary of Test Conditions

Test Description	dh/dx	Voltage Supplied	%SDS (w/w)	Contaminant Injected
Test No.1				6 mL of an
SDS Flushing	0.077[V]	20 V	0.26	equal wt.
with Voltage				BTEX mixture
Test No.2				
Water Flushing	0.333[V]	7.5 V &	0	0.5 mL of
with Voltage		15V		each BTEX
SDS Flushing	0.333[V]	0	0.25	-
SDS Flushing	0.383[V]	7.5	0.25	0.5 mL of
with Voltage			on/off	each BTEX
Test No.3				
Water Flushing	2.0[V]	7.5 V	0	10 mL of
with Voltage	2.6[H]			Model Diesel
SDS Flushing	2.6[H]	7.5 V	1.50	10 mL of
with Voltage				Model Diesel
Test No.4				
SDS Flushing	2.12[H]	20 V	1.50	10 mL of
with Voltage				Model Diesel

[V] = columns in vertical position

[H] = columns in horizontal position

concentration profiles thus increasing the probability of obtaining clear sample results. A cylinder on the outflow tubing of the Mariotte siphon was used to split the tubing six ways for the six soil columns. The flow rate was determined by measuring the amount of outflow collected in 250-mL graduated cylinders over time. After the initial average hydraulic conductivity of the soil columns was determined and prior to hydrocarbon contamination, the soil columns were flushed with surfactant solution to determine the impact of a surfactant on the flow rates in sand.

3.6.3 Voltage Drop and Current Measurement

The measurement of voltage potential gradients and current through the electrical columns was done every 10 min during the test using the data acquisition system. Voltage drops were measured only between the voltage drop ports and, therefore, no voltage drops were measured at the ends of the electrical columns (Fig. 3.3). Since current flow is from negatively charged cathode to positively charge anode (Segall and Bruell 1992), the voltage drops were all positive in this test.

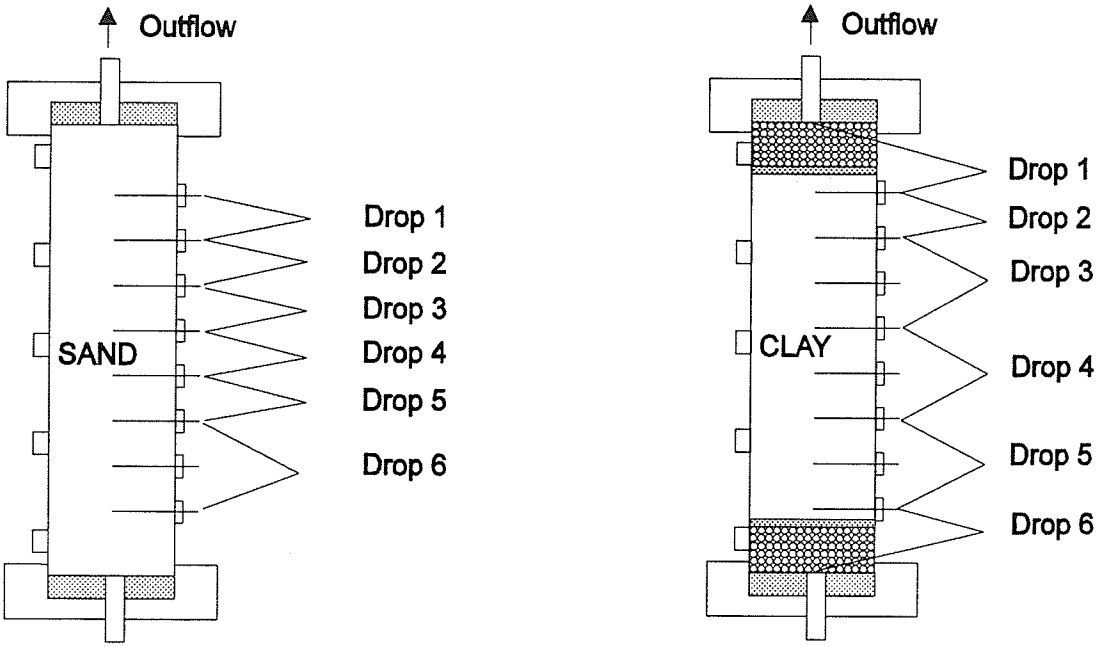

Experiments No.1 and No.2

Experiments No.3 and No.4

Figure 3.3 Experimental set-up for voltage drop measurements.

3.6.4 Hydrocarbon Contamination and Sampling

To determine the efficiency of contaminant removal, 6 mL of an equal weight BTEX mixture was slowly injected into the sampling port closest to the inflow end (2 cm from cathode) in all columns. Sample aliquots of 250 µL were then taken using a 1-mL disposable syringe at various times (approximately every pore volume) from the five sampling ports and effluent to determine the BTEX concentration in the soil columns. The sample aliquots were diluted by a

factor of 1000 with distilled water in a 250 mL-volumetric. A 1.4-mL aliquot was taken from the diluted sample for analysis using an adjustable pipette. Based upon the individual aqueous solubilities of BTEX, a 1000 dilution would ensure that all the compounds went into solution. The 1.4-mL aliquot was placed into a 2-mL screw cap vial sealed with a Teflon-backed silicone septa for SPME-GC-FID analysis. The sampling, if accurate, allows concentration profiles for the BTEX compounds to be determined as a function of time and effluent volume.

3.6.5 Preparation of Surfactant Solution

The 0.26% (w/w) surfactant solution was prepared by first adding 60 g of SDS to 2 L of distilled and de-aired water. The 2-L solution was then stirred overnight to obtain a homogeneous solution before adding to a 23-L glass carboy containing distilled and de-aired water. The 23-L SDS solution was left to equilibrate to ensure complete mixing before use.

3.7 Preliminary Experiment No.2: BTEX in Sand

3.7.1 Experimental Methodology

The second electrokinetic remediation experiment was divided into three parts to allow results for three different sets of test conditions to be determined for the

same sand columns. Part A employed water flushing with an electrical potential gradient to the electrical columns, part B used surfactant flushing only, and part C incorporated surfactant flushing with an applied electrical potential gradient to the electrical columns.

Part A was conducted to determine the effect of electrokinetic remediation using only water as the processing fluid. Three sand hydraulic columns were flushed with water and three sand electrical columns were flushed with water combined with an applied constant voltage potential. A constant voltage potential of 7.5 V was supplied for the first 7 days and then increased to 15 V to 10 days before part B was initiated. The voltage potential was increased during the test to increase the visible effects of electrokinetics. The supplied voltage potential was lower than experiment No.1 to reduce gas production. BTEX was injected into the first sampling port near the inflow end. The electrode configuration was reversed from experiment No.1 with the cathode at the outflow end and the anode at the inflow end. This configuration was chosen to allow electroosmotic flow to act in the same direction as the hydraulic flow and to permit the greater gas production at the cathode to escape through the top of the column.

After 10 days of water flushing, part B of experiment No.2 with surfactant flushing was conducted by

changing the influent to a 0.25% (w/w) SDS solution. The applied voltage to the electrical columns was removed to further evaluate the effect of SDS on the hydraulic conductivity. Surfactant flushing was performed for a period of 8 days.

Part C of experiment No.2 employed flushing with a surfactant combined with an electrical potential gradient in the electrical columns. The columns were once again contaminated with a known amount of BTEX. The electrical potential gradient was applied intermittently (20 min on, 10 min off) to reduce gas accumulation. Surfactant flushing combined with the application of a voltage potential difference of 7.5 V in the electrical columns was carried out for 19 days giving a total time for experiment No.2 as 37 days.

3.7.2 Flow Rate Determination

A constant hydraulic head of was applied to the soil columns using two Mariotte siphons; one for the electrical columns and one for the hydraulic columns. The hydraulic gradient was 0.333 in part A and part B but was increased to 0.75 for 5 hours during surfactant flushing to speed the removal of fines. The hydraulic gradient in part C was 0.383.

There were problems in maintaining a constant flow rate in the columns during the test. Therefore, a new constant head apparatus was designed and built. The new constant head device was incorporated 9 days into the experiment during water flushing with electrical gradient application.

3.7.3 Voltage Drop and Current Measurement

The measurement of voltage potential gradients and current through the electrical columns was done every 10 min during the test. Similar to experiment No.1, voltage drops were measured only between the voltage drop ports. Therefore, no voltage drops were measured at the ends of the electrical columns (Fig. 3.3, page 60). Since the cathode was located at the outflow end, the voltage drops were all negative in this test.

3.7.4 Hydrocarbon Contamination and Sampling

The columns were contaminated by injecting 0.5 mL of each BTEX compound (3 mL total) into the bottom sampling port. A lower amount of BTEX was added in experiment No.2 compared to experiment No.1 to reduce the formation of free-phase and minimize solubility problems in sampling. Contaminant movement was monitored by analysing 1.4-mL aliquots of effluent and from periodic sampling of pore

fluid within the soil column. No dilutions were done on the effluent samples but dilutions of 1000, 10 000, and 100 000 were carried out as necessary for the pore fluid samples following the dilution protocol outlined in section 4.2.

After a surfactant solution had been used to flush the soil columns in part B and the BTEX concentration had been lowered to approximately 1 mg/L, the soil columns were again contaminated by injecting 0.5-mL of each BTEX compound into the sampling port located nearest the inflow end (2 cm from end of column) in each column.

3.8 Experiment No.3: Model Diesel Fuel in Clay

3.8.1 Experimental Methodology

The third electrokinetic remediation experiment with model diesel fuel contaminated clay was performed in two parts. In part A, an electrical potential gradient was applied to the electrical columns and water was used as the influent (water flushing). After 103 days of water flushing, a surfactant was incorporated into the influent and an electrical potential gradient was applied to the electrical columns for 22 days.

Part A, using water flushing combined with an electrical potential gradient for the electrical columns, was applied for a period of 103 days to the clay columns.

The clay columns were contaminated by injecting 10 mL of model diesel fuel into the first voltage port from the inflow end. A constant voltage potential of 7.5 V was supplied to each electrical column.

The influent was changed to a 1.5% (w/w) surfactant solution after approximately four months of water flushing with voltage application. A voltage potential of 7.5 V was constantly supplied to the electrical columns similar to the water flushing section. Surfactant flushing with an electrical potential gradient was applied for a period of 22 days giving the total time for test No.3 as 125 days.

3.8.2 Flow Rate Determination

The hydraulic conductivity of all soil columns in the vertical position was measured by collecting effluent volume in a 100-mL graduated cylinder over time. A constant hydraulic gradient of 2.6 was applied by inverted carboy constant head device. Measurement of hydraulic conductivity in the hydraulic columns was difficult due to the small flow rates.

After 42 days of water flushing the column orientation was changed from vertical to horizontal. The applied hydraulic gradient was 2.12 with the columns in the horizontal position. Switching from the vertical to

horizontal position was needed since the current in the system was higher than anticipated from the results in the experiments with sand. Therefore gas production was also higher than anticipated. A portion of the clay was replaced with glass beads in all the columns to allow gas to escape up and out of the electrical columns at the end sampling ports. The sampling port near the cathode was left open to atmosphere to allow the escape of the produced hydrogen gas. The horizontal position allowed more accurate determination of the hydraulic conductivity and minimized gas accumulation near the electrodes.

The hydraulic conductivities of the hydraulic columns in the horizontal position were measured by the movement of a bubble in the 0.125 cm (1/8") I.D. (cross sectional area 0.07917 cm^2) Nalgene outflow tubing. A bubble was injected with a syringe into the tubing and the distance the bubble moved over a period of time was recorded. Using the inner diameter of the tubing and the distance moved over a period of time, the flow rate could be determined even for the slow flow rates encountered in the hydraulic columns. The hydraulic conductivities of the electrical columns were measured by collecting effluent volume. This method of hydraulic conductivity determination was applied for the electrical columns since the flow rate was greater in the electrical columns and could be measured with available

equipment. In addition, the gas produced by the electrolysis reactions occasionally entered the outflow tube causing confusion in deciding which bubble was to be used for hydraulic conductivity determination. The produced gas also caused air clogging in the tubing. The outflow tubing of the electrical columns was flushed out daily with the column effluent to prevent air bubbles from restricting flow.

The flow rates in part B, with surfactant flushing with an electrical potential gradient, were measured with the same method used in part A.

3.8.3 Voltage Drop and Current Measurement

The measurement of voltage potential gradients and current through the electrical columns was done every 10 min during the test. Voltage drops were measured across the entire soil specimen by connecting the voltage drop wires directly to each electrode at the end of the columns (Fig. 3.3, p. 60). The voltage drops were all negative since the cathode was located at the outflow end.

3.8.4 pH Measurement

The acidity of a solution can be determined by measuring the pH which is equal to the -log {H+} ion

concentration. The instrument used to measure pH was the Corning pH meter 130 with a Corning combination electrode (catalog No. H4333-101). The manufactured specifications give a relative accuracy of ± 0.002 pH, repeatability of ± 0.001 pH over a range of 1 to 14 pH. A saturated KCl solution was used to maintain the electrode fill solution. The instrument calibration was performed with a pH buffer of 7.00 when measuring a solution with a pH close to 7 and with a two point calibration using pH buffers of 4.01 and 7.00 when measuring the pH of highly acidic solutions.

3.8.5 Electrical Conductivity Measurement

The standard method to determine the electrical conductivity is by measuring the electrical conductance which is defined as the inverse of resistance (Gopinath 1994). The electrical conductivity is measured by immersing a conductivity cell in the solution of interest. Electrical conductivity (dS/m) is given by the conductance reading (dS) multiplied by the cell constant of the conductivity cell (1/m). Therefore, the electrical conductivity is given in dS/m. A YSI model 32 conductance meter was used in the measurements.

3.8.6 Hydrocarbon Contamination and Sampling

At the start of both parts, 10 mL of model diesel fuel was injected into the first voltage drop port near the anode at the inflow end (4.5 cm from end of the column). The model diesel was injected slowly over a period of an hour to avoid cracking as well as minimizing the physical disturbance of the clay soil. The injection port was located further from the inflow end of the column than in experiments No.1 and No.2 to reduce the possibility of back diffusion of the contaminants.

One major difficulty encountered in this experiment was the sampling of hydrocarbon contamination from within the clay columns. Pore fluid could not be removed from the clay soil as was done for the sand columns since clay particles clogged the needle of the sampling syringe. To solve this problem, a glass tube was used to create a cylindrical opening within the clay samples at the three middle sampling port locations. No sampling was done at the end sampling ports where glass beads were located. Distilled water was used to fill the openings and left to equilibrate with the surrounding soil before fluid was removed for analysis. Sampling was performed by removing a 200-μL aliquot (or less depending on the amount of fluid able to be withdrawn) of pore fluid and filling up to 1.4 mL in a 2-mL vial using

HPLC grade water. The diluted samples in the vials were taken for SPME-GC-FID analysis to determine the hydrocarbon concentration profiles through the columns during the test.

3.8.7 Destruction of Columns and Extraction of Hydrocarbons

At the completion of experiment No.3, the clay columns were disconnected, sealed at both ends, and chilled to 4°C. The clay was then pushed out from the anode end and sliced into nine segments using dental floss. The nine segments consisted of 2.5-cm long slices at either electrode end and 3-cm long slices from the remaining 21-cm long clay column. The sliced segments were cored with a 2.54 cm (1") diameter glass tube to obtain samples to determine hydrocarbon concentration within the columns by solvent extraction. The cored section was sealed within 25-mL screw cap vials and placed in a deep freezer until extraction was performed.

An extraction procedure was developed to determine the hydrocarbon concentration in the clay samples. The protocol was to place approximately 5 g of clay taken from the clay samples into a tared 25-mL vial with 10 mL of the solvent dichloromethane (DCM). The DCM solvent was chosen because of its solubility in water (19 400 mg/L) (Yaws et al. 1993b) which is necessary for water dilutions needed to perform SPME as well as the high solubility of the model diesel fuel

compounds in DCM. In addition, DCM did not interfere with the acetone chromatographic peak which was desirable. One problem with DCM was the insolubility of SDS in DCM. Therefore, SDS concentration could not be measured in the extracted samples. SDS is also practically insoluble in acetone and ethanol but is moderately soluble in dimethyl sulfoxide (Cheminfo). Dimethyl sulfoxide was not used due to its high health risks associated with absorption through skin and high boiling point which may lead to chromatography problems. Another problem is the inability to separate benzene and DCM chromatographic peaks at low benzene concentrations. Since benzene had the lowest concentration in the model diesel fuel and with the dilutions necessary in the extraction procedure, it is possible that benzene might not have been determined even if another extraction solvent had been used.

After adding 10 mL of DCM to the clay aliquot the 25-mL vial was sealed with a Teflon-lined screw cap to prevent contaminant loss. The sample was then put onto a wrist-action shaker for 150 minutes. A higher agitation time could not be used since the wrist-action shaker overheated with longer extraction times. After shaking, the extract was poured into a 12-mL vial and sealed. The solvent extract was diluted with HPLC grade water by a factor of 100 by taking an aliquot of 100 µL using a 250-µL

adjustable pipette and a 10-mL volumetric flask. Greater dilutions were carried out but there was a loss of resolution in the BTEX chromatographic peaks. The diluted sample was then stirred using a magnetic stir bar until a homogeneous solution with no free-phase was obtained. An aliquot of 1.4-mL was then taken and placed within a 2-mL vial for SPME-GC-FID analysis.

The efficiency of contaminant removal from the clay using the extraction method was determined by analysing various soils contaminated by a known amount. Clay samples were prepared by adding distilled water to the ground clay from Manitoba Hydro cores to a water content similar to the clay columns. Subsamples of approximately 20 g were taken from the prepared clay and put into 25-mL vials. The soil was then contaminated by adding 10, 50, 100, 200, 350, and 500 µL of model diesel fuel. After contamination, the samples were frozen similar to the clay column samples until extraction was performed. Subsample of approximately 5 g were taken twice from the clay samples of known concentration and analysed. The determined concentration of contaminant was divided by the amount of contaminant added to the clay (mg/kg of dry soil) to find the efficiency of removal. The efficiency of removal was determined as 63%, 92%, 78%, 62%, 92%, and 81% for acetone, toluene,

ethylbenzene, *p*-xylene, *m*-xylene, and *o*-xylene respectively. The efficiency of removal was 0.90%, 0.85%, and 0.50% for naphthalene, 2-methylnaphthalene, and phenanthrene respectively. The low recoveries of naphthalene, 2-methylnaphthalene, and phenanthrene indicate that further research should employ a different extraction method to determine the concentration of the PAHs within the soil.

Bulk Density, Water Content, and pH Determination

The remaining portion of the sliced segment was used to determine dry bulk density, gravimetric water content, and *in situ* pH. The pH was measured by placing the pH-electrode in direct contact with the moist clay soil. It is important to note that the pH values measured in soil are not equal to pH values measured in the pore fluid since H+ ions attracted to the clay soil are included in the measurements (Acar et al. 1990b; Hamed et al. 1991; Putnam 1988). Pore fluid pH is generally higher than the *in situ* pH when the pH is acidic and similar pH values are obtained when the *in situ* pH values are basic (Acar and Hamed 1991). The gravimetric water content profile of the clay columns was determined by placing each clay segment on a tared petri dish and weighing the clay sample before and after drying to a constant weight in an oven at 105°C. Dry bulk density was determined by

using the calculated water content to establish the weight of total dry soil in the segment and dividing by the volume of the segment.

3.9 Experiment No.4: Model Diesel Fuel in Clay

3.9.1 Experimental Methodology

The fourth experiment applied surfactant-enhanced electrokinetic remediation to clay columns in the horizontal position contaminated with 10 mL model diesel fuel for a period of 43 days. A constant voltage potential of 20 V was supplied to the electrical columns and the influent was a 1.5% (w/w) SDS solution.

The experimental set-up was modified in this experiment to allow for more accurate flow rate determination in the electrical columns and increased gas venting. With the higher applied voltage and use of a higher SDS concentration in the influent, a higher gas production was anticipated. Therefore, tubing was attached to the end sampling ports above the glass beads in the electrical columns to allow the produced gas to easily escape under the applied hydraulic gradient.

3.9.2 Flow Rate Determination

The flow rates were determined using the same method as for the horizontal hydraulic columns in experiment No.3. A constant hydraulic head of 2.12 was used for the duration of the test. The more accurate flow rate measurement could now be applied to both the electrical and hydraulic columns since the modified experimental set-up allowed the gas to escape through the tubing located at the end sampling ports in the electrical columns.

3.9.3 Voltage Drop and Current Measurement

The measurement of voltage potential gradients and current through the electrical columns was done every 30 min during the test. Voltage drops were measured across the entire soil specimen by connecting the voltage drop wires to the electrodes (Fig. 3.3, page 60). The voltage drops were all negative since the cathode was located at the outflow end.

3.9.4 Hydrocarbon Contamination and Sampling

At the start of the test 10 mL of the model diesel fuel was injected into the second sampling port from the anode (inflow) end (8.5 cm from the end of the columns). The model diesel fuel was injected further from the column end

to try to prevent back diffusion of the hydrocarbons into the influent reservoir.

During injection of the model diesel fuel, the glass column F cracked and broke. Therefore, column F was not included in determining the average hydrocarbon concentrations in the hydraulic columns.

3.9.5 Destruction of Columns and Extraction of Hydrocarbons

Upon completion of the test, the soil columns were disconnected, sealed at both ends to prevent contaminant loss, and stored at 4°C. The columns were removed individually and then the clay was pushed out from the anode end and separated into nine segments similar to experiment No.3. A core of each section was again taken for hydrocarbon analysis and the remaining sample was used for pH, water content, and bulk density determination.

Hydrocarbon extraction was performed according to the same method outlined in experiment No.3 except the solvent extract was diluted by both 100 and 200 by taking 100- and 50-µL aliquots and then adding up to 10 mL with HPLC grade water using 10-mL volumetric flasks. The hydrocarbon concentration was determined by performing SPME-GC-FID analysis on a 1.4-mL aliquot taken from the two dilutions and averaging the results.

4.0 SPME-GC-FID Analysis

4.1 Introduction

Solid-phase microextraction (SPME) with gas chromatography (GC) coupled with a flame ionization detector (FID) was used to determine hydrocarbon concentration and monitor the movement of organic compounds in the soil columns. SPME is a relatively new, fast, simple, inexpensive, and solvent-free extraction method which is easily automated for the determination of hydrocarbon compounds in water (Arthur et al. 1992a; Arthur et al. 1992c; Chai et al. 1993; Louch et al. 1992; Shirey et al. 1993).

Solid-phase microextraction utilizes a fibre coated with an organic phase such as polydimethylsiloxane to extract organic compounds from aqueous samples. The fibre is contained within a syringe-like assembly to protect the fibre between extractions. During extraction, the fibre is exposed directly to the sample or to the headspace over the sample allowing a portion of the analyte to partition from the water to the fibre (Fig. 4.1). After a period of time during which the fibre sorbs the analyte(s), the fibre is removed from the sample and inserted into the injection port of a gas chromatograph (GC). The contaminants are then thermally desorbed and analysed. The samples are quantified by relating detector response to the response of calibration standards.

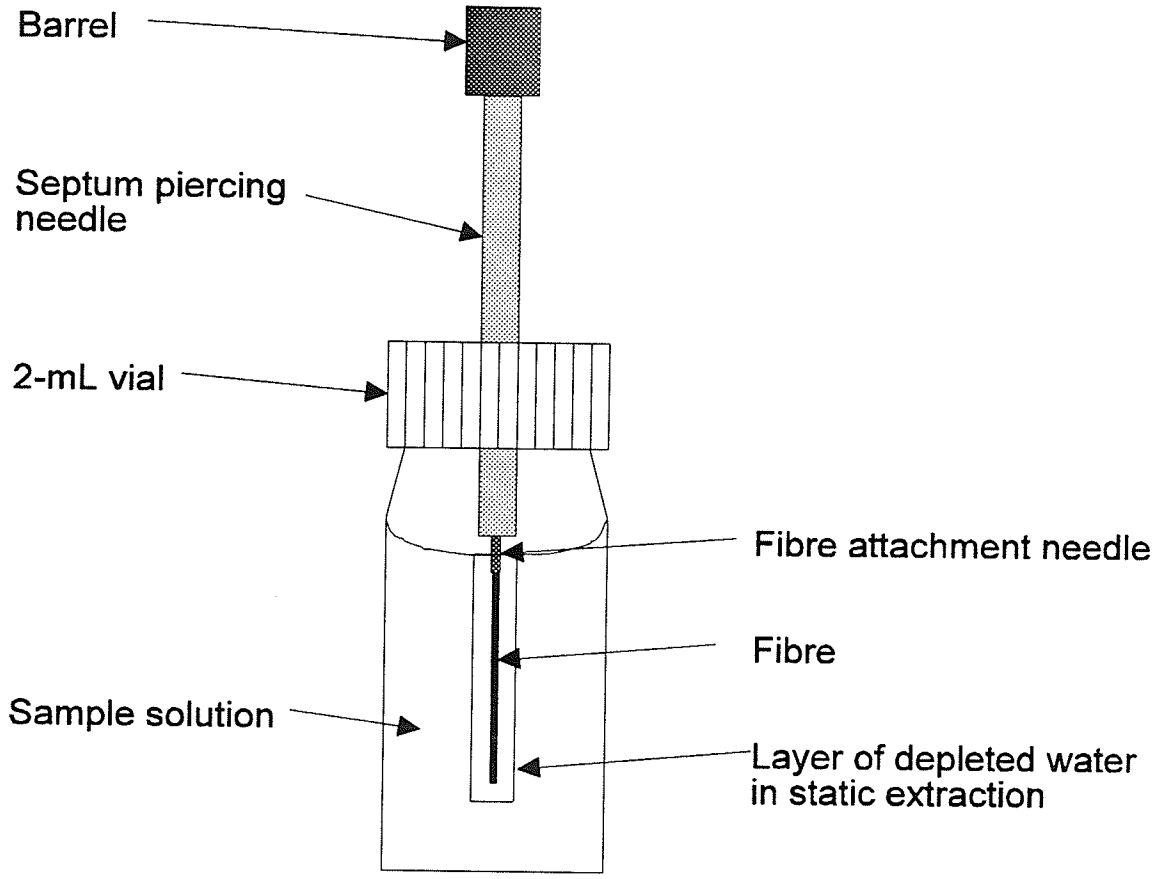

Figure 4.1 Sample vial with SPME fibre during extraction.

A linear relationship exists between the amount of analyte sorbed to the stationary phase and the concentration of the analyte in the sample (Arthur et al. 1992a; Louch et al. 1992; Potter and Pawliszyn 1992; Sarna et al. 1994). The amount of analyte sorbed, represented by the number of moles sorbed by the fibre (n_{mol}) has been shown to be affected by three major factors: (1) the distribution constant of the analyte (K), (2) the volume of the

stationary phase on the fibre (V_s), and (3) the concentration of the analyte in the aqueous phase (C_w). This relationship can be expressed mathematically as

$$n_{mol} = K V_s C_w \quad (9).$$

At equilibrium between the analyte and the fibre, the amount of analyte sorbed is at a maximum. The linear relationship between the analyte concentration and the detector response ranges over several orders of magnitude (Arthur et al. 1992a; Louch et al. 1992; Potter and Pawliszyn 1992). However, all analytes must be in solution to ensure that there is a linear relationship between the detector response and the quantity of analyte in the sample.

4.2 Dilution Protocol

4.2.1 Introduction

Previous research has developed an understanding of how chromatographic and chemical factors affect SPME (Arthur et al. 1992a; Arthur et al. 1992b; Arthur and Pawliszyn 1990; Arthur et al. 1992c; Buchholz and Pawliszyn 1993; Chai et al. 1993; Louch et al. 1992; MacGillvray and Pawliszyn 1994; Potter and Pawliszyn 1992; Potter and Pawliszyn 1994; Sarna et al. 1994; Zhang and Pawliszyn 1993). However, previous research with SPME has focussed on the determination of sub-milligrams-per-litre levels of BTEX to establish the

limits of detection. The maximum reported BTEX concentration determined by SPME which fit the linear response range was 3 mg/L (Arthur et al. 1992b). However, remediation projects typically encounter both high and low concentrations of hydrocarbons. In order to use SPME to analyse environmental samples containing free-phase or high concentrations of BTEX, samples must be diluted because of solubility and linear response problems. Using the dilution protocol described in the next sections, environmental samples containing free-phase or high concentrations of BTEX and PAHs samples containing free-phase or high concentrations of BTEX can be analysed with the automated SPME-GC-FID analysis method.

The effects of mixtures of organic compounds on the aqueous solubility of individual organic compounds play an important role in the preparation of high-concentration standards and dilution of high-concentration samples. In any environmental remediation project, contamination seldom involves a single compound, and analysis is often required for many compounds. It is crucial to keep in mind that the aqueous solubility of a single BTEX compound is significantly decreased with the addition of other BTEX compounds (Sanemasa et al. 1987). This decrease in aqueous solubility lowers the maximum concentration of standards that can be used for quantification with SPME. Information concerning the aqueous solubilities of organic compounds in

complex mixtures is limited (Sanemasa et al. 1987). However, Raoult's Law has been shown to predict the equilibrium aqueous concentrations of aromatic organic hydrocarbons in miscible two-compound mixtures (Lane and Loehr 1992; Sanemasa et al. 1987). Using Raoult's Law, the aqueous solubility of a compound in a complex mixture (S_i) can be predicted by multiplying the mole fraction of the compound in the mixture (X_i) by its individual aqueous solubility (S_{wi}) as described by

$$S_i = X_i S_{wi} \qquad (10).$$

To ensure an accurate determination of BTEX in a sample using SPME-GC-FID analysis, analyte concentrations should remain below their aqueous solubility limits to preclude the formation of a free-phase. It is more convenient to prepare standards as a mixture rather than as individual compounds to reduce the analysis time on the gas chromatograph. For example, one could prepare a 10 mg/L standard for each BTEX compound individually resulting in six analyses to be done or one analysis of a BTEX standard containing 10 mg/L of each compound. However, solubility problems may be encountered for the analysis of complex mixtures. These solubility problems can be avoided considering that Raoult's Law can be used to predict the maximum concentration of the BTEX mixture.

The effect of a co-solvent influences the dilution and analysis of environmental samples containing free-phase or high concentrations of BTEX. One difficulty in analysing high concentration samples with solid-phase microextraction using a polydimethylsiloxane fibre is the limitation of 1% organic co-solvent in the sample (Arthur et al. 1992a). It has been shown that the accuracy of SPME is unaffected by organic co-solvent concentrations at or below 1% (Arthur et al. 1992a). However, as the co-solvent concentration increases, the distribution constant decreases, and less analyte is taken up by the fibre. Therefore, the 1% organic co-solvent limit restricts the ability to significantly increase analyte solubility with the addition of a co-solvent. Data available on aromatic solubility in miscible solvent/water mixtures is limited (Fu and Luthy 1986) and the solubility effect of 1% co-solvent in the sample can be confusing. For example, a linear semi-log relationship between naphthalene solubility and percentage of acetone in an acetone/water mixture shows that the solubility of naphthalene increased slightly from 30.9 mg/L to 33.2 mg/L with 1% acetone in solution (Fu and Luthy 1986). In contrast, the aqueous solubility of naphthalene, phenanthrene, and pyrene has been reported to be enhanced by ≈20-30% relative to their aqueous solubilities when 1% methanol is included in the solution (Edwards et al. 1991c).

This confusion in the significance of the effect of a 1% co-solvent can be minimized by restricting the maximum concentration that can be analysed with SPME to the aqueous solubility of the compound. The 1% co-solvent concentration limit also forces the dilution of free-phase or high concentration samples to be performed in two steps. The first step is to add a sufficient amount of co-solvent to increase the solubility of the analytes and achieve a single phase sample. The second step is to dilute the single phase sample with distilled water by at least a factor of 100 to keep the solvent concentration at or below the 1% concentration limit. To avoid the formation of free-phase, the second dilution must also ensure that all analytes are below their aqueous solubility limits as indicated by Raoult's Law. The effects of co-solvency and complex mixtures on solubility can be minimized by diluting the sample well below the aqueous solubility limits to ensure all the analytes are in solution prior to analysis.

The main objectives of the dilution protocol experiments were to (1) test the applicability of using Raoult's Law to predict the aqueous solubility in the complex six-compound BTEX mixture; (2) identify the concentration limit at which equally weighted BTEX mixture standards could be prepared for SPME without affecting the linear relationship between concentration and detector

response; and (3) develop a protocol for accurately diluting free-phase or high concentration BTEX samples. The development of this protocol would allow the relatively fast, simple, and cost-effective automated SPME-GC-FID analysis method to be used in remediation projects where samples contained free-phase or high concentrations of BTEX.

4.2.2 Solubility of BTEX Mixtures

The aqueous solubilities of the BTEX compounds, when combined in a mixture, were found by injecting 1 mL each of the BTEX compounds into two replicate separatory funnels containing 250 mL of distilled water. The separatory funnels were shaken occasionally over three days to ensure equilibration and then left two days without shaking to allow separation. The lighter BTEX compounds that were not in solution accumulated at the top of the separatory funnel and a saturated solution of BTEX compounds was left in the remainder of the separatory funnel. An aliquot of 2.5 mL was removed from the bottom of the separatory funnels and diluted by 0, 10, and 100 with 0, 25, and 250 mL of distilled water in volumetrics. Replicate 1.2 mL aliquots were taken from the samples and put into 2-mL vials with silicone Teflon-backed septa for analysis by gas chromatography with an autosampler modified for SPME.

4.2.3 Testing Linear Response Limits

The limit of the linear response was estimated by analysing high concentration BTEX standards in water prepared by diluting solutions of 20 000, 10 000, and 1000 mg/L BTEX prepared in acetone and 5000 mg/L BTEX made up in methanol. These solutions were diluted to a range of standards from 200 to 0.01 mg/L with a maximum co-solvent concentration of 1%. Three replicate aliquots of 1.2 mL were taken from the prepared standards and put into 2-mL vials for GC analysis.

4.2.4 Dilution Experiments

The first step in diluting a sample containing free-phase BTEX was to add sufficient organic co-solvent such as acetone to ensure that all the analytes were in solution. Acetone was chosen because BTEX is miscible with acetone and acetone is miscible with water. Methanol could also be used since it has similar properties. The amount of solvent needed depended on the concentration of BTEX which was originally unknown in the sample. However, it was better to err on the side of diluting more rather than less to ensure that all compounds were in solution. In addition, with the low detection limits accessible through SPME-GC-FID, excess dilution was not expected to significantly decrease the accuracy of BTEX determination.

In this study, a BTEX mixture containing equal weight fraction of each BTEX compound was used to represent the free-phase sample (i.e., 0.167 g of each compound was in 1 g of the BTEX mixture). A sample of 250 µL of the BTEX mixture was added to five different volumes (1.0, 2.5, 5.0, 10 and 25 mL) of acetone using 1-mL disposable syringes. These five samples were diluted by combining 250 µL subsamples from each of the solutions with 25 and 250 mL of distilled water in volumetrics. This represented a second dilution factor of 100 and 1000 respectively. The samples were then vigorously shaken for 2 min before aliquots were taken for analysis. The final concentrations for each of the BTEX compounds in the 10 samples were 15, 37, 73, 147, 366 mg/L with the second dilution factor of 100 and 1.5, 3.7, 7.3, 14.7, and 36.6 mg/L with the second dilution factor of 1000. Replicate aliquots 1.2 mL were removed from the volumetric flasks using a pipette and placed within 2-mL screw cap vials with silicone Teflon-backed septa for GC analysis.

Standards

Standard solutions were prepared to quantify the results. Standards of 10, 5, 1, and 0.1 mg/L were prepared in HPLC grade water by diluting a 1000 mg/L BTEX solution

prepared in acetone. Replicate aliquots of 1.2 mL were placed in 2-mL screw-cap vials with rubber Teflon-backed septa for GC analysis.

Standard solutions of individual BTEX compounds were also run to check for the effects that mixtures might have on the SPME extraction process. Separate standard solutions containing 1000 mg/L benzene, toluene, ethylbenzene, *p*-xylene, *m*-xylene, and *o*-xylene were diluted to standards of 10, 1, and 0.1 mg/L for GC analysis.

4.2.5 Results of the Solubility of BTEX Mixtures Experiment

The results of the separatory funnel experiments showed that the aqueous solubilities of BTEX compounds in a mixture were much lower than the individual aqueous solubilities of the BTEX compounds. Considering the six-compound complex mixture to follow Raoult's Law, the mole fraction of the analyte in the mixture multiplied by the individual aqueous solubility was expected to give a good prediction of the mixture solubility (Lane and Loehr 1992; Sanemasa et al. 1987). This prediction was shown to be true for the complex mixture for all six BTEX compounds (Table 4.1). Therefore, the aqueous solubilities of BTEX compounds in complex mixtures can be predicted using Raoult's Law. The aqueous solubilities of the six BTEX compounds in an equal weight

mixture were approximately one-sixth their individual aqueous solubility. Therefore, to ensure that all the compounds are in solution, the maximum BTEX standard concentration recommended for equal weight mixtures is 25 mg/L.

Table 4.1 Mixture Solubility Experiment Results

BTEX Compound	Aqueous Solubility (mg/L)*	Mole Fraction	Predicted Solubility in Mixture (mg/L)	Measured Solubility in Mixture (mg/L)
benzene	1750	0.211	369	349.0
toluene	515	0.176	91	78.7
ethyl benzene	152	0.153	23	25.3
p-xylene	198	0.152	30	21.0
m-xylene	158	0.153	24	21.0
o-xylene	152	0.155	24	22.3

* From: Knox et al. (1993)

Note *p*- and *m*-xylene not separable on the DB5 column and, therefore, values shown are half of the combined GC-FID results.

For unequally weighted BTEX concentrations, if the changes in mole fraction are taken into account, Raoult's Law could still be used to predict the solubility of the compounds. Therefore, the effects of unequally weighted BTEX concentrations would be similar to the effects of equal weight BTEX concentrations. For example, when the concentration of benzene is greater than other BTEX compounds in the sample, its mole fraction increases and therefore the apparent solubility of benzene increases. The mole fractions of the other compounds in the sample decrease leading to a decrease in their apparent solubilities. Calculations of aqueous solubility are more difficult with unequally weighted BTEX concentrations and with a greater number of compounds in the mixture. However, Raoult's Law is still applicable to these complex mixtures. In order to ensure that the analyte is in solution, the measured concentration must be less than the solubility predicted by Raoult's Law.

4.2.6 Results of Testing for Linear Response Limits

Separate linear relationships were determined for the results of the standards concentrations 10 mg/L and lower and for all of the standard concentrations from 0.01 to 200 mg/L using the least-squares technique (Draper and Smith

1981; Neter et al. 1985). The linear regression models originally included an intercept term but statistical analysis indicated that the intercepts were not different from zero at the 1% significance level. Consequently, the data was fitted without an intercept term. In addition, F tests indicated that a linear model significantly accounted for the variance in the data and, therefore, more complicated nonlinear models were not fitted to the data. The fitted regression lines indicated that a linear line fitted through the 10 mg/L and lower concentration standards gave a more linear response (higher r^2 value) than a linear line fitted through all the data except for the more water-soluble benzene (Fig. 4.2). The distribution of the three replicates at higher concentrations indicates that the error variance increased with increasing concentration above 10 mg/L. Therefore, as concentration increased above 10 mg/L the accuracy of the BTEX determination decreased. A comparison of the slope of the regression line fitted through the 10 mg/L and lower concentrations to the slope of the regression line fitted through all the data indicated that the slopes were statistically significantly different for each compound except for the more water-soluble benzene. The results indicate that if the concentration of the sample is above 10 mg/L the samples should be quantified with a different slope than the lower concentration samples. The

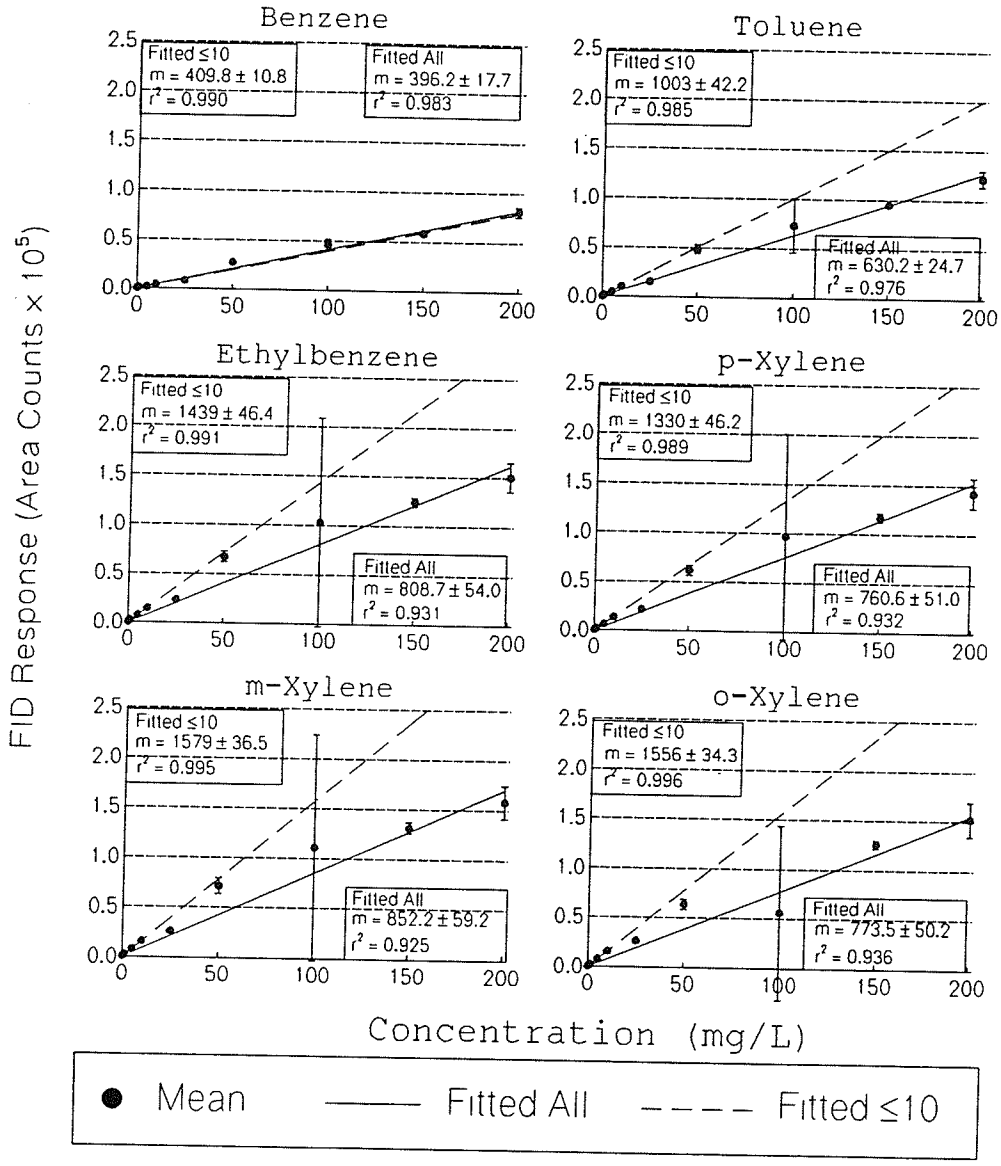

Figure 4.2 Standard results showing the regression lines fitted through the 10 mg/L and lower concentrations and all the standards. The 95% confidence interval is given with the slope (m) and is indicated on the sample points with error bars. The regression line in the 10 mg/L and lower standards gave higher r^2 values than the regression line fitted through all the data. No difference was found for the more water-soluble benzene.

aqueous solubility limits predicted by Raoult's Law for ethylbenzene and the xylenes correspond well with the decrease in the linear response of the high concentration standards. Therefore, the decrease in linearity in the higher concentration standards was attributed to compounds no longer being in solution. Chromatography limitations were not expected to cause the decrease in linearity since the 5-min extraction and 2-min desorption times used allow equilibration between the BTEX and the fibre and ensure complete desorption of BTEX from the fibre at BTEX concentrations below 0.850 µg/µL (Sarna et al. 1994). Any BTEX not desorbing from the fibre would not be sufficient enough to cause the lower detector response. In addition, if the fibre's capacity was limiting the results, the reduction in linearity would also be shown for benzene. The results of the analysis of the higher concentration standards show that the concentrations should be kept below 25 mg/L for equal weight BTEX mixture standards to ensure a good linear response and accurate BTEX determination.

4.2.7 Comparison of Individual BTEX Standard Results to BTEX Mixture Standards

The results for individually run BTEX compound standards were very similar to the results from the analysis

of standard BTEX mixtures. Since there were no effects of complex mixtures on SPME, standards having mixtures of BTEX compounds with concentrations below aqueous solubility limits could be analysed more cost effectively compared to the separate analysis of individual standard compounds.

4.2.8 Results of Dilution Experiments

Measured concentrations of the dilution samples were determined from an average of two replicate aliquots from each dilution. If the BTEX determination was accurate, the measured concentrations should plot directly on a line with a unity slope on a graph of measured concentration against predicted concentration. The results show that the samples from the second dilution of 1000 gave deviations from the expected results in the 36.6 mg/L sample and the samples from the second dilution of 100 gave deviations from expected in the samples above 73 mg/L (Fig. 4.3). In the samples from the second dilution of 100, more accurate results were obtained in the 15 mg/L samples compared to the higher concentration samples. The measured concentrations were slightly higher than the predicted concentrations due to higher volatile losses in the standards compared to the dilutions samples. It is important to note that the difference between the two replicate samples from each dilution sample was much larger in the 36.6 mg/L and higher

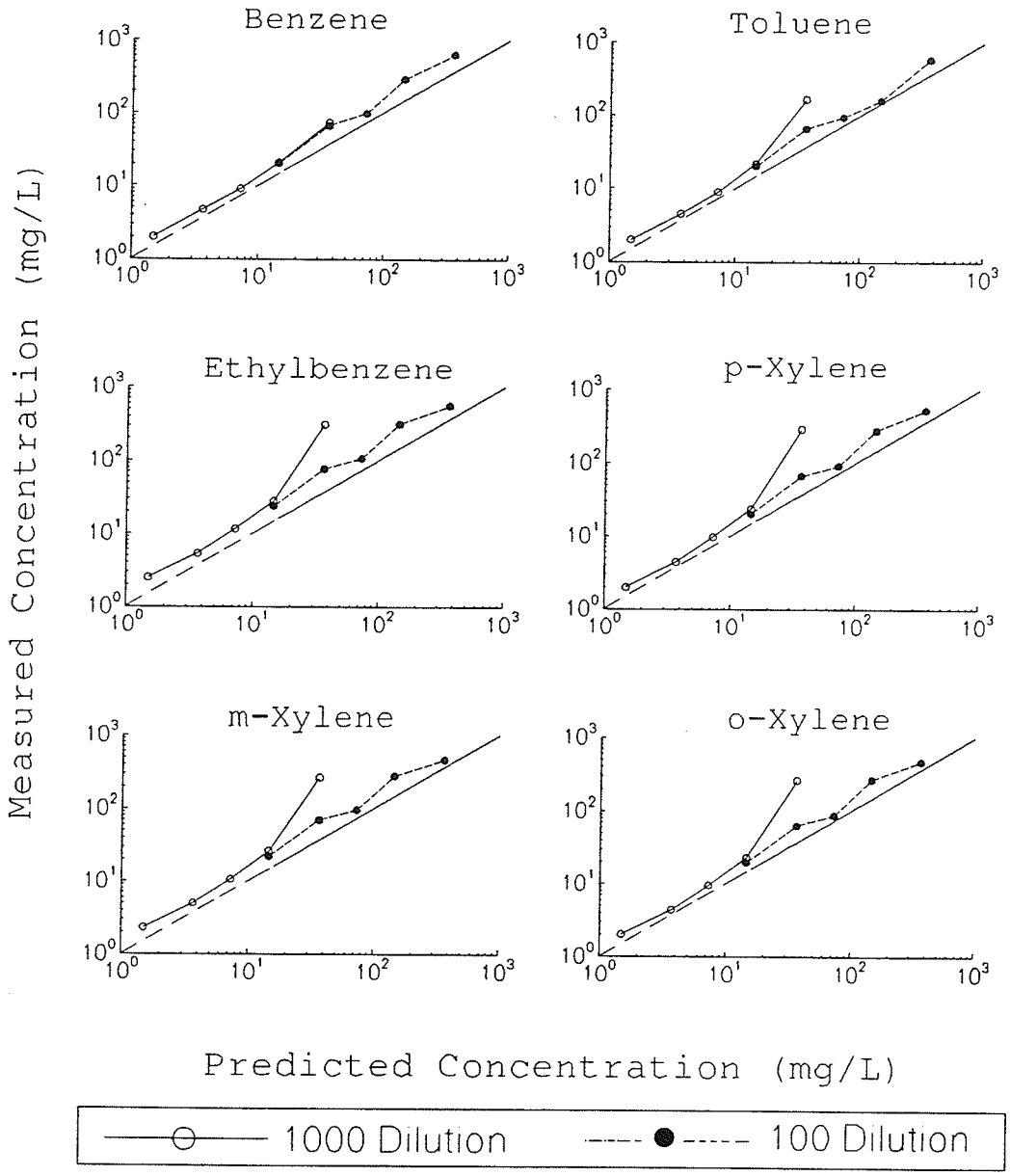

Figure 4.3 Dilution method results for each of the BTEX compounds. Deviations from expected results are indicated by the proximity to the unity line. The large deviation in the 36.6 mg/L sample from the second dilution of 1000 is attributed to the formation of a free-phase in the sample at this concentration.

concentration samples compared to the samples having concentrations below 36.6 mg/L. In addition, the replicates in all the dilution samples indicated that the BTEX compounds with lower solubilities had a higher difference between replicates than the higher solubility compounds.

The lower precision of the results between replicates and the lower accuracy at the higher concentrations suggest that solubility problems are limiting the results. The deviation of the measured concentration from the predicted concentration indicates that the dilution of high concentration samples gives more accurate results when the final concentrations of the BTEX compounds were ≤25 mg/L. Also, the more accurate results in the 37 mg/L sample obtained from the second dilutions of 100 compared to the 37 mg/L sample from the second dilution of 1000 indicates that a higher percentage of acetone (1% compared to 0.1%) can help increase the solubility of the BTEX compounds and improve the accuracy of BTEX determination at higher concentrations. The 0.1% acetone in the 37 mg/L sample from the second dilution of 1000 is not large enough to keep the BTEX compounds in solution at this concentration. These results indicate a final dilution sufficient to reduce the BTEX concentration below their aqueous solubility as indicated by Raoult's Law is necessary for accurate analysis. The second dilution should be by a factor of 100

to give 1% acetone in solution which will not significantly affect the distribution coefficient of the compound but will improve accuracy of the determination of BTEX when the concentrations are close to their aqueous solubilities.

A real sample with unknown initial concentrations should be diluted with a sufficient amount of acetone to solubilize all the free-phase BTEX in the sample. A second dilution by at least a factor of 100 should be performed to keep the maximum organic concentration below 1%. After the concentration of BTEX is determined from SPME-GC-FID analysis, a check should be made to ensure that the measured concentration is not larger than the solubility predicted by Raoult's Law. If the analyte concentration determined is above the solubility predicted by Raoult's Law, a greater second dilution is necessary to ensure that all BTEX compounds are in solution.

4.3 Vibration-Enhanced SPME of Hydrocarbons in Water

4.3.1 Introduction

The demand for a fast and efficient analytical method to determine hydrocarbon concentration has increased due to the growing environmental concern over hydrocarbon contamination of soil and groundwater. Solid-phase microextraction has been shown to be a fast, simple, and

inexpensive method for analysing organic compounds in water (Arthur et al. 1992b; Arthur et al. 1992c; Chai et al. 1993; Louch et al. 1992; Shirey et al. 1993). However, without sample agitation, the amount of organic compound extracted is limited by the rate of diffusion of the compound through water (Louch et al. 1992). To overcome this limitation and to improve the SPME method, an innovative sample carousel agitation device (SAMCAD) was designed and built to vibrate the sample carousel of a Varian 8200 autosampler. Sample agitation provided by the SAMCAD increases the efficiency of SPME by increasing the amount of analyte extracted over a period of time prior to equilibration between the compound and the fibre. Vibration-enhanced extraction leads to a reduction in equilibration time and improvement in the limits of detection.

The time required to reach equilibrium can be decreased with agitation, temperature, and chemical changes. Without agitation, the contaminants must diffuse across a static layer of water surrounding the fibre in order to come into contact with the coating on the fibre (Louch et al. 1992; Zhang and Pawliszyn 1993) (Fig. 4.1, p. 79). For compounds which have high distribution constants, the static water layer at the fibre/solution interface can significantly limit the rate of sorption by the fibre. The higher the distribution constant the greater the amount of analyte that

must pass through the static water layer to reach the fibre (Louch et al. 1992; Zhang and Pawliszyn 1993). Stirring a sample solution using a magnetic stir bar within the sample has been shown to increase the amount of analyte that can be sorbed over a specific period of time leading to a reduction in equilibration time (Arthur et al. 1992a; Arthur et al. 1992b; Arthur et al. 1992c; Louch et al. 1992; Zhang and Pawliszyn 1993). Samples that are stirred attain the maximum sorption in a shorter time compared to unstirred samples for both liquid and headspace extractions (Zhang and Pawliszyn 1993). In addition, when equilibrium has not been reached, increasing the temperature of the sample can increase the rate of diffusion through water and lead to an increase in the amount of analyte sorbed by the fibre (Arthur et al. 1992a). Higher temperatures reduce equilibration time in headspace analysis by increasing Henry's constants (Zhang and Pawliszyn 1993). Reducing the volume of headspace during headspace extraction also lowers equilibration time by reducing the distance that a compound must diffuse across to reach the fibre (Zhang and Pawliszyn 1993). Saturating a sample with salt and lowering pH are other methods that can be used to increase the response (Arthur et al. 1992a; Buchholz and Pawliszyn 1993).

The SAMCAD is an innovative and simple apparatus which works with a Varian 8200 autosampler to provide sample

agitation. The SAMCAD consists of a vibrating mechanism which agitates the samples in the autosampler carousel when the SPME fibre is in the extraction position. The vibration on/off time is controlled by two optical sensors mounted on the autosampler to ensure agitation only takes place when the fibre is exposed to the sample. The optical sensors as well as an external power supply are used to control the SAMCAD to ensure consistent vibration.

The SAMCAD provides many improvements over current agitation techniques. The SAMCAD requires no sample modification such as the insertion of magnetic stir bars which may expose the samples to contamination and cause possible loss of volatile compounds. Compared to other agitation techniques such as sonification which require expensive equipment (Zhang and Pawliszyn 1993), the SAMCAD provides improved extraction efficiency at a much lower cost. The SAMCAD is also easily incorporated with automated extraction and can provides consistent agitation that can improve the response of SPME for all samples in the autosampler carousel.

The main objective of the research using the SAMCAD was to compare the standard static extraction method to the effects of vibration-enhanced extraction. To meet this objective, sorption profiles and calibration curves were obtained for both static and vibration-enhanced extraction

for benzene, toluene, ethylbenzene and the xylene isomers (BTEX), three polycyclic aromatic hydrocarbons (PAHs) (naphthalene, 2-methylnaphthalene, and phenanthrene), and acetone.

4.3.2 Static and Vibration-Enhanced Extraction Sorption Profiles

Vibration-enhanced and static equilibration curves were developed for BTEX, naphthalene, 2-methylnaphthalene, phenanthrene, and acetone. A standard solution containing 1000 ppm each of the BTEX and PAH compounds was prepared in acetone. This standard solution was diluted by a factor of 5000 using HPLC grade water to obtain a solution containing 0.5 mg/L of the BTEX and PAH compounds. Six aliquots of 1.4 mL each were taken at the same time from the 0.5 mg/L solution and placed in 2-mL screw cap vials with Teflon-backed silicone septa for GC analysis with either static or vibration-enhanced SPME. To obtain the sorption profiles for the compounds, the samples were run in triplicate at extraction times of 1, 3, 5, 15, and 30 min for both static and vibration extraction.

The results of the sorption profiles indicated a significantly higher response in the samples that were extracted with vibration compared to samples with static

extraction for both the BTEX and PAH compounds (Fig. 4.4 and 4.5). The error bars in the figures indicate 95% confidence interval. The vibration-enhanced extraction gave a significantly higher response than static extraction for 5, 15, and 30 min extraction times for all compounds except benzene, toluene, and acetone which reached equilibrium within the 30 minute extraction time. No significant increase was found for acetone. It is important to note that the vibration-enhanced extraction of benzene and toluene reached equilibrium faster than the static extraction as indicated by the levelling off of the sorption profile at a shorter time (Fig. 4.4). This trend of reduced equilibration time with vibration-enhanced extraction should be apparent if extraction times were extended to equilibrium for the other compounds. The higher distribution constants for the other compounds can explain the increased equilibration time. Sample agitation with stirring has not been found efficient enough to allow all BTEX compounds to reach equilibrium in a few minutes (Arthur et al. 1992a). However, since the GC analysis run time is greater than the extraction time, the extraction can be performed during the gas chromatographic runs without increasing analysis time. In addition, equilibration need not be reached as long as calibration is performed using the same extraction time.

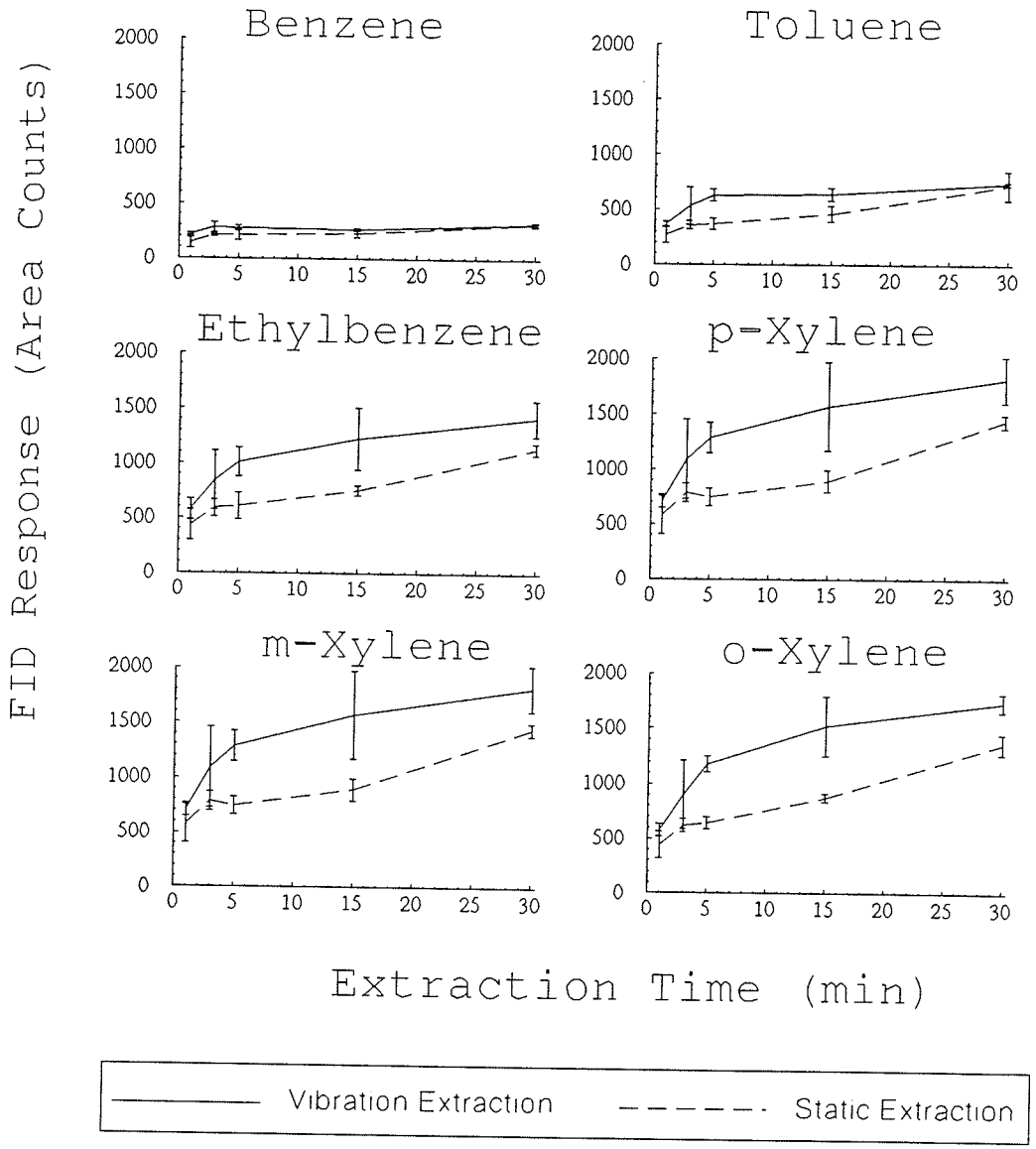

Figure 4.4 Comparison of static and vibration-enhanced extraction sorption profiles for BTEX with the 95% confidence limits indicated by error bars.

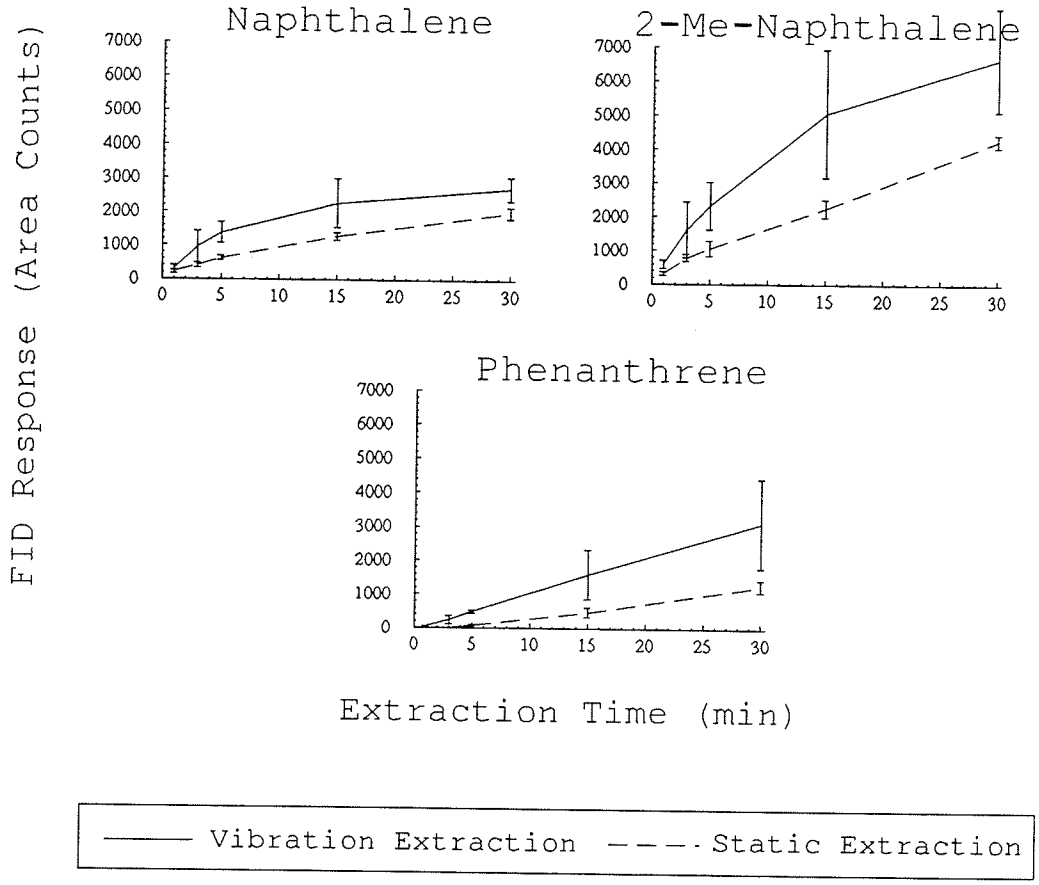

Figure 4.5 Comparison of static and vibration-enhanced extraction profiles for naphthalene, 2-methylnaphthalene, and phenanthrene with the 95% confidence limits indicated by error bars.

The percent increase in response of vibration-enhanced extraction over static extraction was calculated by

$$\%\ increase = \frac{average\ vibration\ value - average\ static\ value}{average\ static\ value} \times 100 \quad (11).$$

The average % increase in detector response for all extraction times was 44.0% and 163.7% for the BTEX and PAH compounds respectively (Table 4.2). Detector response was observed for phenanthrene at 1 and 3 min vibration-enhanced extraction but not at 1 and 3 min for static extraction. The equilibration curves with the agitation provided by the SAMCAD improved the sensitivity of SPME and lowered the limits of detection for the three PAHs. Therefore, the SAMCAD allows determination of trace concentrations for analytes having low distribution constants.

Table 4.2 % Increase in Vibration-Enhanced Extraction Response over Static Extraction for the Sorption Profiles

Compound	1 min	3 min	5 min	15 min	30 min
acetone	4.8	12.9	-16.6	21.0	2.3
benzene	56.4	33.4	27.9	15.1	-0.4
toluene	37.3	48.1	71.7	38.0	2.0
ethylbenzene	32.8	43.4	66.6	63.3	24.3
p-xylene	25.1	44.3	80.7	80.2	34.4
m-xylene	22.2	38.9	72.3	75.8	26.1
o-xylene	31.1	45.2	82.9	74.0	27.6
naphthalene	33.9	136.2	122.6	77.2	35.0
2-Me-naphthalene	88.2	108.3	120.7	123.9	56.0
phenanthrene	-	-	545.5	238.5	148.1

The precision of the results was measured using the percent relative standard deviation value. The average % RSDs for the selected PAHs were 30.4% and 12.3% for vibration-enhanced and static extraction respectively (Fig. 4.6). The average % RSD values for both the static and vibration extraction data are higher compared to the approximate 5% relative standard deviation found in previous work (Arthur et al. 1992a; Potter and Pawliszyn 1992). However, % RSD values of 10% and 20% have been reported for PAHs and polychlorinated biphenyl respectively using a 15-μm polydimethylsiloxane fibre (Potter and Pawliszyn 1994). The relatively high % RSD values in the sorption profile results were attributed to the lack of sensitivity in the older CLOT column used in the analysis and not related to the SPME method. The improvement in % RSD shown in the calibration curve results can be attributed to the use of a new column. Since there was no trend in % RSD with extraction time, the % RSD was independent of the extraction time used. There was also a higher % increase in the % RSD for the PAHs compared to the BTEX compounds.

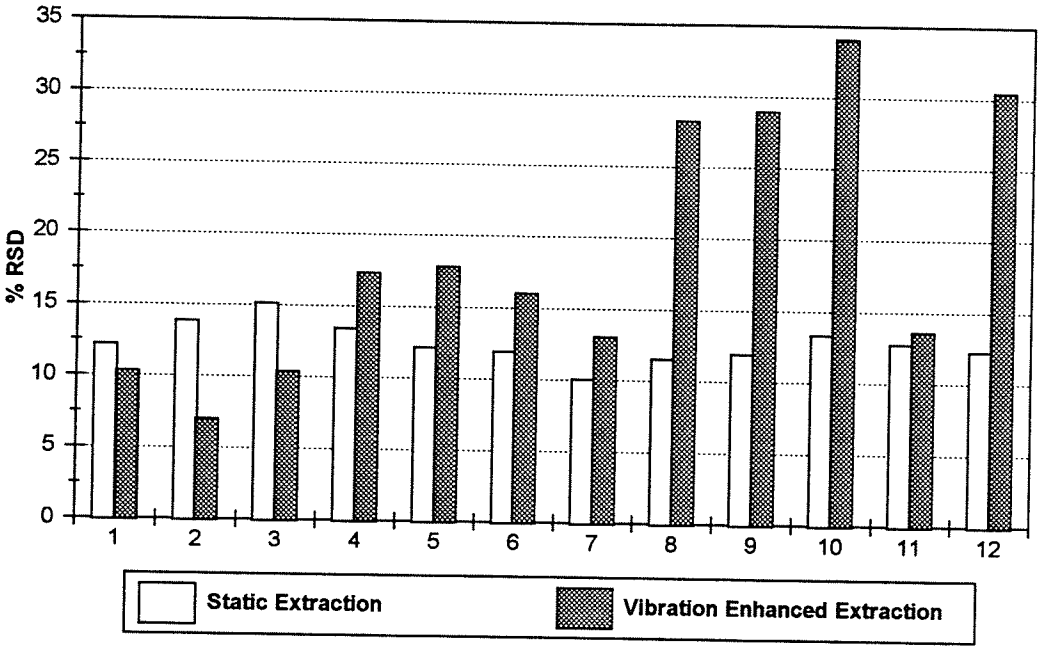

Figure 4.6 % RSD comparison for static and vibration-enhanced extraction in the sorption profiles: 1- acetone, 2- benzene, 3- toluene, 4- ethylbenzene, 5- *p*-xylene, 6- *m*-xylene, 7- *o*-xylene, 8- naphthalene, 9- 2-methylnaphthalene, 10- phenanthrene, 11-average BTEX, 12- average of naphthalene, 2-methylnaphthalene, and phenanthrene.

4.3.3 Static and Vibration-Enhanced Extraction Calibration Curves

Calibration curves for both the vibration-enhanced extraction and static extraction were developed by diluting a solution containing 1000 mg/L of each of the BTEX compounds and 50 mg/L of PAH in acetone by a factor of 100, 200, 1000, 2000, and 10 000. The corresponding concentrations analysed were then 10, 5, 1, 0.5, and

0.1 mg/L for BTEX and 0.5, 0.25, 0.05, 0.025, 0.005 mg/L for the three PAHs. Six aliquots of 1.4 mL each were taken at the same time from the dilutions and placed in 2-mL screw cap vials with Teflon-backed silicone septa for GC analysis. Three of the aliquots were used for static extraction and the other three for vibration-enhanced extraction.

The calibration curves indicate a significant increase in detector response for the BTEX and PAH compounds with vibration-enhanced extraction over static extraction. Calibration curves were determined by fitting a linear relationship between the detector response and the compound concentration (mg/L) through the intercept. The vibration-enhanced calibration curves gave a % increase in fitted slopes of 78.6% for the BTEX compounds and 103.1% for the PAH compounds (Table 4.3). Therefore, vibration-enhanced extraction increases the fitted slope by a factor of 1.5 for BTEX and 2.0 for the PAHs.

The average % RSD with vibration and static extraction were 7.4% and 6.2% for BTEX and 12.0% and 5.7% for the selected PAHs respectively (Fig. 4.7). The % RSD was found to increase with increasing distribution constants with vibration-enhanced extraction but not with static extraction. The increase in % RSD with increasing K values is attributed to the increased amount of analyte sorbed over a specific period of time before equilibrium is reached

(Potter and Pawliszyn 1992). Since vibration-enhanced extraction increases the amount absorbed compared to static extraction, the %RSD should be higher for vibration-enhanced extraction prior to equilibrium. The % RSD is expected to similar for both extraction methods if the extractions were performed at equilibrium conditions.

Table 4.3 Fitted Slope Comparison of Vibration-Enhanced and Static Extraction

Compound	Static		Vibration		% Increase
	Slope	r^2	Slope	r^2	in slope
acetone	36	0.994	33	0.990	-7.6
benzene	22687	0.998	28517	0.985	25.7
toluene	45776	0.999	68285	0.984	49.2
ethylbenzene	50620	0.998	106246	0.947	109.9
p-xylene	51073	0.998	128047	0.915	150.7
m-xylene	98460	0.993	155874	0.998	58.3
o-xylene	77501	0.999	137865	0.980	77.9
naphthalene	77865	0.994	132516	0.981	70.2
2-methyl naphthalene	95931	0.994	186283	0.975	94.2
phenanthrene	128177	0.999	314022	0.997	115.0
average BTEX	-	-	-	-	78.6
average PAHs	-	-	-	-	103.1

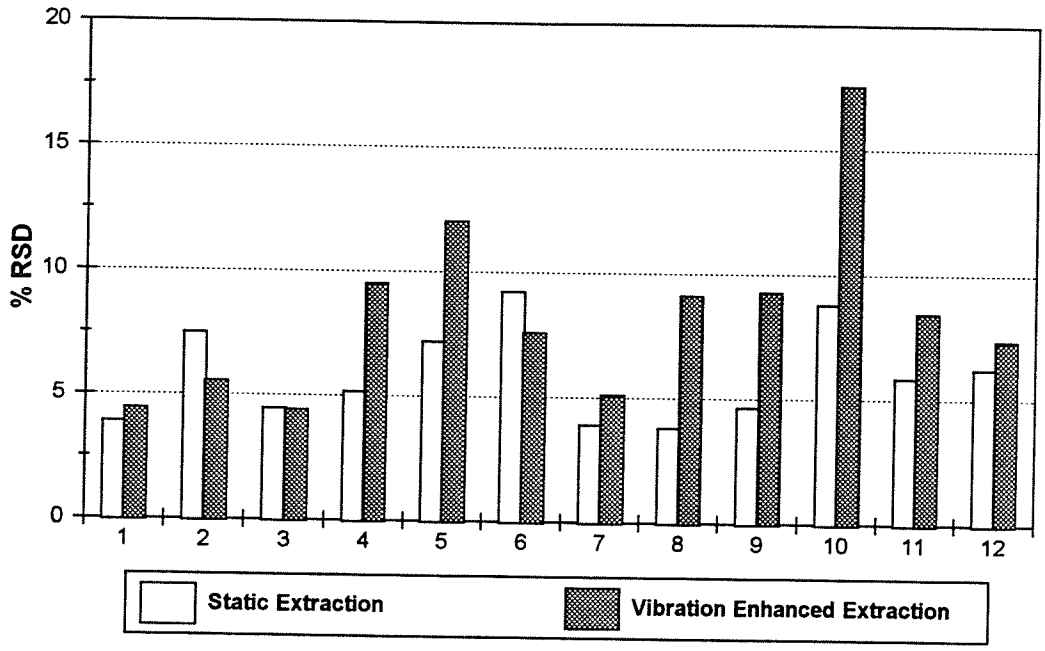

Figure 4.7 % RSD comparison for static and vibration-enhanced extraction in the calibration curves: 1- acetone, 2- benzene, 3- toluene, 4- ethylbenzene, 5- *p*-xylene, 6- *m*-xylene, 7- *o*-xylene, 8- naphthalene, 9- 2-methylnaphthalene, 10- phenanthrene, 11-average BTEX, 12- average of the naphthalene, 2-methylnaphthalene, and phenanthrene.

The limits of detection were improved using vibration-enhanced extraction. The limit of detection (LOD) was calculated by determining the integrated area count corresponding to a peak in the baseline noise. The integrated peak area with a signal to noise ratio of 4:1 of a baseline peak was conservatively measured as ≈5. Therefore, with the definition of the LOD being an analyte

signal three times the baseline noise (Potter and Pawliszyn 1992), the LOD was taken as a concentration corresponding to an integrated peak area of 15 counts. The LOD ranged from 47.8-526 pg/mL and 117-661 pg/mL for vibration-enhanced and static extraction respectively (Table 4.4). Furthermore, the limits of detection for the compounds would improve as the amount of analyte sorbed by the fibre increases up to equilibrium between the compounds and the fibre. The limit of detection can also be improved by increasing the sample volume and volume of the stationary phase (Potter and Pawliszyn 1994). The observed LOD improved with increasing distribution constants. This corresponds to other work where the LOD improved by an order of magnitude as the distribution constant increased by an order of magnitude (Potter and Pawliszyn 1994).

Based on the hypothesis that high distribution constant compounds have a greater restriction to diffusion through water to reach the fibre, there should be a greater % increase in response with vibration extraction with increasing values for the distribution constants (Zhang and Pawliszyn 1993). To test this hypothesis, a linear regression line was fitted to the increase in vibration-enhanced extraction over static extraction with distribution constants found in the literature for benzene (200), toluene

Table 4.4 Limits of Detection for Vibration-Enhanced and Static Extraction

Compound	Static LOD (pg/L)	Vibration LOD (pg/L)	% Improvement
benzene	661	526	20.4
toluene	328	220	32.9
ethylbenzene	296	141	52.4
p-xylene	294	117	60.2
m-xylene	152	96	36.7
o-xylene	194	109	43.8
naphthalene	193	113	41.5
2-methylnaphthalene	156	81	48.4
phenanthrene	117	48	59.1

(759), ethylbenzene (2138), and *o*-xylene (1820) that used a 100-µm polydimethylsiloxane fibre similar to the one employed in this study (Potter and Pawliszyn 1992).

$$\%\ Increase\ in\ slope = 0.0392\ K + 17.44 \qquad (12)$$

The fitted equation (12), $r^2 = 0.95$, shows the % increase of vibration-enhanced extraction over static extraction with the increase in the distribution constant of the compound (Fig. 4.8). The *p*- and *m*-xylene were not included in the regression because the individual distribution constants under similar experimental conditions were not available in

the source literature. Therefore, it is expected that compounds with high distribution constants can be efficiently analysed with vibration-enhanced SPME made possible by the SAMCAD. The % increase also shows that the effect of agitation on the LOD is more pronounced for compounds having a higher distribution constant.

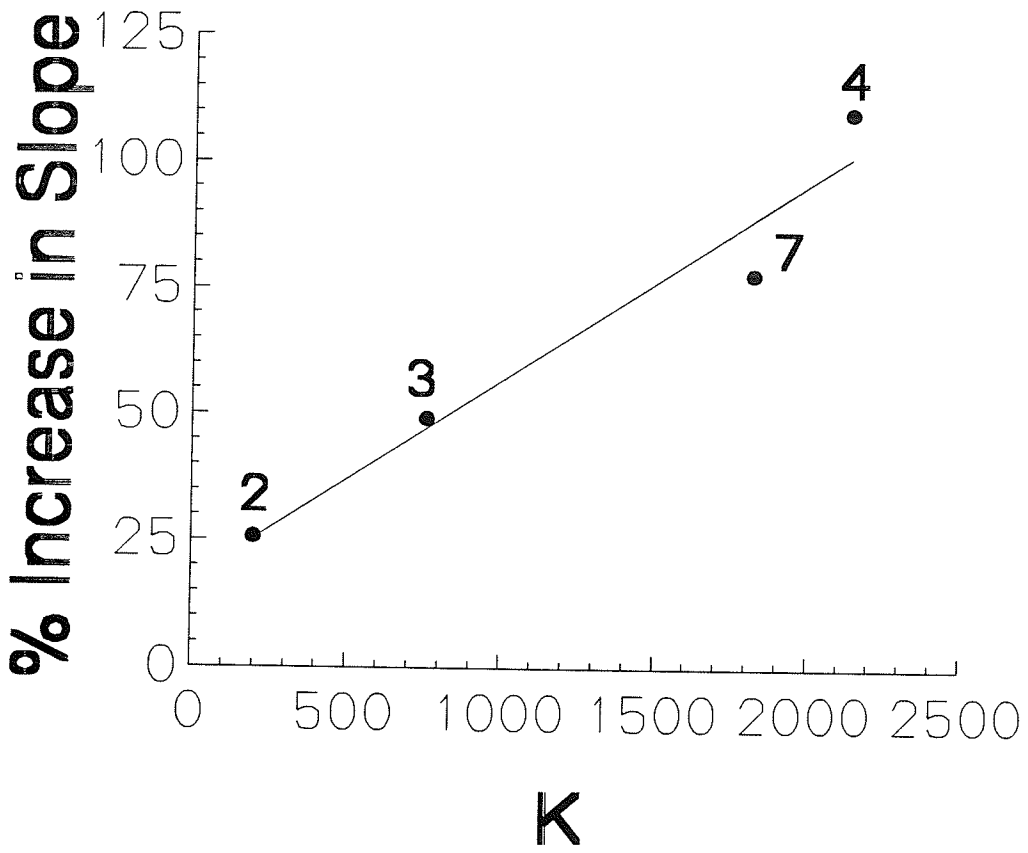

Figure 4.8 Relationship of % increase in the slope of calibration curves obtained from vibration-enhanced extraction over static extraction as a function of distribution constants found in the literature: 2- benzene, 3- toluene, 4- ethylbenzene, and 7- *o*-xylene.

4.4 Methods of SPME-GC-FID Analysis of Hydrocarbon Samples

Extraction was performed using a 100-μm polydimethylsiloxane fibre with a Varian 8200 autosampler modified to perform SPME. A 5-min extraction time and 2-min thermal desorption time were used for BTEX analysis in experiments No.1 and No.2. In experiments No.3 and No.4 with the model diesel fuel, 30-min vibration extraction and 2-min thermal desorption were used. A Varian 3400 gas chromatograph equipped with a flame ionization detector (FID) was used for separation and analysis. Separation was performed using a Supelco 30 m x 0.32 m I.D. carbon-layer open tubular (CLOT) column. The chromatographic conditions for BTEX analysis were as follows: detector 250°C; injector 200°C (2 min), 5°C/min to 150°C, hold (3 min); flow rates, He carrier plus makeup 30 mL/min, air 300 mL/min, H_2 30 mL/min. For the analysis of the model diesel compounds the chromatographic conditions were detector 250°C; injector 200°C; column 40°C (2 min), 5°C/min to 220°C, 2°C/min to 280°C, hold (2 min); flow rates, He carrier plus makeup 30 mL/min, air 300 mL/min, H_2 3.0 mL/min. Standard calibration curves were determined for each experiment and as necessary to ensure accurate sample quantification.

5.0 Development of the Contaminant Transport Equation for Surfactant-Enhanced Electrokinetic Remediation

5.1 Introduction

The analytical modelling of contaminant movement during electrokinetic remediation with a surfactant is based upon classical transport equations. An analytical model was chosen since it has the ability to screen and test numerical models, it is more computationally efficient, and is physically based. In addition, because relatively little attention has been focussed on mathematical modeling of SEAR to date (Brown and Pope 1994), a simpler model is appropriate. With increased knowledge of surfactant-enhanced remediation, more complicated models will be warranted. However, even with the simplifying assumptions involved, the analytical model is useful for modelling surfactant-enhanced electrokinetic remediation and for identifying the effects of various physical and chemical factors in electrokinetic remediation.

The new model integrates electrokinetic phenomena with the effects of a surfactant to predict the transport of contaminants in soil during surfactant-enhanced electrokinetic remediation. Electroosmotic flushing of dissolved organic chemicals under steady-state uniform flow through fine-grained soils can be modelled using the

traditional advection-dispersion-sorption equation for solutes in saturated homogeneous isotropic media (Bruell et al. 1992). In addition, enhanced transport of trace organic compounds with the presence of surfactant micelles can be explained quantitatively by a modified retardation factor which takes into account surfactant effects (Kan and Tomson 1986). Therefore, electrokinetic remediation with a surfactant can be modeled by adapting the advection-dispersion-sorption equation to include a modified retardation factor and electrokinetic effects.

5.2 Modified Retardation Factor

Surfactant-enhanced remediation can be modeled with the help of a modified retardation factor (Kan and Tomson 1986). The modified retardation factor takes into account partitioning of the organic compound between the sorbed soil phase, the aqueous phase, and the surfactant micelles during transport. This includes the enhanced contaminant transport due to the increased partitioning of the organic compounds into the aqueous phase with the addition of a surfactant. The general retardation factor can be used in electrokinetic remediation modelling since it has been noted that an electrical field, generated by electroosmosis, has minimal effect, if any, on adsorption (Bruell et al. 1992). The

general equation for the retardation factor is given as (Freeze and Cherry 1979)

$$R = 1 + \frac{\rho_b}{n} K_d \qquad (13)$$

where:

ρ_b = dry bulk density (g/cm^3),

K_d = distribution coefficient (mL/g),

n = porosity (dimensionless),

R = retardation factor (dimensionless).

The definition of the distribution coefficient in a porous medium is the mass of solute on the solid phase per unit mass of solid phase over the concentration of solute in solution which gives units similar to mL/g (Freeze and Cherry 1979). Including the effects of a surfactant, the distribution coefficient can be expressed as (Jafvert 1991)

$$K_d = \frac{C_{soil}}{C_w + C_{mic}} \qquad (14)$$

where:

K_d = distribution coefficient (mL/g),

C_{soil} = concentration of hydrocarbon sorbed onto the soil (mol/g),

C_w = concentration of hydrocarbon in the aqueous phase expressed as moles per millilitre of solution (mol/mL),

C_{mic} = concentration of hydrocarbon in surfactant micelles expressed as moles per millilitre of solution (mol/mL).

The concentration in the aqueous phase refers to the solute dissolved in either water only or water plus a surfactant concentration equal to or below the CMC. The concentration in the solution phase refers to both the aqueous phase concentration and the concentration in micelles which are formed at surfactant concentrations above the CMC, i.e. $(C_w + C_{mic})$.

The micelle-water partition coefficient, K_{mc}, in concentration-based units is given by (Jafvert 1991)

$$K_{mc} = \frac{C_{mic}}{C_w\ (C_{surf} - CMC)} = \frac{C_{mic}}{C_w\ DS_{mic}} \qquad (15)$$

where:

K_{mc} = micelle-water partition coefficient expressed in concentration-based units (mL/mol of micelle),

C_w = concentration of hydrocarbon in the aqueous phase expressed as moles per millilitre of solution (mol/mL),

C_{mic} = concentration of hydrocarbon in surfactant micelles expressed as moles per millilitre of solution (mol/mL),

C_{surf} = surfactant concentration (mol/mL),

CMC = critical micelle concentration (mol/mL),

DS_{mic} = moles of surfactant in micellar form per millilitre of solution (mol of micelle/mL), i.e., (C_{surf}-CMC).

The partition coefficient of a compound between soil and the aqueous phase based upon the amount of organic carbon can be expressed as (Jafvert 1991)

$$K_{oc} = \frac{C_{soil}}{C_w f_{oc}} \qquad (16)$$

where:

K_{oc} = partition coefficient of a compound between organic carbon and the aqueous phase (cm^3/g),

C_{soil} = concentration of hydrocarbon sorbed onto the soil (mol/g),

C_w = concentration of hydrocarbon in the aqueous phase expressed as moles per millilitre of solution (mol/mL),

f_{oc} = weight fraction of organic carbon (dimensionless).

By combining equation (14) for the distribution coefficient and equation (15) for the micelle-water partition coefficient in concentration-based units with equation (16) for K_{oc}, one can express the distribution coefficient as

$$K_d = \frac{K_{oc} f_{oc}}{1 + K_{mc} DS_{mic}} \qquad (17)$$

where:

K_d = distribution coefficient (mL/g),

K_{oc} = partition coefficient of a compound between organic carbon and the aqueous phase (cm^3/g),

f_{oc} = weight fraction of organic carbon (dimensionless),

K_{mc} = micelle-water partition coefficient (mL/mol),

DS_{mic} = moles of surfactant in micellar form per millilitre of solution (mol/mL).

Therefore, a modified retardation factor that takes into account the partitioning of the compound between the soil, water, and micelles with a surfactant concentration equal to or greater than the CMC is given by

$$R_f = 1 + \frac{\rho_b K_{oc} f_{oc}}{n (1 + K_{mc} DS_{mic})} \qquad (18)$$

where:

R_f = modified retardation factor (dimensionless),

ρ_b = dry bulk density (g/cm^3)

K_{oc} = partition coefficient of a compound between organic carbon and the aqueous phase (cm^3/g),

f_{oc} = weight fraction of organic carbon (dimensionless),

n = porosity,

K_{mc} = micelle-water partition coefficient (mL/mol),

DS_{mic} = moles of surfactant in micellar form per millilitre of solution (mol/mL).

In order to integrate the modified retardation equation with reported micelle-water partition coefficients given in the mole-fraction based dimensionless units, the micelle-water partition coefficient expressed in concentration-based units must be converted. The conversion of the micelle-water partition coefficient in concentration-based units to the dimensionless mole fraction ratio is accomplished by using the relationship of Jafvert (1991),

$$K_{mc} = K_{mm} V_{mol} \frac{(62+N)}{62} \times 1000 \qquad (19)$$

where:

K_{mc} = micelle-water partition coefficient expressed as concentration-based units (mL/mol),

K_{mm} = micelle-water partition coefficient expressed as a dimensionless mole fraction ratio (dimensionless),

N = the mean occupancy number of the organic molecules in SDS micelles at saturation,

V_{mol} = the molar volume of water (0.01805 L/mol at 25°C).

The number 62 comes from the fact that SDS has an aggregation number of 62, i.e., 62 SDS molecules are in every SDS micelle (Almgren et al. 1979).

Table 5.1 Mean Occupancy Numbers for Selected Hydrocarbons

Organic Compound	Mean Occupancy Number (N) *	SDS Concentration (mol/L)
benzene	35	0.05
toluene	35	0.05
p-xylene	30	0.05
naphthalene	6.25	0.04
anthracene	0.09	0.02

* From: Almgren et al. (1979)

The (62+N)/62 term is included because the concentration-based units are inconsistent with the mole fraction units for more water-soluble compounds such as BTEX (Jafvert 1991). Since the mean occupancy number of a compound decreases with decreasing aqueous solubility, the (62+N)/62 term can be neglected for highly hydrophobic compounds without serious error. However, the mean occupancy number should be include to predict the retardation of BTEX and other less hydrophobic organic compounds. The mean occupancy number has not been included in other similar modified retardation factors (Kan and

Tomson 1986; Valsaraj and Thibodeaux 1989). The modified retardation equation with the micelle-water partition coefficient in dimensionless mole fraction-based units can be written as

$$R_f = 1 + \frac{\rho_b K_{oc} f_{oc}}{n\left(1 + K_{mm} V_{mol}\, DS_{mic}\, \frac{(62+N)}{62}\right)} \qquad (20)$$

where:

R_f = modified retardation factor (dimensionless),

ρ_b = dry bulk density (g/cm^3)

K_{oc} = partition coefficient of a compound between organic carbon and the aqueous phase (cm^3/g),

f_{oc} = weight fraction of organic carbon (dimensionless),

n = porosity (dimensionless),

K_{mm} = micelle-water partition coefficient (dimensionless),

DS_{mic} = moles of surfactant in micellar form per millilitre of solution (mol/L),

N = the mean occupancy number of the organic molecules in SDS micelles at saturation,

V_{mol} = the molar volume of water (L/mol).

The concentration of surfactant micelles is expressed in mol/L to match the units of molar volume in equation (19) and avoid the multiplication factor of 1000.

5.3 Modified Organic Carbon-Water Partition Coefficient

The amount that partitions onto the organic carbon of a soil decreases as aqueous solubility of a compound increases. Since the solubility in the aqueous phase increases with a surfactant concentration equal to or greater than the CMC, the organic carbon-water partition coefficient, K_{oc}, must be modified. The value of log K_{oc} has been related to the solubility of compound by Kenaga and Goring (1980) (Domenico and Schwartz 1990)

$$\log K_{oc} = 3.64 - 0.55 \log S \qquad (21)$$

where:

K_{oc} = partition coefficient of a compound between organic carbon and the aqueous phase (cm^3/g),

S = hydrocarbon solubility in the aqueous phase (mg/L).

The relationship of hydrocarbon solubility at the CMC (mg/L) with log K_{ow} found from the micellar solubilization experiments in section 6.1.1 can be combined with equation (21) to obtain a relationship for a modified log K_{oc}. The equation for the modified organic carbon partition coefficient taking into account the increased solubility in the aqueous phase due to SDS in terms of log K_{ow} is given as

$$\log K_{oc,cmc} = 0.5353 + 0.5223 \log K_{ow} \quad (22)$$

where:

$K_{oc,\ cmc}$= modified partition coefficient of a compound between organic carbon and the aqueous phase taking into account surfactant effects (cm^3/g),

K_{ow} = octanol-water partition coefficient (dimensionless concentration ratio).

Equation (22) accounts for the lower log K_{oc} values present when the hydrocarbon solubility increases in the aqueous phase due to the presence of a surfactant at a concentration equal to or greater than the CMC.

The log K_{oc} value can also be expressed in terms of log K_{ow} without including the effects of a surfactant. This relationship is needed to predict the effects of remediation with water flushing. The linear regression relationship of the log of aqueous solubility (S_{wi})(mg/L) for the individual BTEX and PAH compounds in the model diesel fuel to their log K_{ow} values is given by ($r^2 = 0.91$),

$$\log S_{wi} = 4.6922 - 0.7358 \log K_{ow} \quad (23).$$

Combining equation (23) with equation (21), the log K_{oc} values for the model diesel fuel compounds in the absence of a surfactant can be calculated from

$$\log K_{oc} = 1.059 + 0.4047 \log K_{ow} \quad (24)$$

where:

K_{oc} = partition coefficient of a compound between organic carbon and the aqueous phase (cm^3/g),

K_{ow} = octanol-water partition coefficient (dimensionless concentration ratio).

Since there is a linear relationship between log K_{mm} and log K_{ow}, log K_{mm} can be expressed in terms of the log K_{ow} of the compound (section 6.1.1). Therefore, the modified retardation factor can be expressed in terms of dry bulk density, porosity, mean occupancy number, fraction of organic carbon and log K_{ow}. The relationship between log K_{ow} and log R_f for different SDS concentrations using typical parameters for sand indicates that the retardation factor decreases as surfactant concentration increases (Fig. 5.1). However, at SDS concentrations greater than 2% (w/w) there is little decrease in the modified retardation factor with an increase in surfactant concentration. Therefore, an optimum SDS surfactant solution should not have a

concentration greater than 2% (w/w). In addition, figure 5.1 indicates that compounds with log K_{ow} values less than 1.5 will not experience significantly enhanced recovery with the use of surfactants because SDS has little effect on the solubility of less hydrophobic compounds.

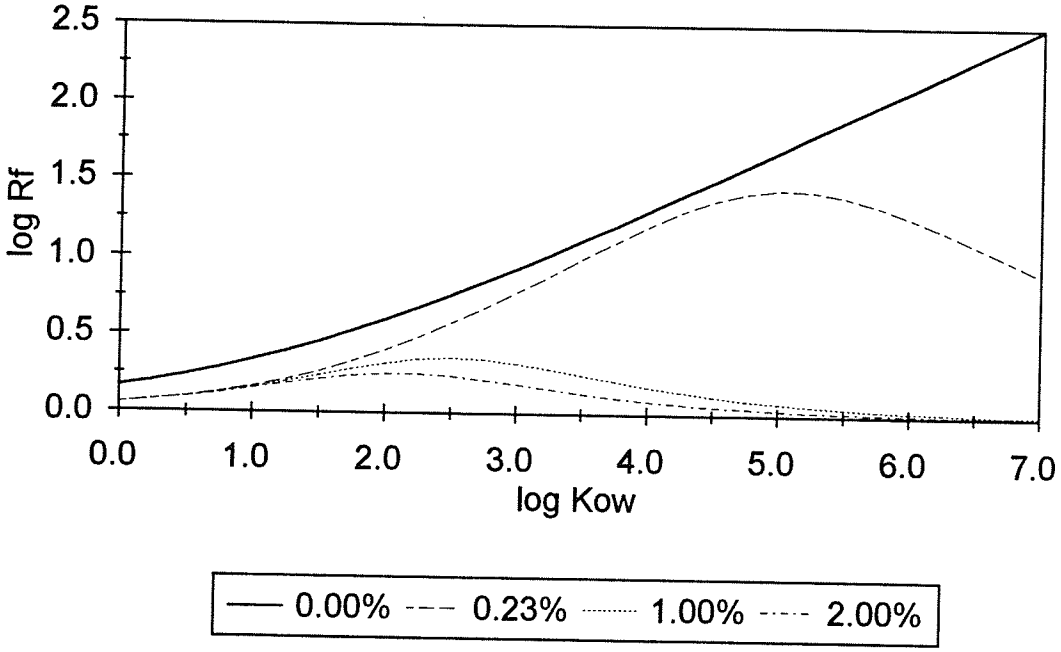

Figure 5.1 Relationship between log K_{ow} and log R_f for different SDS concentrations (bulk density = 1.60 g/cm^3, f_{oc} = 0.01, N = 0, porosity = 40%).

5.4 Development of the Advection-Dispersion-Retardation Electrokinetic Equation

The classical advection-dispersion equation can be modified to include the effects of both electroosmosis and

electrophoresis. The rate of advective transport is equal to the average linear groundwater velocity and is given by the sum of the hydraulic and electroosmotic velocities.

$$v_w = v_h + v_{eo} \tag{25}$$

where:

v_w = average linear groundwater velocity (cm/sec),

v_h = average linear hydraulic flow velocity (cm/sec),

v_{eo} = average linear electroosmotic flow velocity (cm/sec).

The concentration of the solute in the solution phase, C, is defined as the mass of solute per unit volume of solution. Therefore, the mass of solute per unit volume of porous media is nC, where n = porosity (Freeze and Cherry 1979). The mass of solute transported in the x direction by dispersion, hydraulic flow, electroosmotic flow, advection, and electrophoresis is given as

$$\textit{transport by dispersion} = nD_x \frac{dC}{dx} \tag{26}$$

$$\textit{transport by hydraulic flow} = v_h nC \tag{27}$$

$$transport\ by\ electroosmotic\ flow = v_{eo} nC \quad (28)$$

$$transport\ by\ advection = v_w nC \quad (29)$$

$$transport\ by\ electrophoresis = v_{ep} nC_{mic} \quad (30)$$

where:

D_x = hydrodynamic dispersion coefficient in the x direction (cm/sec),

n = porosity (dimensionless),

v_w = average linear groundwater velocity (cm/sec),

v_{ep} = electrophoretic velocity or the velocity of the micelles (cm/sec),

C_{mic} =concentration of hydrocarbon in surfactant micelles expressed as milligrams per litre of solution (mg/L).

C = hydrocarbon concentration in the solution phase (mg/L).

The transport due to dispersion is given by Fick's First Law. The term C_{mic} takes into account only the fraction of the contaminant attached to the charged micelles moving due to electrophoresis.

The electrophoresis transport equation (30) can be written in terms of the concentration of the solute in the bulk solution, C, rather than the concentration of solute in micelles. The bulk concentration of a solute in solution is given by

$$C = C_w + C_{mic} \tag{31}$$

where:

C = hydrocarbon concentration in the solution phase (mol/L),

C_w = concentration of hydrocarbon in the aqueous phase expressed as moles per litre of solution (mol/L),

C_{mic} = concentration of hydrocarbon in surfactant micelles expressed as moles per litre of solution (mol/L),

Rearranging equation (15) for the micelle-water partition coefficient to solve for the concentration of solute in the aqueous phase gives,

$$C_w = \frac{C_{mic}}{K_{mc}\, DS_{mic}} \tag{32}$$

where:

K_{mc} = micelle-water partition coefficient (L/mol),

C_w = concentration of hydrocarbon in the aqueous phase expressed as moles per litre of solution (mol/L),

C_{mic} = concentration of hydrocarbon in surfactant micelles expressed as moles per litre of solution (mol/L),

DS_{mic} = moles of surfactant in micellar form per litre of solution (mol/L).

Substituting equation (31) into equation (32) and rearranging to solve for the solute concentration in micelles in terms of the bulk solution concentration gives

$$C_{mic} = \frac{C}{1 + \frac{1}{K_{mc} DS_{mic}}} \qquad (33).$$

Therefore, the fraction of hydrocarbon in surfactant micelles is given by

$$f_{HCmic} = \frac{C}{C_{mic}} = \frac{1}{1 + \frac{1}{K_{mc} DS_{mic}}} = \frac{K_{mc} DS_{mic}}{K_{mc} DS_{mic} + 1} \qquad (34)$$

where:

f_{HCmic} = fraction of hydrocarbon in surfactant micelles (dimensionless),

K_{mc} = micelle-water partition coefficient (L/mol),

C_w = concentration of hydrocarbon in the aqueous phase expressed as moles per litre of solution (mol/L),

C_{mic} = concentration of hydrocarbon in surfactant micelles expressed as moles per litre of solution (mol/L),

DS_{mic} = moles of surfactant in micellar form per litre of solution (mol/L).

The determined fraction of hydrocarbon in surfactant micelles is similar to that determined by Valsaraj et al. (1988). The micelle-water partition coefficient expressed as concentration based units in equation (34) is converted into dimensionless mole fraction units for use in the modelling equations. The fraction of hydrocarbons in micelles is a dimensionless constant at a specific surfactant concentration above the CMC. Therefore, the solute electrophoresis transport equation (30), which takes into account the fraction of solute in the micellar phase moving by electrophoresis, can be written as

$$v_{ep} n C f_{HCmic} \qquad (35)$$

where:

f_{HCmic} = fraction of hydrocarbon in surfactant micelles (dimensionless),

n = porosity,

v_{ep} = electrophoretic velocity or the velocity of the micelles (cm/sec),

C = hydrocarbon concentration in the solution phase (mg/L).

If J_x represents the mass flux transported in the x direction per unit time, then

$$J_x = v_w nC - nD_x \frac{\partial C}{\partial x} - V_{ep} nC f_{HCmic} \quad (36).$$

The negative sign before the electrophoretic term indicates that the negatively charged micelles are moving in the opposite direction as the advective flow. Assuming the complete conservation of mass in the system

$$\frac{\partial J_x}{\partial x} = -n \frac{\partial C}{\partial t} \quad (37).$$

Substituting for J_x and cancellation of n from both sides gives:

$$D_x \frac{\partial^2 C}{\partial x^2} - v_w \frac{\partial C}{\partial x} + V_{ep} f_{HCmic} \frac{\partial C}{\partial x} = \frac{\partial C}{\partial t} \quad (38)$$

where x is the direction along the flow line. This is the classical advection-dispersion equation including electroosmosis and electrophoresis.

Including the modified retardation factor in the advection-dispersion-electrokinetic equation gives

$$\frac{D_x}{R_f} \frac{\partial^2 C}{\partial x^2} - \frac{v_w}{R_f} \frac{\partial C}{\partial x} + \frac{V_{ep} f_{HCmic}}{R_f} \frac{\partial C}{\partial x} = \frac{\partial C}{\partial t} \quad (39).$$

The concentration distribution of a contaminant during electrokinetic remediation with a surfactant can be given by the advection-dispersion-retardation electrokinetic (ADRE) equation.

The ADRE equation can be solved using the initial and boundary conditions where the contaminant is assumed to originate as an instantaneous point source at x=0 with a mass M_o (Baetsle 1969). The contaminant concentration at a given distance and time in one dimension by an instantaneous point source is given by the probability function (Baetsle 1969),

$$C(x,t) = \frac{M_o}{2\sqrt{\frac{\pi D_x t}{R_f}}} \exp\left(-\frac{X^2}{\frac{4D_x t}{R_f}}\right) \qquad (40)$$

where:

$$X = x - \frac{v_w t}{R_f} + \frac{v_{ep} f_{HCmic} t}{R_f} \qquad (41)$$

x = distance travelled in the x direction (cm),

C = hydrocarbon concentration in the solution phase (µg/mL),

M_o = mass of contaminant added to the system (μg),

D_x = hydrodynamic dispersion coefficient (cm^2/sec),

v_w = advective flow velocity (cm/sec),

v_{ep} = electrophoretic flow velocity (cm/sec),

f_{HCmic} = fraction of hydrocarbon in surfactant micelles (dimensionless),

R_f = modified retardation factor (dimensionless),

t = elapsed time (sec).

Equations (40) and (41) describe a bell-shaped curve (Gauss curve) as the concentration profile.

5.5 Determination of Equation Parameters

The terms in the ADRE equation can be quantified either from laboratory results or literature values. The model input parameters determined from experimental data were the hydraulic conductivity, coefficient of electroomostic permeability, voltage potential gradient, hydraulic gradient, surfactant concentration, K_{mm}, K_{oc}, dry bulk density, and mass of contaminant added. Values for the mean occupancy number, fraction of organic carbon, CMC, electrophoretic mobility of SDS micelles, and hydrodynamic dispersion were estimated from values found in the literature.

The hydrodynamic dispersion coefficient is expressed in terms of two components (Freeze and Cherry 1979)

$$D_x = \alpha_l v_w + D^* \quad (42)$$

where:

α_l = dispersivity (cm),

D^* = coefficient of molecular diffusion for the solute in the porous medium (cm^2/sec),

D_x = hydrodynamic dispersion coefficient (cm^2/sec),

v_w = advective flow velocity (cm/sec).

The dispersivity is usually neglected in fine-grained soils due to low advective flow velocities (Acar et al. 1990a). However, with the increased flow due to electrokinetic effects and the higher flow in sandy soils, the dispersivity term was included in the model. The dispersivity values for laboratory columns packed with quartz sand have been measured as 0.061 and 0.060 (Pennel et al. 1993), 0.029, 0.018, 0.225, and 0.072 (Pennel et al. 1994), and 0.1 cm (Borden and Kao 1989). An average value of 0.081 cm was used as a typical input parameter for sandy soils in the model. An overview of reported dispersivity values from a number of sources obtained from different methods indicate a range from 0.01 to 1 cm for a wide range of soil types (Knox et al. 1993).

Diffusion coefficients of selected organic compounds in water are given in Table 5.2. The diffusion coefficients for the xylene isomers and naphthalene were estimated as 0.8×10^{-5} cm^2/sec. The diffusion coefficients of phenanthrene and 2-methylnaphthalene were estimated as 0.7×10^{-5} and 0.65×10^{-5} cm^2/sec respectively. Therefore, using the estimated values for the diffusion coefficient and dispersivity from the literature with porosity of the soil, the effective coefficient of hydrodynamic dispersion can be determined.

Table 5.2 Diffusion Coefficients of some Model Diesel Fuel Compounds

Chemical	Diffusion Coefficient × 10^{-5} (cm^2/sec) @ 20°C [A]	Diffusion Coefficient × 10^{-5} (cm^2/sec) @ 25°C [B]
benzene	1.02	1.08
toluene	0.85	-
ethylbenzene	0.81	-
acetone	-	1.28

[A] From: Lymann et al. (1992)
[B] From: Louch et al. (1992)

The model input values for the mean occupancy number were taken from Table 5.1. A mean occupancy number of 30 was taken for ethylbenzene and the xylene isomers. The mean occupancy number was neglected for the more hydrophobic compounds of 2-methylnaphthalene and phenanthrene.

The hydraulic, electroosmotic, and electrophoretic flow velocity can be expressed in terms of the gradient which causes the flow. The hydraulic flow is given by Darcy's Law

$$v_h = K_h \frac{dh}{dx} \tag{43}$$

where:

v_h = hydraulic flux (cm/sec),

K_h = hydraulic conductivity (cm/sec),

dh/dx= hydraulic gradient.

The hydraulic flux can be calculated from the measured hydraulic conductivity in the experiments with the applied hydraulic gradient.

The electroosmotic flux given in equation (5) is given by

$$v_{eo} = K_{eo} \frac{dE}{dx} \tag{44}$$

where:

v_{eo} = electroosmotic flux (cm/sec),

K_{eo} = coefficient of electroosmotic permeability (cm/sec)/(V/cm),

dE/dx= electrical potential gradient (V/cm).

The electroosmotic flux was calculated from experimental measurement of K_{eo} and the measured voltage potential gradient in the soil during the course of the experiments.

In electrophoretic flow the charged particle is moving due to the imposed electrical gradient but the liquid surrounding the charged particle is moving in the opposite direction. Therefore, predicting electrophoretic flow becomes a difficult task. The electrophoretic velocity is the terminal velocity at which the frictional drag of the surrounding fluid moving in the opposite direction balances the electric force. The frictional drag can be approximated by Stoke's Law. One equation for electrophoretic velocity or the velocity of the micelles is Hückel's equation

$$v_{ep} = u_{ep}\frac{dE}{dx} = \frac{2D_o\zeta_{mic}}{3(4\pi\eta)}\frac{dE}{dx} \qquad (45)$$

where:

u_{ep} = electrophoretic mobility of the micelle (cm/sec)/(V/cm),

D_o = permittivity of the aqueous phase (C/V/cm or mN/V^2),

η = viscosity of the pore fluid (mPa sec),

ζ_{mic} = zeta potential of the micelles (V),

dE/dx= electrical potential gradient (V/cm).

Similarly, the electrophoretic velocity can be given by the Helmholtz-Smoluchowski equation

$$v_{ep} = \frac{D_o \zeta_{mic}}{4\pi\eta} \frac{dE}{dx} \quad (46).$$

The two electrophoretic equations differ by a factor of two thirds. Both equations are valid but are to be applied to different situations based upon the diffuse double layer thickness (κ^{-1}) and the radius of the charged particle (R_p). For log κR_p values < 0 Hückel's equation applies and for log κR_p values > 2 the Helmholtz-Smoluchowski equation applies (Vold and Vold 1983). Unfortunately the known κR_p values for SDS micelles fall between the valid ranges of the equations (Vold and Vold 1983). The log κR_p values for SDS ranges from -0.2 in water up to 0.4 in a 0.1 mol/L NaCl solution (Stigter and Mysels 1955). Therefore, for aqueous solution with ionic concentrations used in the experiments log κR_p values will fall below 0 and Hückel's equation can be used. In addition, the zeta potential determines which equation will be valid. In the intermediate range between the equations, the higher the zeta potential the greater the error of the equations (Vold and Vold 1983). The zeta potential predicted for SDS micelles range from 60 to 100 mV (Stigter and Mysels 1955). It is assumed that with the increasing acidity in the soil during electrokinetic treatment the zeta potential would be reduced and,

therefore, the region in which Hückel's equation is valid would include SDS micelles. Therefore, Hückel's equation is chosen over the Helmholtz-Smoluchowski equation.

Electrophoretic mobilities for SDS micelles have been measured as 4.55×10^{-4} $cm^2/(V\ sec)$ at the CMC in water (Stigter and Mysels 1955). The electrophoretic mobilities have been shown to decrease with increasing surfactant concentration and increasing ionic concentration. This indicates that there is an interaction between micelles. Electrophoretic mobilities ranged from 4.55×10^{-4} $cm^2/(V\ sec)$ at 0.23% (w/w) (CMC) to 3.75×10^{-4} $cm^2/(V\ sec)$ at 3.5% (w/w) in water (Stigter and Mysels 1955). Therefore, the electrophoretic mobility of SDS micelles is approximately an order of magnitude greater than the coefficient of electroosmotic permeability.

5.6 Relative Importance of Electroosmosis and Electrophoresis

In electrokinetic remediation with a surfactant it is important to determine the relative importance of electroosmosis and electrophoresis. One way to determine whether electroosmosis or electrophoresis is the dominant electrokinetic transport mechanism is to take the ratio of v_{eo} to v_{ep}. However, in terms of contaminant transport, the

amount of compound partitioning into the micelles must be included. The ratio of the rate of the amount of contaminant transported by electroosmosis in equation (28) and electrophoresis in equation (35), named the Thomas ratio, T_e, is given by

$$T_e = \frac{v_{eo}}{v_{ep} f_{HCmic}} \tag{47}$$

where:

T_e = Thomas ratio (dimensionless),

v_{eo} = electroosmotic flow velocity (cm/sec),

v_{ep} = electrophoretic flow velocity (cm/sec),

f_{HCmic} = fraction of hydrocarbon in surfactant micelles (dimensionless).

Electroosmotic transport dominates when the Thomas ratio is greater than one and electrophoretic transport in micelles dominates when the Thomas ratio is less than one. Substituting the Helmholtz-Smoluchowski equation (4) for electroosmotic flow and the Hückel's equation (45) for electrophoretic flow and cancelling terms gives

$$T_e = \frac{3\zeta_{soil}}{2\zeta_{mic} f_{HCmic}} \tag{48}$$

where:

T_e = Thomas ratio (dimensionless),

ζ_{soil} = zeta potential of the soil (V),

ζ_{mic} = zeta potential of the micelles (V),

f_{HCmic} = fraction of hydrocarbon in surfactant micelles (dimensionless).

The fraction of hydrocarbon in surfactant micelles ranges from close to 1 for high K_{ow} compounds and high surfactant concentrations. Therefore, when there is no surfactant or when the analyte is completely soluble in water, the fraction of analyte being transported by electrophoretic flow in micelles goes to zero and the Thomas ratio goes to infinity. Therefore, the more hydrophobic the compound and the greater the surfactant concentration the lower the Thomas ratio and the more dominant the electrophoretic transport.

For SDS concentrations ranging from 0.5% to 5% (w/w), mean occupancy numbers ranging from 0 to 35, and log K_{ow} values ranging from 2 to 7, the fraction of hydrocarbons in micelles ranges from 0 to 1. Therefore, the Thomas ratio can be expressed as

$$T_e = \frac{\zeta_{soil}}{B\,\zeta_{mic}} \qquad (49)$$

where B ranges from 0 to 0.667. Sandy material normally has a zeta potential of less than -20 mV whereas clayey material can have a zeta potential of up to -100 mV. Using zeta potential for soils ranging from -10 mV to -100 mV and zeta potential of SDS micelles ranging from 40 to 120 mV, the Thomas ratio ranges from 0.125 to ∞. Since the Thomas ratio is both below and above one under typical conditions, the dominance of electroosmosis and electrophoresis changes with changing chemistry of the system. Considering an average zeta potential of -10 mV typically associated for clay soils during electrokinetic processing with toluene as the organic compound (log K_{ow}=2.69, log K_{mm}=3.25, N=35), a typical surfactant concentration of 2% (w/w), and a conservative estimate of the zeta potential of the micelles as 60 mV, the Thomas ratio is given as 0.221. This shows that electrophoretic transport for toluene is 4.5 times greater than the electroosmotic transport at these typical conditions. When the SDS concentration is 2% (w/w) electrophoretic transport would be greater than the electroosmotic transport for organic compounds having log K_{ow} values greater that 1.5. Therefore, for the majority of hydrocarbons under typical treatment conditions, electrophoretic transport in SDS micelles will be greater than electroosmotic transport.

5.7 Modelling Assumptions

The proposed model for electrokinetic remediation with a surfactant makes some important assumptions. First, the model assumes the soil is homogeneous and saturated. Secondly, it assumes that a constant hydraulic potential and electrical potential gradient are applied across the soil. The steady-state assumption has been used in other research and steady-state flow has been shown during electroosmotic experiments (Acar et al. 1990a; Bruell et al. 1992). However, other research has reported that non-linearities and non-uniform pore water pressures which develop during electrokinetic remediation are not adequately described by classical equations (Eykholt and Daniel 1994). Since the zeta potential of both the soil and the micelles and the electrical potential gradient are transient processes the steady-state assumption can lead to errors (Eykholt and Daniel 1994). The dominant factor which leads to an error with this assumption is the pH. Both the electroosmotic flow and electrophoretic flow depend on the zeta potential which changes with changing pH over time. The affect of pH is included indirectly in the modelling within the calculated value of the coefficient of electroosmotic permeability.

A third assumption of the model is that all the soil pores are available for flow. Neglecting the true "effective porosity" may lead to an error since the anionic surfactant may disperse clay particles and clog the soil pores.

Another assumption of the model is the absence of ionic migration which should be included when the concentration profile for ionic species such as hydrogen ions and metal ions is desired.

A major limitation of the model is the assumption that only one phase is involved in the transport. No free-phase transport of organic compounds is considered. This leads to errors in modelling surfactant-enhanced remediation since the increase in compound solubility with a surfactant is not included. The compounds are considered to be immediately in solution and therefore surfactant addition will not increase the amount in solution. In addition, the amount of contaminant should be such that the concentration does not exceed the aqueous solubility of the compound.

The model also assumes that the hydrocarbons are immediately partitioned into the solution phase and transported under the hydraulic and electrical potential gradient. Other work reported in the literature indicates that surfactant-enhanced remediation (solubilization) is rate-limited, rather than instantaneous (Abriola et al. 1993; Pennel et al. 1994).

The model does not account for the loss of surfactant due to adsorption. Since an anionic surfactant was used, ignoring adsorptive loss is a valid assumption. Constant surfactant concentrations were assumed.

6.0 Results and Discussion

6.1 Solubilization Experiments

6.1.1 Introduction

Micellar solubilization experiments were conducted to determine the SDS micelle-water partition coefficients for toluene, ethylbenzene, and the xylene isomers. The micelle-water partition coefficients can be used to predict the increase in hydrocarbon aqueous solubility in the presence of a surfacant at concentrations above the CMC. The micelle-water partition coefficients can also be used to predict the amount of hydrocarbon transported by electrophoresis in micelles. The electrical conductivity of various surfactant solutions saturated with hydrocarbons can be used to predict the influence of hydrocarbons on the CMC. The effect of hydrocarbons on the CMC changes the amount of micelles available for micellar solubilization and electrophoretic transport in micelles.

6.1.2 Determination of the SDS Micelle-Water Partition Coefficients

Separatory funnel experiments were conducted to determine the apparent solubilities of toluene, ethylbenzene, and the three xylene isomers at SDS concentrations ranging from 0 to 2% (w/w) or 0 to 69 mmol/L

(Fig. 6.1). The molar solubilization ratio (MSR) is the slope of the line fitted through apparent solubility as a function of SDS concentration above the CMC (Fig. 6.1). The MSR and the measured aqueous solubility at the CMC can be used with equation (3) to calculate the SDS micelle-water partition coefficient, K_{mm}, for the compounds (Table 6.1).

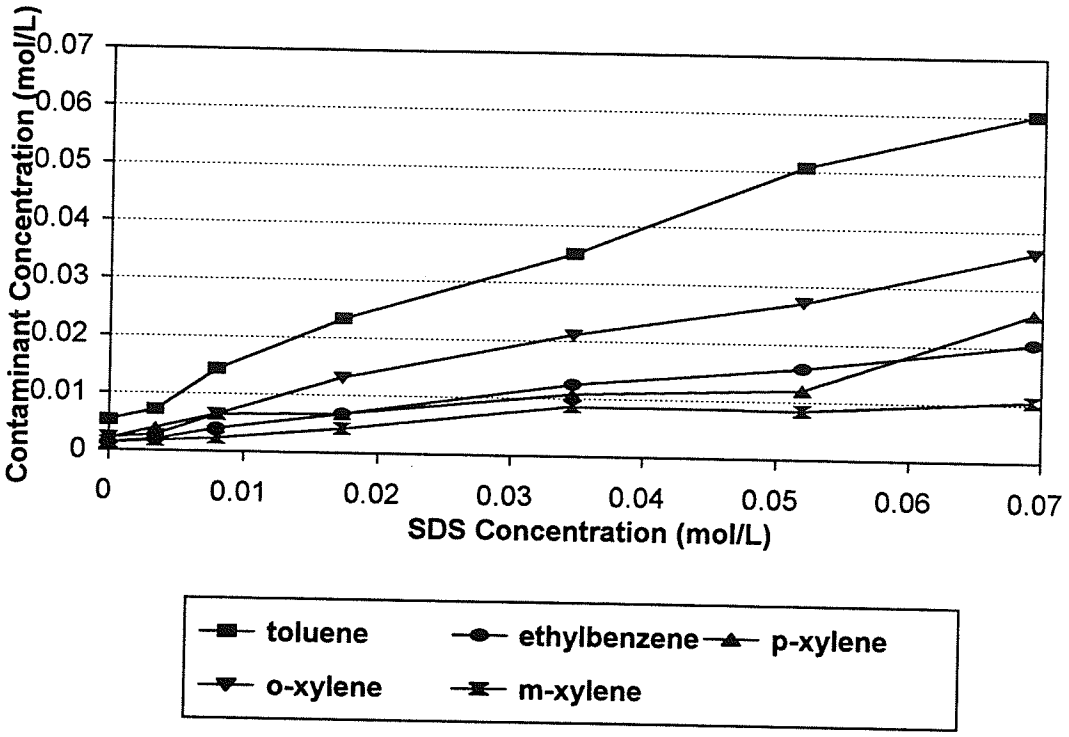

Figure 6.1 Aqueous solubility (mol/L) of toluene, ethylbenzene, and the xylene isomers at SDS concentrations ranging from 0 to 2% (w/w) or 0 to 0.069 mol/L.

The aqueous solubilities of toluene, ethylbenzene, and the xylene isomers were found to increase at the CMC (Table 6.1). The solubility at the CMC was increased by a

factor of 1.6 for *m*-xylene and up to 3.2 for ethylbenzene. The increase in solubility leads to a decrease in the calculated MSR and SDS micelle-water partition coefficients. The increase in solubility at the CMC has not been taken into account in previously reported determinations of K_{mm} even though the increase in the hydrocarbon solubility at the CMC have been reported (Edwards et al. 1991a; Kile and Chiou 1989).

Table 6.1 Calculated SDS Micelle-Water Partition Coefficients for Toluene, Ethylbenzene, and Xylene Isomers

Compound	Measured Aqueous Solubility		Measured Solubility at CMC		MSR	log K_{mm}
	mmol/L	mg/L	mmol/L	mg/L		
toluene	5.35	493	14.4	1326	0.752	3.19
ethylbenzene	1.39	148	4.45	472	0.264	3.42
p-xylene	2.09	222	6.48	688	0.284	3.45
m-xylene	1.45	154	2.38	253	0.169	3.39
o-xylene	2.35	249	6.52	692	0.464	3.36

The octanol-water partition coefficient, K_{ow}, is a measure of the hydrophobicity of a compound. Since the tendency to partition into micelles increases as a compound becomes more hydrophobic, it is reasonable to assume that there is a relationship between K_{mm} and K_{ow}. It has been

demonstrated in the literature that a linear relationship between log K_{mm} and log K_{ow} (Edwards et al. 1991c; Valsaraj and Thibodeaux 1989). A fitted linear regression line through the experimentally measured data for toluene, ethylbenzene, and the xylene isomers relating the log K_{mm} (dimensionless mole fraction ratio) to log K_{ow} (dimensionless concentration ratio) is given by ($r^2 = 0.95$),

$$\log K_{mm} = 2.089 + 0.421 \log K_{ow} \qquad (50)$$

The equation indicates that the more hydrophobic a compound the greater its tendency to partition into micelles.

In order to determine the most accurate K_{mm}-K_{ow} relationship possible, literature values for the SDS micelle-water partition coefficient were compiled for a number of organic compounds (Table 6.2). There is some discrepancy in the reported literature values for K_{mm}. For example, Valsaraj et al. (1989) reported log K_{mm} values for 1-methylnaphthalene, anthracene, and biphenyl determined from Almgren et al. (1977) as 4.35, 5.09, and 4.36 respectively. However, reported values in Jafvert (1991) determined from the same source were given as 4.71, 5.21, and 4.79 respectively. A linear regression line fitted through all data found in the literature presented in Table 6.2 along with the measured data is given by ($r^2 = 0.91$),

$$\log K_{mm} = 0.843 + 0.948 \log K_{ow} \quad (51a),$$

$$K_{mm} = 6.966\, K_{ow}^{0.948} \quad (51b).$$

The log K_{mm}-log K_{ow} relationship in equation (51) can be used to predict the solubilization of other contaminants based upon a compound's K_{ow} value. The K_{mm} value can then be used to predict contaminant transport in surfactant-enhanced remediation. A plot of log K_{mm} against log K_{ow} is given in Figure 6.2 along with the fitted regression line represented by equation (51).

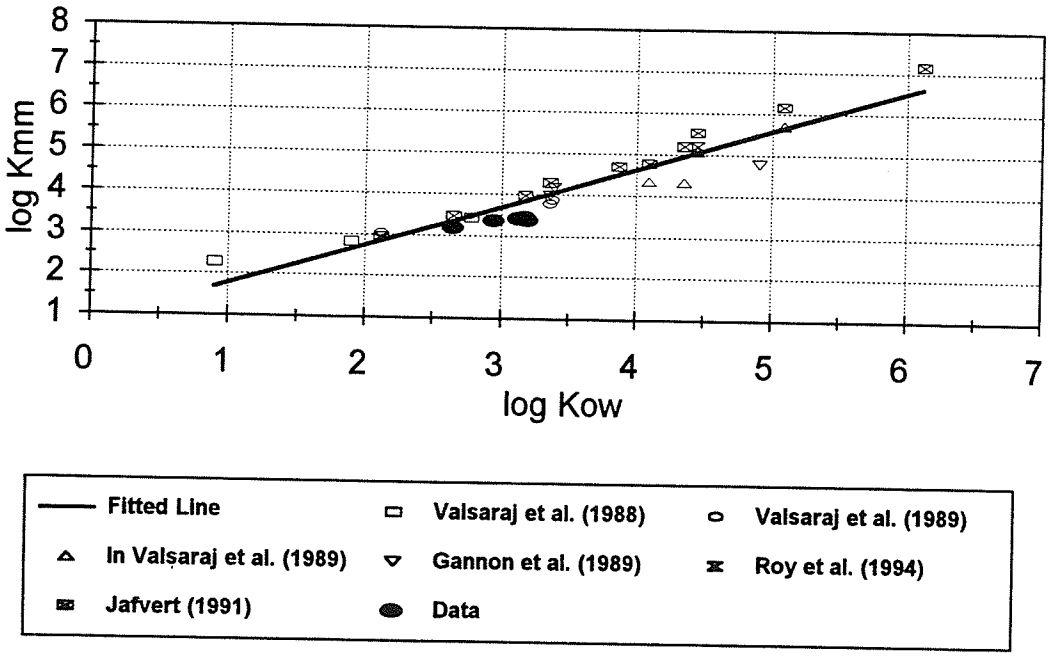

Figure 6.2 Relationship between log K_{ow} and log K_{mm} for SDS from reported literature and determined values.

Table 6.2 Literature Reported log K_{mm} Values

Organic Compound	log K_{mm}	log K_{ow}
methyl chloride	2.29[A]	0.90[G]
chloroform	2.83[A]	1.90[G]
carbon tetrachloride	3.44[A]	2.78[G]
benzene	3.04[B]	2.12[G]
toluene	3.22[B]	2.65[G]
m-dichlorobenzene	2.88[B]	3.38[G]
naphthalene	3.79[B]	3.36[G]
pyrene	5.72[B]	5.09[G]
1-methylnaphthalene	4.35[C]	4.35[B]
anthracene	5.09[C]	4.45[G]
biphenyl	4.36[C]	4.09[B]
dichlorobenzene	4.19[D]	3.39[G]
naphthalene	4.01[D]	3.36[G]
biphenyl	4.80[D]	4.91[H]
anthracene	5.21[e]	4.45[G]
perylene	7.18[F]	6.12[H]
pyrene	6.18[F]	5.09[G]
anthracene	5.55[F]	4.45[G]
1-bromonaphthalene	5.21[F]	4.35[H]
biphenyl	4.79[F]	4.09[H]
1-methylnaphthalene	4.71[F]	3.87[H]
naphthalene	4.31[F]	3.36[G]
p-xylene	3.98[F]	3.18[G]
toluene	3.48[F]	2.65[G]
benzene	2.96[F]	2.12[G]

[A] From: Valsaraj et al. (1988)

[B] From: Valsaraj and Thibodeaux (1989)

[C] From: Almgren et al.(1979)in Valsaraj and Thibodeaux(1989)

[D] From: Gannon et al. (1989) [E] From: Roy et al. (1994)

[F] From: Almgren et al. (1979) in (Jafvert 1991)

[G] From: Knox et al. (1993) [H] From: Jafvert (1991)

A linear relationship between log K_{mm} and log K_{ow} has also been found for the nonionic surfactant Triton X-100 (Edwards et al. 1991c). Using the log K_{ow} values for the toluene, ethylbenzene, and the xylene isomers, the log K_{mm} values for SDS calculated from equation (51) are lower than the log K_{mm} values predicted for Triton X-100. Therefore, SDS has a lower capacity to solubilize organic compounds compared to Triton X-100. This result follows the hypothesis that the ability to increase the solubility of organic compounds is in the order nonionic > cationic > anionic for surfactants of the same non-polar chain length (Kile and Chiou 1989). This order of solubilization may be caused by the hydration of the surfactant micelles which limits access to the micelle core and reduces the partitioning efficiency of the solute (Kile and Chiou 1989). Therefore, based upon micellar solubilization, a nonionic surfactant may be more suited to surfactant-enhanced remediation.

A linear relationship between the log of apparent compound solubility at the CMC (mg/L) measured in the micellar solubilization experiments and log K_{ow} can be developed to predict the apparent solubility of other organic compounds at the CMC ($r^2 = 0.69$),

$$\log C_{CMC} = 5.645 - 0.950 \log K_{ow} \qquad (52)$$

where:

C_{CMC} = apparent hydrocarbon solubility at the CMC (mg/L),

K_{ow} = octanol-water partition coefficient (dimensionless concentration ratio).

The negative sign indicates that solubility at the CMC decreases with increasing K_{ow} consistent with expectations. The apparent solubility at the CMC can be used to predict the modified organic-carbon partition coefficient ($K_{oc,\ cmc}$) which includes surfactant effects. The log of apparent solubility at the CMC (mg/L), predicted log $K_{oc,\ cmc}$ for SDS concentrations greater than the CMC from equation (18), and predicted log K_{mm} values are shown in Table 6.3 for the model diesel fuel compounds.

6.1.3 Effect of Organic Compounds on the CMC

The critical micelle concentration of solutions saturated with toluene, ethylbenzene, *p*-xylene, *m*-xylene, and *o*-xylene were determined as 0.0056, 0.0057, 0.0045, 0.0052, and 0.0056 mol/L respectively. There was an average decrease of 33% in the CMC in the presence of organic compounds under saturated conditions. Therefore, the literature value of CMC under estimates the effects on micellar solubilization and the amount of hydrocarbon

transported by electrophoresis in micelles with surfactant-enhanced remediation at high hydrocarbon concentrations.

Table 6.3 Predicted solubility at the CMC (mg/L), predicted log $K_{oc,\ cmc}$, and log K_{mm} for Model Diesel Fuel Compounds

Compound	log K_{ow}*	Predicted Solubility at the CMC (mg/L)	Predicted log $K_{oc,cmc}$ (cm^3/g)	Predicted log K_{mm}
acetone	-0.24	746284	0.962	0.584
benzene	2.12	4284	1.917	2.853
toluene	2.65	1344	2.131	3.355
ethylbenzene	3.13	471	2.326	3.810
p-xylene	3.18	422	2.346	3.858
m-xylene	3.20	404	2.354	3.877
o-xylene	2.95	698	2.253	3.640
naphthalene	3.36	285	2.419	4.028
2-Me-naphthalene	4.11	55	2.722	4.739
phenanthrene	4.52	23	2.888	5.128

* From: Knox et al. (1993)

6.2 Preliminary Experiment No.1 on BTEX-Contaminated Sand

6.2.1 Flow Rate

The preliminary experiment No.1 on sand, with an electrical potential difference of 20 V and electrode configuration causing electroosmotic flow to retard the hydraulic flow, gave higher flow rates in the hydraulic columns than the electrical columns. A summary of the experimental treatment conditions is given in Table 3.2 (p. 58). The difference in flow rates between the electrical and hydraulic columns was attributed to gas produced by electrolysis reactions clogging the soil pores in the electrical columns rather than electroosmotic flow retarding the hydraulic flow. The addition of a surfactant increases the current and the production of gases by electroylsis of water. The hydrogen gas produced at the cathode was not able to escape from the electrical columns and consequently air bubbles clogged the soil pores. An important observation is the reduced flow rate in the electrical column C even though a loose electrode wire prevented the constant application of current to the sample. Therefore, the reduced flow rate was attributed to the build-up of gases in the soil pores and not to electroosmotic flow retarding hydraulic flow.

The average of the individual hydraulic conductivities of the hydraulic columns was determined to be 2.38×10^{-3} cm/sec (% RSD = 30.0%) which is not significantly different from the initial hydraulic conductivity of 1.70×10^{-3} cm/sec (% RSD = 1.35%) with water flushing. Therefore, the surfactant did not have an effect on the flow rate of the sand columns under the given treatment conditions.

Another important observation made in experiment No.1 was that the flow rate could not be re-established by flushing the accumulated gases with an increased hydraulic gradient. This is a result of foaming of the SDS surfactant solution induced by gas production. Once foam has formed with SDS it is very stable and resistant to breakdown. Therefore, SDS foam can significantly disrupt flow through soil.

6.2.2 Current as a Function of Time

The current in experiment No.1 peaked at approximately 1.60 mA after 2 days and then slowly decreased to a steady 0.5 mA after 7 days. Similar profiles showing initial increase then decrease in current over time to some asymptotic value have been obtained in other research (Gopinath 1994). The decrease in current is a result of the overall increase in the resistance of the soil column.

6.2.3 Gas Production

The volume of hydrogen and oxygen gas produced at the electrodes over time can be calculated from the current. Since one coulomb is equal to 1 amp × 1 second, the number of coulombs produced in one hour by a 0.5 mA current measured in experiment No.1 is given by the expression

$$coulombs\ produced = 0.5 mA \times \frac{1 A}{1000 mA} \times 3600 \frac{\sec}{hr} \qquad (53).$$

Since the charge on one 1 mole of electrons is 96845 C (Faraday's constant) (Gillespie et al. 1989), the number of moles of electrons produced in one hour is 1.859×10^{-5}. The electrolysis reactions of water indicate that 4 moles of electrons produce 1 mole oxygen gas at the anode and 2 moles electrons produce 1 mole of hydrogen gas at the cathode. This corresponds to 4.648×10^{-6} ($1.859 \times 10^{-5}/4$) moles of oxygen gas and 9.295×10^{-6} ($1.859 \times 10^{-5}/2$) of hydrogen gas produced by the 0.5 mA current in one hour. From the ideal gas law, 1 mole of an ideal gas occupies 22.4 L at standard temperature and pressure (Gillespie et al. 1989). Therefore, 0.10 mL oxygen gas and 0.21 mL hydrogen gas could be produced in an hour. In the course of the 15 day test, 36 mL oxygen gas and 72 mL hydrogen gas would have been produced.

The sand columns had a pore volume of 214 mL. Therefore, at the end of the test, approximately one third of the pore volume was filled with hydrogen gas. The amount of hydrogen gas produced would be significant to account for the decreased flow rates in the electrical columns.

6.2.4 Voltage Potential Gradient Profile

At the start of the test, the voltage distribution across the soil columns was linear indicating initial homogeneous electrical properties. However, the voltage potential gradients changed over time with changing resistance of the soil column. It was observed that the first voltage potential gradient near the outflow end increased during the initial part of the test. The first voltage gradient peaked at 2.5 V/cm at 3 days for column A and at 2.75 V/cm at 5 days for column E. The second voltage gradient then decreased and the third voltage gradient increased to a peak of 3.75 V/cm after 7 days for column A and to a peak of 2.75 V/cm at 8 days for column E. This trend of increasing then decreasing voltage gradients with growing distance from the anode was shown to continue up to the end of the test for the fourth voltage gradient. The trend was attributed to the formation of gases clogging the soil pores which increased the soil electrical resistance and the voltage potential gradient measurements.

The summation of the voltage drops across the columns should be equal to the voltage applied. However, the sum of the voltage drops were only about 15 V compared to the 20 V supplied by the constant power supply. This corresponds to a 25% loss in applied voltage at the ends of the columns and at the electrodes. With a current of 0.5 mA the voltage drop across the 1000 ohm resistor is only 0.5 V and does not account for the lower applied voltage. The lower effective voltage is believed to be caused by the increased resistance from air bubbles clogging the ends of the soil columns and the polarization of the electrodes by the electrolysis reactions (Hamed et al. 1991). The effects of the electrolysis reactions are more important with the addition of a surfactant since the rate of electrolysis reactions are increased with the increased current in the presence of surfactant micelles. Since electrolysis reactions reduce the conversion of electrical energy to electrokinetic energy used to transport contaminants, they could be a major problem in the cost of applying electrokinetic remediation (Runnells and Wahli 1993).

6.2.5 Hydrocarbon Concentration Profiles

The results of the hydrocarbon concentration determination in experiment No.1 were erratic and

inconsistent. Problems associated with the determination of BTEX concentration was attributed to solubility problems which were not apparent at the time of sampling. The 250-μL sample aliquots taken from the soil columns were diluted by a factor of 1000 to keep the concentrations below the individual aqueous solubilities of the BTEX compounds. However, it was later discovered that the dilution should keep the hydrocarbon concentration of the sample below the solubilities indicated by Raoult's Law due to the reduction in aqueous solubilities with complex mixtures. Since each column was sampled 15 times from each sampling port (450 samples), and each sample involved at least one hour of sampling and analysis time, a proper dilution protocol could have saved at least 450 hours of work if previously known. Based upon these findings, a new dilution protocol was developed for use in subsequent experiments. This new analytical technique is discussed in section 4.0.

6.3 Preliminary Experiment No.2 on BTEX-Contaminated Sand

6.3.1 Flow Rate

The application of a 7.5 V and 15 V potential difference with water flushing did not result in a significant difference ($\alpha = 0.05$) in the flow rates between the electrical and hydraulic columns. A summary of the

experimental treatment conditions is given in Table 3.2 (p. 58). The average hydraulic conductivity of the hydraulic columns in part A of experiment No.2 was determined as 2.20×10^{-3} cm/sec (% RSD = 40.8%).

During part B of experiment No.2 with 0.25% (w/w) SDS flushing, the average outflow volumes of the electrical and hydraulic columns were not significantly different (α=0.05) similar to part A. During the application of a surfactant solution to the sand columns the effluent became cloudy as a result of the displacement of fines. The average hydraulic conductivities were determined as 1.20×10^{-3} cm/sec (% RSD = 45.6%) and 1.07×10^{-3} cm/sec (% RSD = 37.0%) for the electrical and hydraulic columns respectively. Although there was an increase the average hydraulic conductivity with surfactant flushing in part B, it was not significantly different (α = 0.05) from the average hydraulic conductivity with water flushing.

In part C of experiment No.2 with surfactant and voltage application, the flow rates in the electrical and hydraulic sand columns were not significantly different (α = 0.05). The average hydraulic conductivity of the hydraulic columns was 0.79×10^{-3} cm/sec (% RSD = 44.8%).

6.3.2 Current as a Function of Time

The current in part A of experiment No.2 with a voltage potential difference of 7.5 V was a steady 0.004 mA. When the voltage potential difference was increased to 15 V in part A, the current increased to 0.025 mA after 10.3 days of water flushing. Therefore, 0.0005 mL/h of oxygen gas and 0.0011 mL/h of hydrogen gas would have been produced at the start of part A and 0.008 mL/h of oxygen gas and 0.00168 mL/h at the end of part A. Compared to the measured current in experiment No.1, the addition of SDS at a concentration 0.26% (w/w) increased the current by a factor of 20 with a electrical potential difference of 15 V. The lower gas production in experiment No.2 with water flushing compared to experiment No.1 with surfactant flushing did not lead to clogging of the soil pores as in experiment No.1. The electrical energy for electroosmosis depends upon the fraction of current carried by water relative to the amount of current carried by the other species in solution (Runnells and Wahli 1993). Therefore, the current increase in the presence of a surfactant reduces the amount of energy applied to electroosmotic flow.

Surfactant flushing with a 0.25% SDS solution and an intermittent (20 min on, 10 min off) voltage potential difference of 7.5 V in part C resulted in a current ranging

from 0.2 mA to 0.25 mA. The increase in the current caused by the 0.25% (w/w) surfactant solution caused an increase in the electrolysis of water. Therefore, the effects of pH changes and gas production should increase with the addition of a surfactant.

6.3.3 Voltage Potential Gradient Profile

The average voltage potential gradients in part A of experiment No.1 with a 7.5 V voltage potential difference were initially approximately 0.1 V/cm except near the cathode. Voltage gradients 1 to 5 near the anode (Fig.3.3, p. 59) were increased to 0.2 V/cm when the electrical potential difference was increased to 15 V. The voltage gradient near the cathode was always greater than the other measured voltage gradients. Voltage gradient at the cathode was initially 0.3 V/cm with 7.5 V applied and increased to approximately 1.0 V/cm with 15 V applied after 10.3 days.

In part C with the intermittent application of a 7.5 V potential difference and surfactant flushing with a 0.25% (w/w) solution, the voltage gradients remained relatively constant over 19 days at 0.15 V/cm except near the cathode. The voltage potential gradient near the cathode was higher at approximately 0.25 V/cm for the duration of part C.

6.3.4 Hydrocarbon Concentration Profiles

After injecting 0.5 mL of each BTEX compound into the soil columns, the effluent concentration profiles were measured. The hydrocarbon profiles show the BTEX passing quickly through the sand with the concentration peaking during the first day of the test for both the electrical and hydraulic columns. Benzene was the highest concentration measured in the effluent which is attributed to its relatively higher aqueous solubility. Toluene had the second highest measured concentration since toluene has the second highest solubility among the BTEX compounds. The profiles show toluene peaking at a later time than benzene due to its higher retardation. No clear peak was shown for ethylbenzene and the xylene isomers. The concentration of ethylbenzene and the xylene isomers were measured as approximately 20 mg/L at the start of the test and slowly reduced to less than 5 mg/L after 10 days of water flushing.

With the addition of a surfactant in part B, the hydrocarbon concentration in the effluent increased and the percent of compound removed increased. Therefore, SDS addition improved the efficiency of removal even without the application of a voltage potential.

The measured concentration profiles in part C with surfactant and electrical potential gradient application

were lower than in part A with the largest measured concentration at the first sampling time. It was believed that the BTEX passed through the columns faster than with water flushing and samples could not be taken early enough to obtain a clear concentration profile. The time of peak concentration was probably missed with the sampling leading to lower measured concentrations.

6.4 Experiment No.3 - Model Diesel Fuel in Clay

6.4.1 Flow Rate

Application of water flushing with a constant voltage potential difference of 7.5 V to the electrical columns resulted in the outflow in the electrical columns being significantly higher than the hydraulic columns (Fig. 6.3). This is anticipated because the effects of electrokinetics would be more prominent in clayey soils than the sandy soils used in preliminary experiments No.1 and No.2. A summary of the experimental treatment conditions is given in Table 3.2 (p. 58).

The decrease in the hydraulic conductivity after 42 days is related to the change in the column orientation from the vertical to the horizontal position (Fig. 6.4). The determination of hydraulic conductivity with the columns in the vertical position had errors associated with collecting

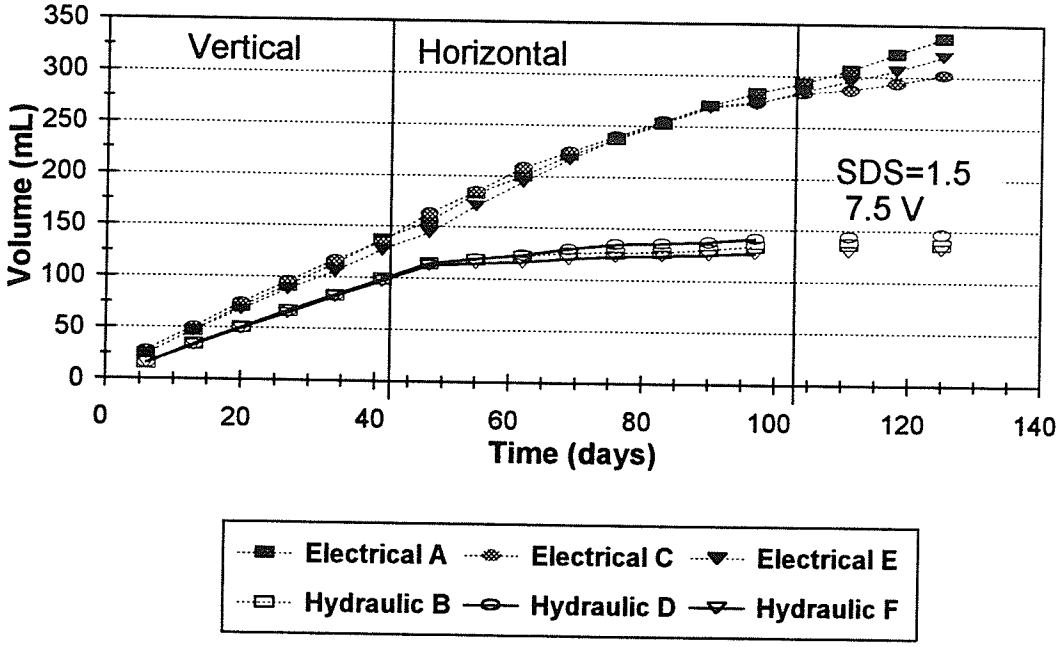

Figure 6.3 Effluent volume collected over time for the six columns in experiment No.3.

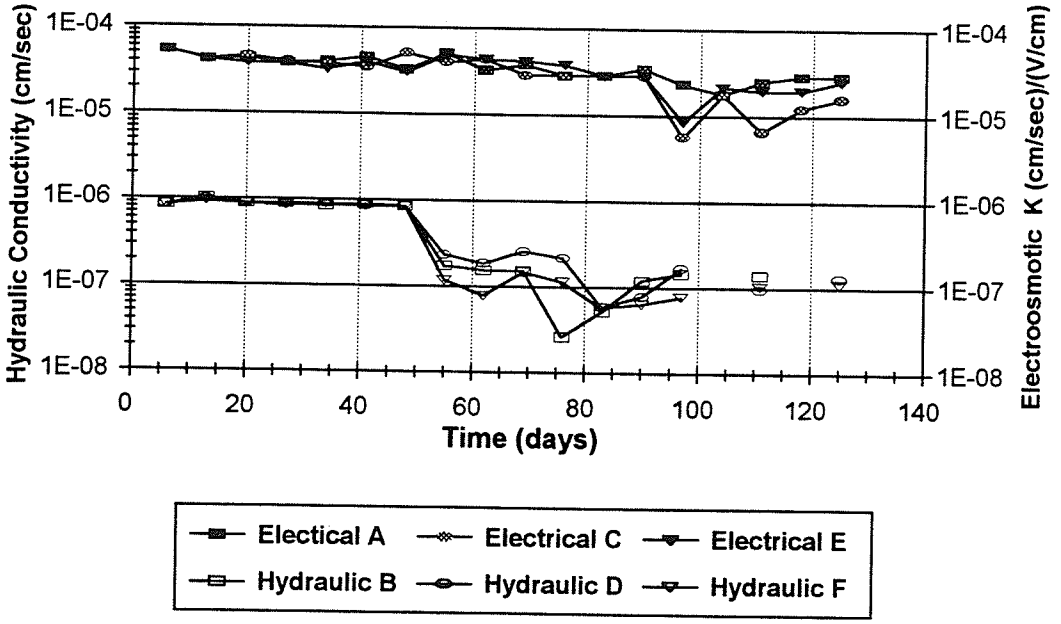

Figure 6.4 Coefficient of electroosmotic permeability of the electrical columns and hydraulic conductivity of the hydraulic columns as a function of time in experiment No.3.

and measuring the small outflow volume collected over time. However, with the set-up changed to the horizontal position, a small volume of outflow could be measured more accurately by bubble movement in the outflow tubing. The average hydraulic conductivity in the hydraulic columns were 8.83×10^{-7} cm/sec (% RSD = 5.4%), 1.28×10^{-7} cm/sec (% RSD = 36.0%), and 1.17×10^{-7} cm/sec (% RSD = 4.7%) with the vertical orientation, horizontal orientation, and addition of surfactant respectively.

There was no effect of the surfactant on the flow rates in the clay columns. The lack of surfactant effects was attributed to the attraction of the anionic surfactant to the anode and the low flow rates. The experimental set-up of locating the anode at the inflow end of the column may have prevented the surfactant from permeating into the electrical columns since the anionic surfactant SDS is attracted to the anode.

The coefficient of electroosmotic permeability remained relatively constant over time (Fig. 6.4). The average coefficient of electroosmotic permeability with water flushing using a voltage potential gradient of 0.05 V/cm was determined as 3.76×10^{-5} (cm/sec)/(V/cm) (% RSD=27.8%). With the application of a surfactant in part C, the coefficient of electroosmotic permeability was measured as 2.00×10^{-5} (cm/sec)/(V/cm) (% RSD = 33.1%) using a voltage

potential gradient of 0.1 V/cm. Acar et al.(1990a) has reported the coefficient of electroosmotic permeability to decrease over time by an order of magnitude. The coefficient of electroosmotic permeability did decrease over time but not to the extent indicated in the literature.

The relatively constant coefficient of electroosmotic permeability and non-reversal of electroosmotic flow can be explained by the uniform pH values measured. The pH of the soil, with the exception of the soil near the electrodes, remained close to 7 and did not drop below the isoelectric point. As defined in section 2.2.2.1, the isoelectric point is the pH where a molecule bears no net charge so that the zeta potential is zero. Below the isoelectric point, the zeta potential changes sign and the electroosmotic flow is reversed. A pH value greater than the isoelectric point keeps the zeta potential of the soil negative and the electroosmotic flow moving toward the cathode. Since the zeta potential of the soil, and hence the coefficient of electroosmotic permeability, is dependent on pH, a uniform pH profile led to a uniform coefficient of electroosmotic permeability. In addition, with the test treatment of a relatively low voltage potential gradient within the clay and a higher hydraulic gradient applied, the hydraulic inflow prevented desaturation of parts of the clay. One of

the reasons that has been attributed to the decrease in electroosmotic flow is the formation of partially unsaturated conditions (Gopinath 1994). Therefore, with the lower voltage potential gradient and higher hydraulic gradient, the formation of partially unsaturated conditions were reduced leading to a steady electroosmotic flow.

6.4.2 Current as a Function of Time

The current at the start of the experiment No.3 with water flushing was 0.6 mA and peaked at 1.7 mA after 65 days of water flushing. At the end of part A, the current decreased to 1.4 mA. With the application of a constant voltage potential difference of 7.5 V with a surfactant concentration of 1.5% (w/w) in part B, the current was initially measured as 1.4 mA and decreased to 1.0 mA after 22 days of treatment. Since the current did not increase with the addition of a surfactant as in the preliminary experiments in sand, it is believed that the surfacant did not permeate into the soil.

The oxygen gas produced at the anode and the hydrogen gas produced at the cathode with an average current of 1.5 mA in part A was calculated at 0.3 mL/hr and 0.63 mL/hr respectively. This corresponds to 7.6 mL and 15.1 mL of oxygen and hydrogen gas produced per day. With the soil

columns in the vertical position, the produced gas partially filled the glass beads at the ends of the soil columns. The produced gases were removed daily to prevent flow restriction. The produced gases caused erratic voltage gradient and current measurements. Since gases were removed from the columns easier when the columns were in the horizontal position, the build-up of gases was reduced resulting in a more uniform current in the electrical columns.

6.4.3 Voltage Potential Gradient Profile

The voltage potential gradients within the clay columns (voltage drops 2 to 5 on Fig. 3.3, p.60) in the vertical position in part A were measured as 0.05 V/cm. This was much lower than the anticipated voltage gradient of 0.25 V/cm due to the voltage loss at the electrodes and electrical resistance of air clogging in the glass beads at the ends of the columns. Higher voltage drops at the cathode have also been found in other research and attributed to increased resistant due to gas formation (Gopinath 1994). Erratic voltage potential gradient measurements were made with the columns in the vertical position due to entrapped gas near the inflow port. With the column orientation changed to the horizontal position,

the voltage potential gradients within the columns were more steady and increased to 0.1 V/cm. The voltage potential gradients at the cathode and anode with the columns in the horizontal orientation were 0.8 V/cm and 0.4 V/cm in part A respectively.

In part B with the addition of a surfactant, the voltage gradients within the columns were measured as 0.1 V/cm similar to the end of part A with water flushing. The voltage potential gradient at the anode remained near 0.4 V/cm and the voltage gradient at the cathode decreased to 0.6 V/cm. The voltage potential gradient remained relatively constant during the electrokinetic treatment and no change with the addition of a surfactant was shown.

6.4.4 Hydrocarbon Concentration Profiles

With the injection of 10 mL of model diesel fuel, the measured concentration profiles gave a much lower concentration than anticipated. The lower concentration was attributed to the contaminants remaining at the injection port due to solubility limitations and to contaminant loss by back diffusion into the influent reservoir. The extraction profiles as shown in section 6.4.5 indicates that most of the model diesel compounds remained at the injection port and did not reach the sampling ports. During the

injection of the model diesel fuel into the clay columns a white cloud and white precipitate formed in the glass beads at the inflow end. This is attributed to the PAHs coming out of solution and precipitating. The presence of a white solid believed to be PAH precipitate was also found during column destruction. In addition, the problem of contaminant loss by back diffusion has been reported in the literature (Hamed et al. 1991). Therefore, measured contaminant concentrations lower than anticipated could partially be due to contaminants back diffusing through the inflow tubing to the constant head source. Contaminant loss may have also occured in the electrical columns during the removal of gases from electrolysis reactions.

The measured concentration profiles indicated that the movement of acetone was greater compared to the other hydrocarbons. In addition, higher acetone concentrations were found closer to the cathode in the electrical columns compared to the hydraulic columns. Therefore, acetone transport was enhanced with the application of the electrical gradient. There were also increased benzene and toluene concentrations toward the cathode indicating that the compounds were moving toward the cathode. There was no apparent concentration difference for the other more hydrophobic model diesel fuel compounds in the electrical and hydraulic columns. Therefore, the more hydrophobic

compounds did not significantly move from the point of injection even in the electrical columns. In addition, the xylene isomers and PAHs were not measured at the sampling ports 10.5 and 17.0 cm from the point of injection (15 and 21.5 cm from anode).

6.4.5 Hydrocarbon Extraction Profiles

The hydrocarbon concentration profiles from the extraction samples indicate that there was little contaminant transport for the model diesel fuel compounds (Fig. 6.5). Naphthalene, 2-methylnaphthalene, and phenanthrene all remained at the point of injection. This corresponded well with the measured concentration profiles determined from pore fluid sampling. The more water-soluble acetone was the only compound that moved throughout the soil column during the test. Toluene, ethylbenzene, and the xylene isomers were not found near the outflow end in both the hydraulic and electrical columns. However, the concentration extraction profiles indicate that toluene, ethylbenzene, and the xylene isomers all had significantly higher concentrations in the hydraulic columns compared to the electrical columns. Based upon the higher flow rate in the electrical columns compared to the hydraulic columns and the lower concentrations of ethylbenzene and xylene isomers

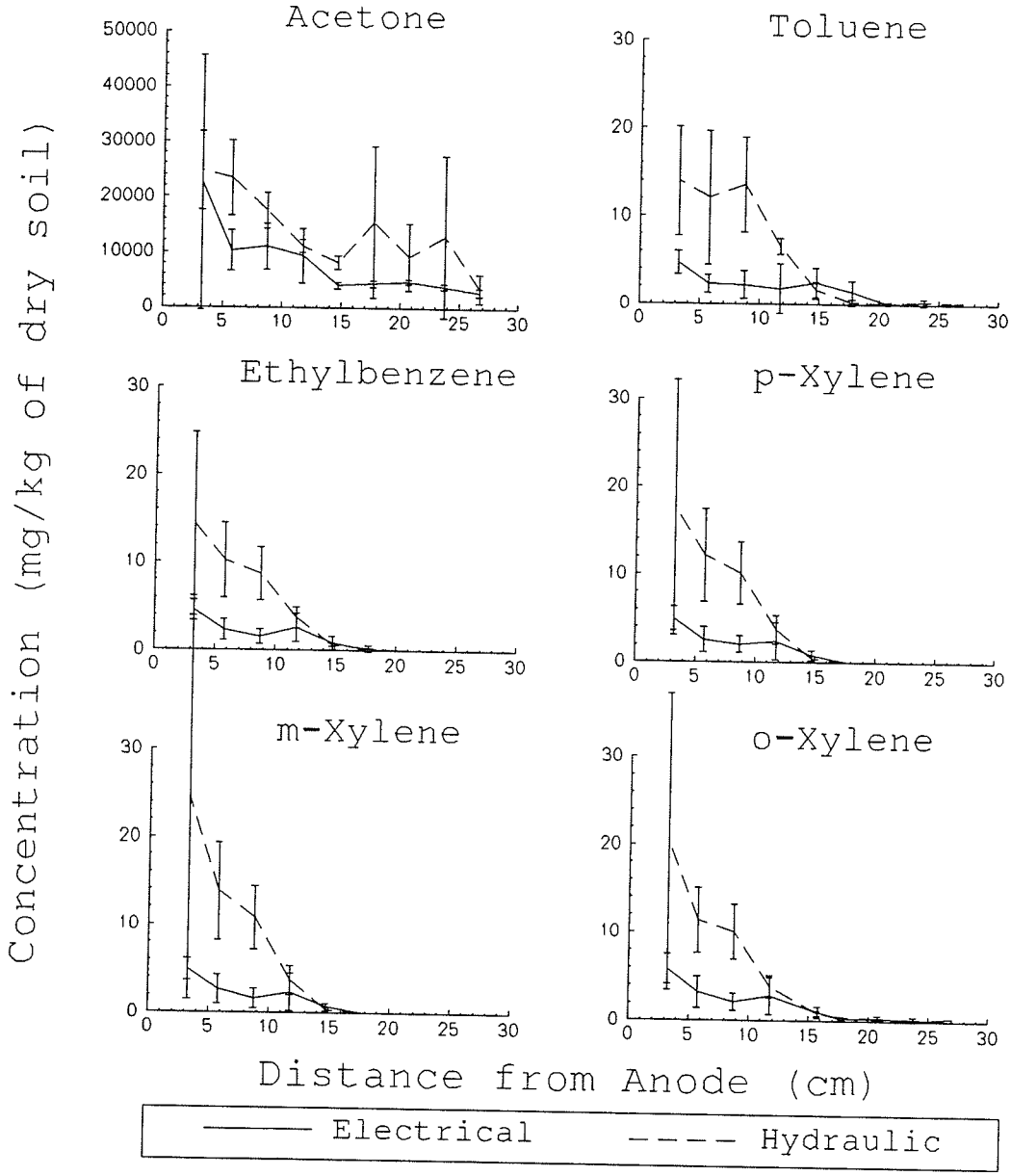

Figure 6.5 (a) Hydrocarbon concentration extraction profiles for acetone, toluene, ethylbenzene, and the xylene isomers at the end of experiment No.3 with the 95% confidence limits indicated by error bars.

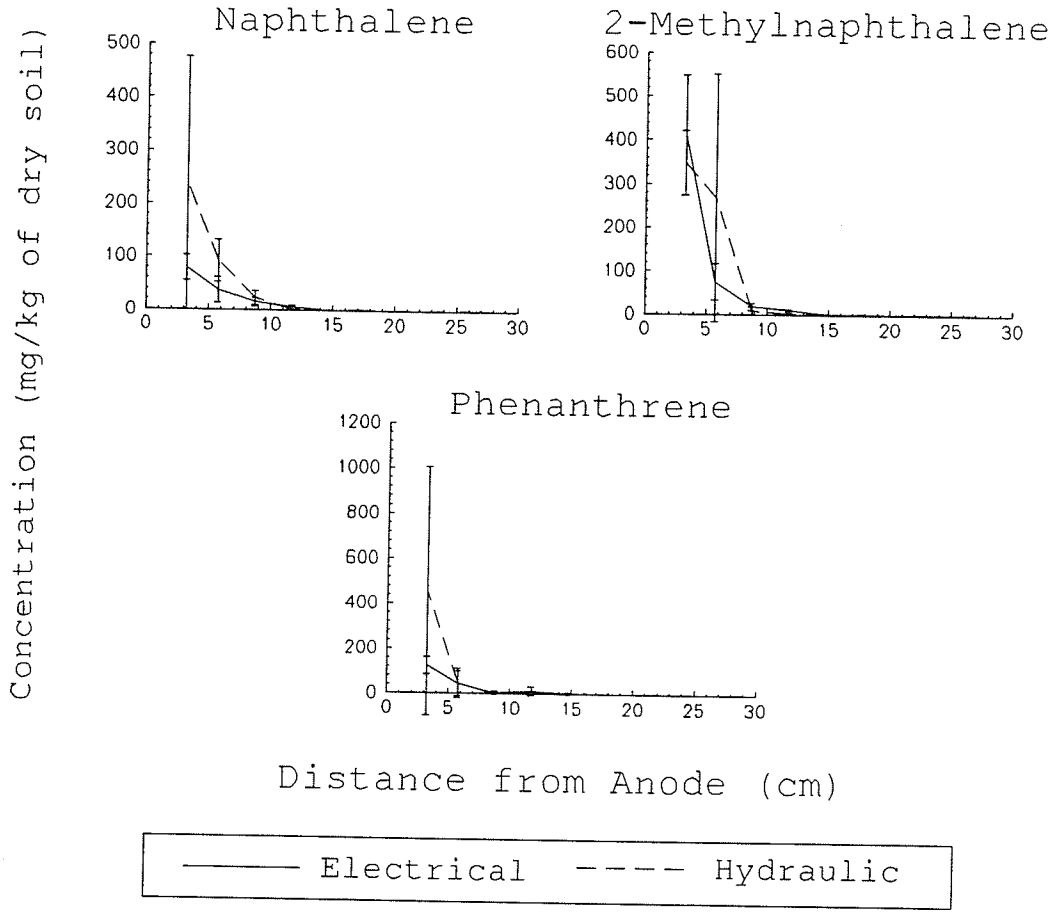

Figure 6.5 (b) Hydrocarbon concentration extraction profiles for naphthalene, 2-methylnaphthalene, and phenanthrene at the end of experiment No.3 with the 95% confidence limits indicated by error bars.

compounds in the electrical columns, the compounds should have been transported further into the columns than indicated in the extraction concentration profiles. The

reason for this discrepency is attributed to greater contaminant loss in the electrical columns occuring when removing gases generated by the elecrolysis reactions.

6.4.6 pH Profile

The pH profile of the electrical columns was similar to other soil columns after electrokinetic treatment in that a highly acidic pH of 2.7 was measured at the anode and a highly basic pH of 11.2 was measured at the cathode (Fig. 6.6). The pH at the anode sharply increased to 6.1 over a distance of 3 cm. The measured pH profiles differ from other research which found that the acidic front was transported throughout the soil and only the cathode region remained alkaline (Acar et al. 1990a; Acar et al. 1990b). The lack of the formation of an acid front in the soil columns anticipated after long periods of electrokinetic remediation can be explained by the clay soil having a high buffering capacity and the limited inflow into the clay columns. However, the lack of acid front formation has also been found in other work (Gopinath 1994).

The pH profile of the hydraulic columns was uniform with the pH close to 7. There was a trend to more acidic values toward the cathode.

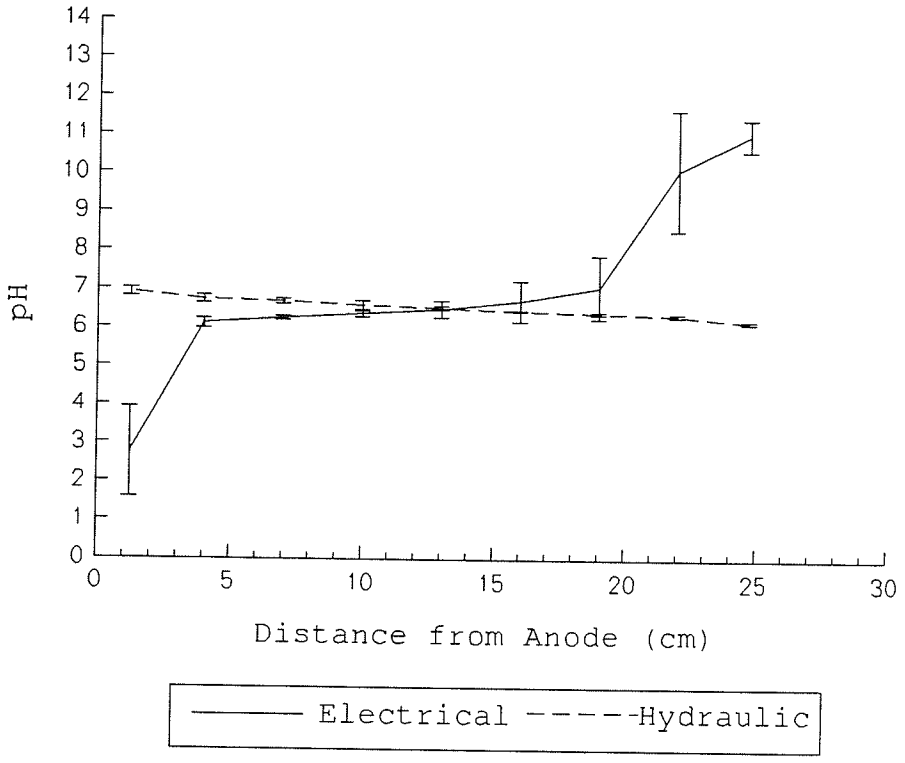

Figure 6.6 pH profiles of the electrical and hydraulic columns at the end of experiment No.3 with the 95% confidence interval indicated by error bars.

6.4.7 Water Content Profile

The water content profile indicated that the electrical columns had a lower water content than the hydraulic columns (Fig. 6.7). However, the gravimetric water contents were only significantly different at the cathode. This is anticipated since electroosmotic flow, especially with the higher voltage potential gradient at the cathode, drains the pore fluid from the clay faster than can be replenished from the anode.

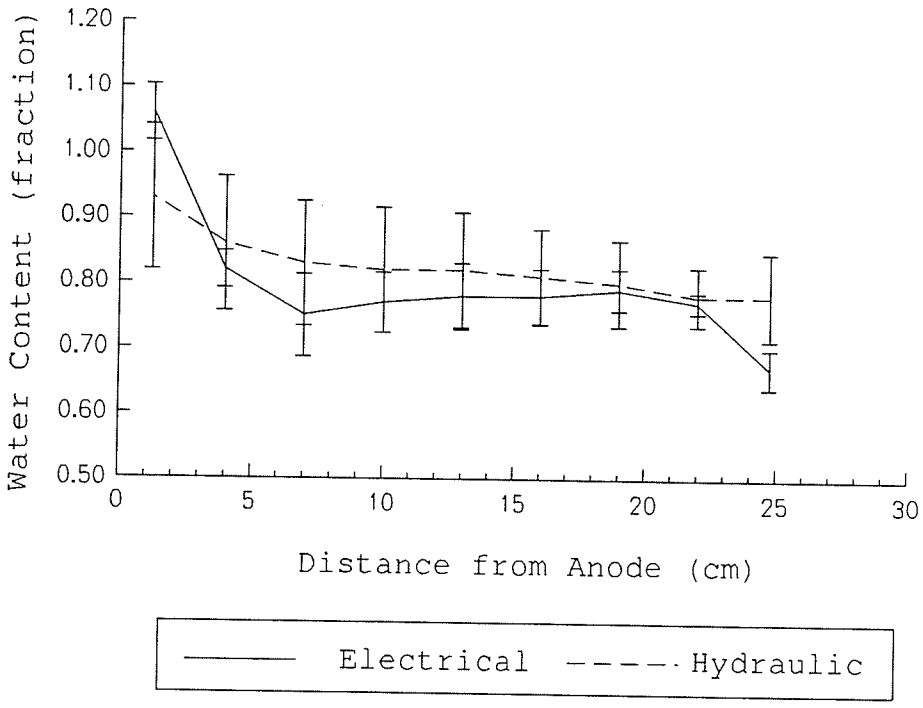

Figure 6.7 Gravimetric water content profile of the electrical and hydraulic columns at the end of experiment No.3 with the 95% confidence interval indicated by error bars.

6.4.8 Dry Bulk Density Profile

The dry bulk density of the hydraulic and electrical were not significantly different (α = 0.05) (Fig. 6.8). The dry bulk density of the clay columns ranged from 0.55 g/cm^3 to 0.85 g/cm^3 with the lower dry bulk density being at the inflow end of the columns.

When the columns were switched to the horizontal position after 42 days of remediation treatment the top 3 cm of clay soil near the cathode was replaced with glass beads to allow gas to escape. During the removal of the clay, it was observed that the clay had become consolidated and stronger than the rest of the column. The strengthened clay was more difficult to remove in the electrical columns compared to the hydraulic columns.

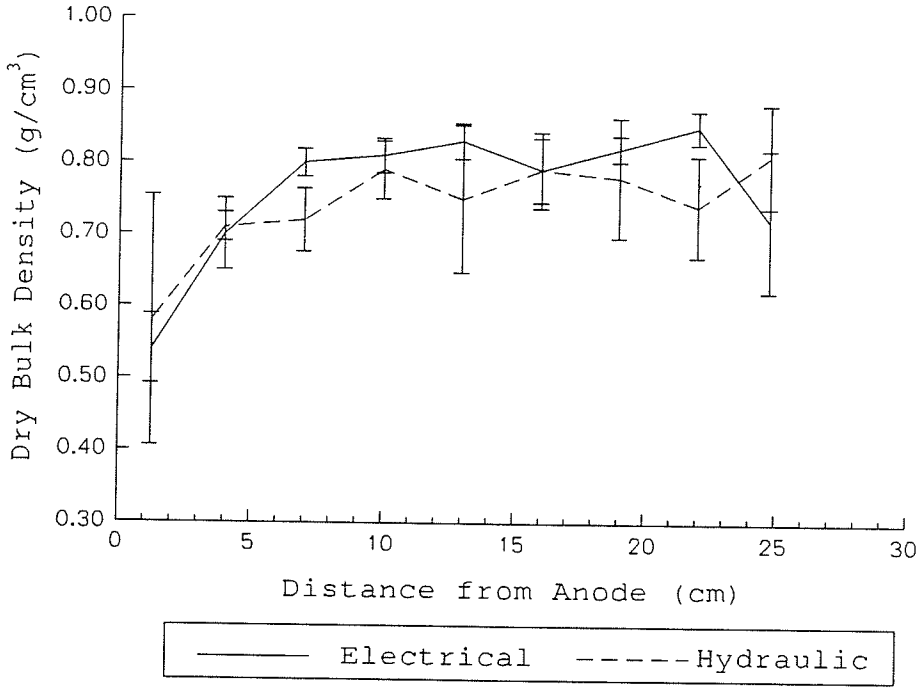

Figure 6.8 Dry bulk density profiles of electrical and hydraulic columns at the end of experiment No.3 with the 95% confidence interval indicated by error bars.

6.5 Experiment No.4 - Model Diesel Fuel in Clay

6.5.1 Flow Rates

The flushing of a surfactant with a concentration of 1.5% (w/w) with a voltage potential difference of 20 V resulted in the electrical columns having significantly higher outflow than the hydraulic columns (Fig. 6.9). The average coefficient of electroosmotic permeability was determined as 1.11×10^{-5} (cm/sec)/(V/cm) (% RSD = 34.2%) (Fig. 6.10) and average hydraulic conductivity was measured as 2.54×10^{-7} cm/sec (% RSD = 43.6%) (Fig. 6.11).

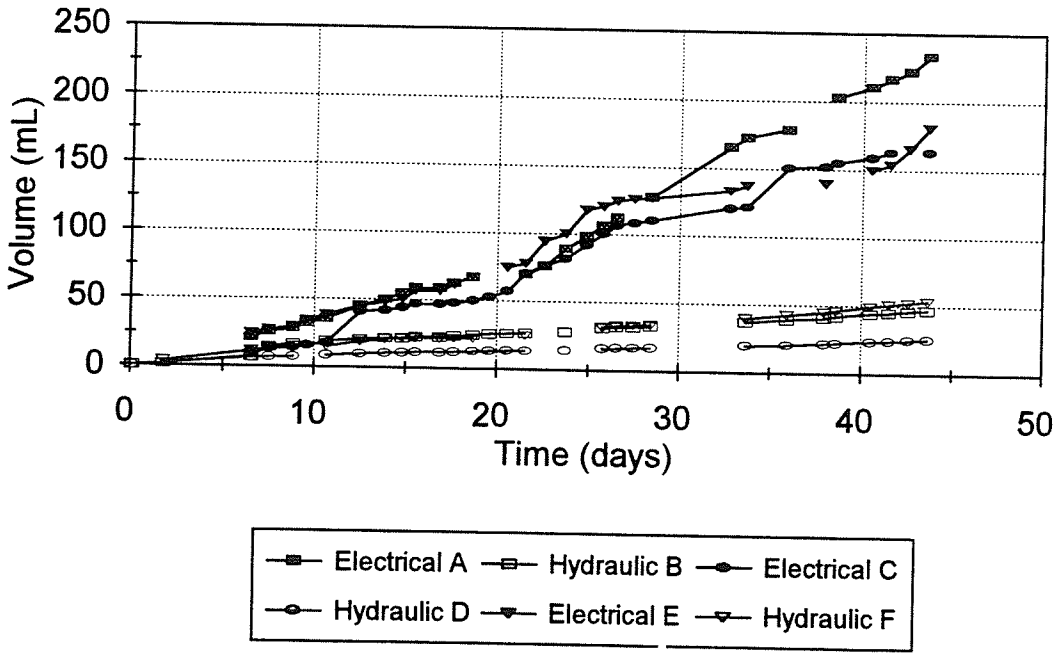

Figure 6.9 Effluent volume collected over time for the six columns in experiment No.4.

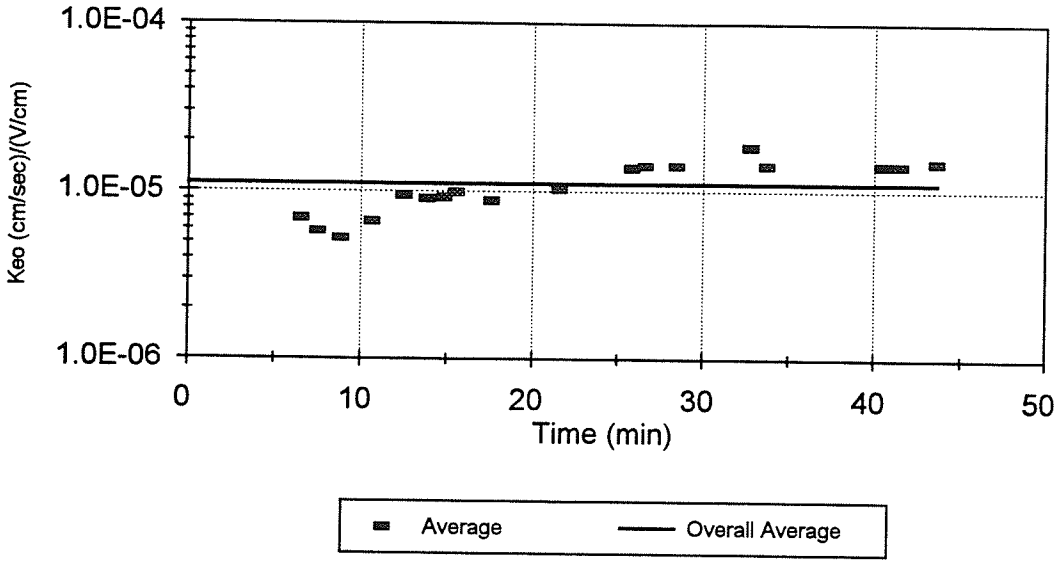

Figure 6.10 Average coefficient of electroosmotic permeability measured in experiment No.4.

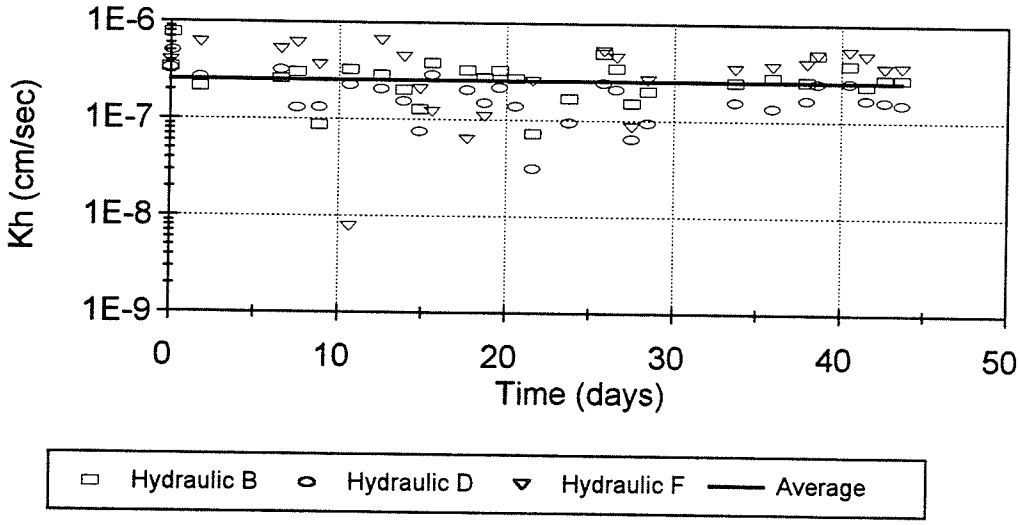

Figure 6.11 Average hydraulic conductivity measured in experiment No.4.

6.5.2 Current as a Function of Time

The average current at the start of the experiment was 3.75 mA and increased to 6.0 mA after 43 days of treatment. The rate of oxygen and hydrogen gas production was calculated as 0.75 mL/h and 1.6 mL/h at the start of the test and 1.2 mL/h and 2.5 mL/h at the end of the test respectively.

6.5.3 Voltage Potential Gradient Profiles

The average voltage gradients within the clay column were initially 0.1 V/cm and increased to 0.25 V/cm at the end of the test. The voltage potential gradients at the electrodes were higher than the gradients measured within the clay columns. The voltage potential gradient at the cathode was initially 0.75 V/cm and increased to 3.0 V/cm after 10 days, then decreased to 1.25 V/cm after 43 days at the end of the test. The gradient at the anode was initially 1.75 V/cm and decreased to 0.4 V/cm at the end of the test.

The sum of the average voltage drops across the columns was equal to the applied voltage. Therefore, the voltage potential gradient measurements were accurate in all the experiments.

6.5.4 Electrical Conductivity and pH Measurement

The electrical conductivity of the influent reservoir containing the 1.5% (w/w) SDS solution was a constant 1.5 dS/m (Fig. 6.12). The electrical conductivity of the combined anode fluid of the electrical columns ranged from 4 to 5 dS/m. The electrical conductivity of the effluent of the electrical samples steadily increased over time up to 23 dS/m after 40 days (Fig. 6.13). The linear relationship of electrical conductivity at the cathode as a function of time fitted through the origin is given as ($r^2 = 0.87$),

$$EC = 0.619\ days \tag{54}$$

where:

EC = electrical conductivity (dS/m),

days = time (days).

Since the outflow volume was accumulated over time, the increase in electrical conductivity is related to the increased OH^- concentration caused by the electrolysis of water over time.

The pH of the effluent of the electrical columns was within the range of 12-13 during the electrokinetic treatment (Fig. 6.14). The pH of the combined anode fluid in the electrical columns was constantly acidic at a pH

value close to 2. The influent reservoir originally had a neutral pH but grew more acidic with the back diffusion of the hydrogen ion from the anode into the reservoir over time. The pH values of the influent and effluent are similar to other results reported in the literature (Acar and Alshawabkeh 1993).

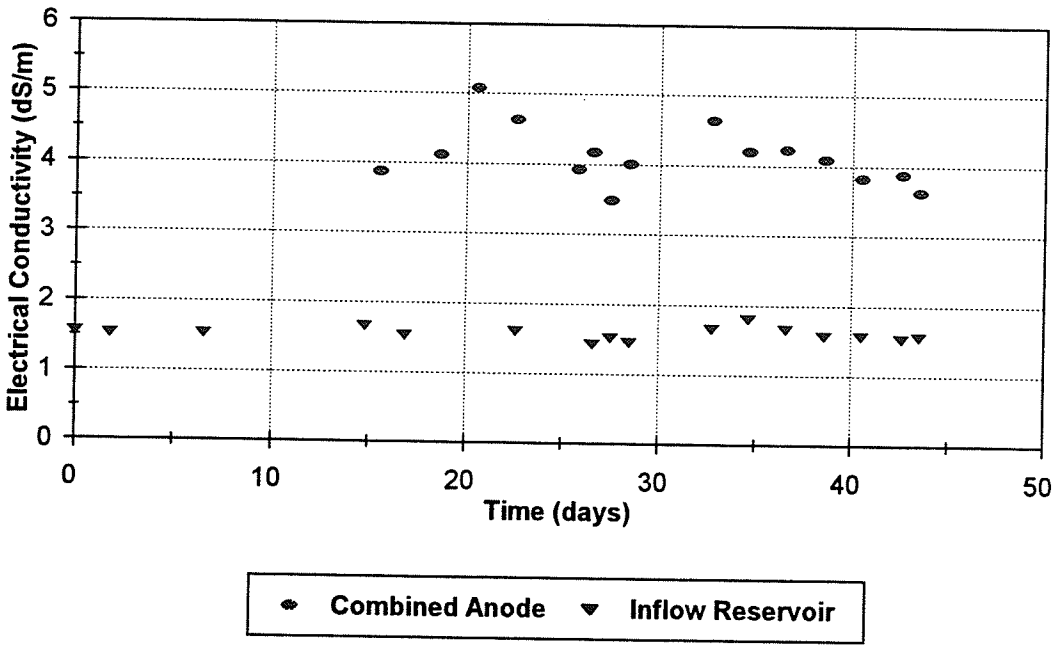

Figure 6.12 Electrical conductivity measured at the anode and the influent reservoir over time in experiment No.4.

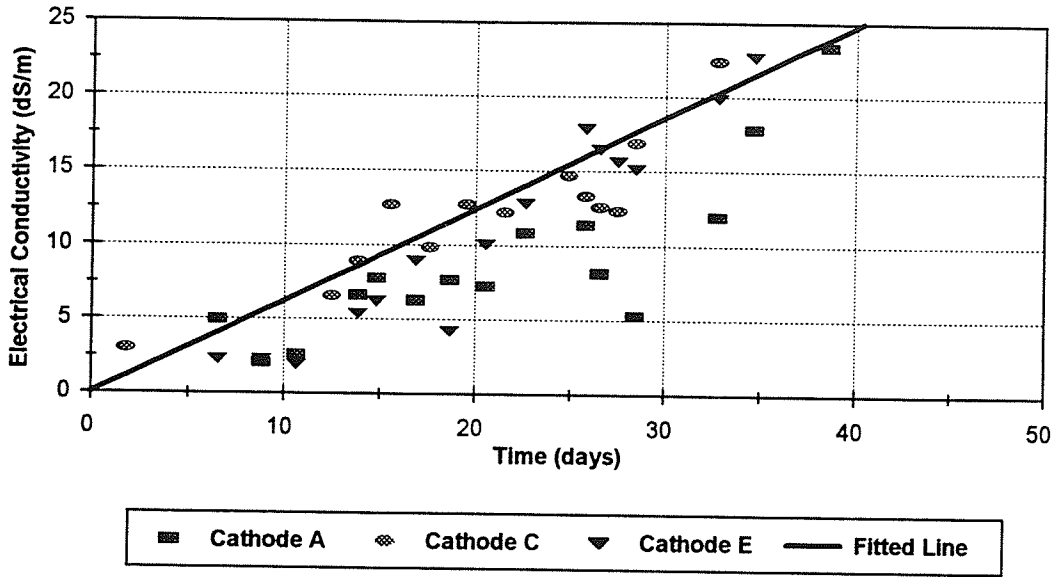

Figure 6.13 Electrical conductivity of the effluent in the electrical columns over time in experiment No.4.

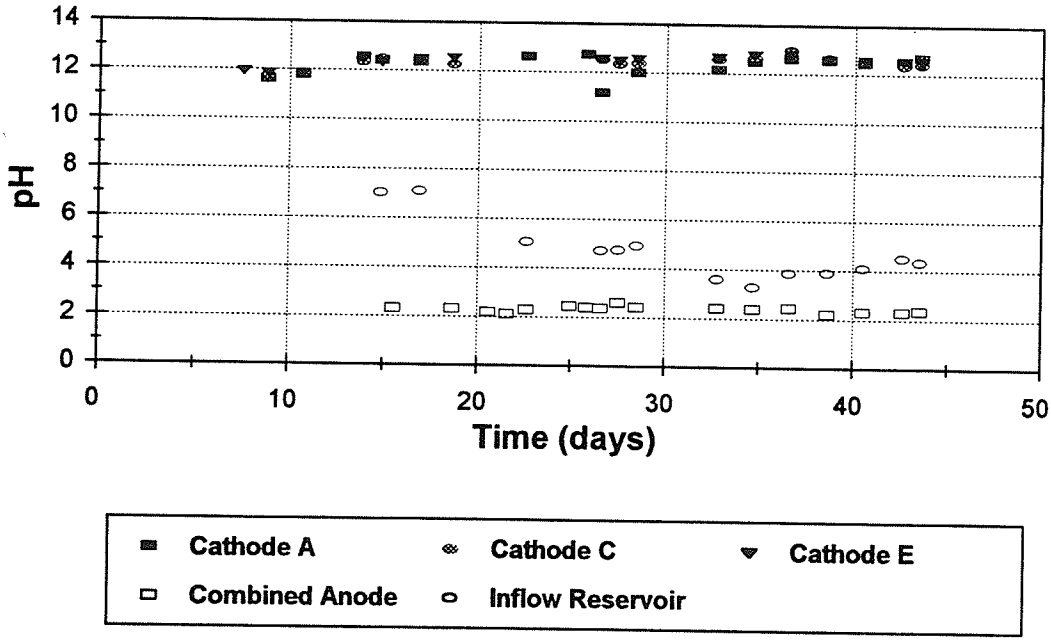

Figure 6.14 pH measured at the cathode, anode, and influent reservoir over time in experiment No.4.

6.5.5 Hydrocarbon Concentration Profiles

The concentration profiles indicate the more water-soluble acetone moved faster in the electrical columns compared to the hydraulic columns. The acetone concentration at the injection port steadily dropped and the acetone concentration at sampling ports further along the column increased over time. The average acetone concentration in the hydraulic columns was higher at the injection port and lower at the other sampling ports compared to the electrical columns. Therefore, acetone was transported more efficiently in the electrical columns.

The concentration profiles for benzene and toluene were similar to acetone. The concentrations were reduced over time at the injection port and increased over time at the sampling ports. However, there was no difference in concentration profiles in the electrical and hydraulic columns for benzene and toluene.

The hydrocarbon concentration measured at the injection port for ethylbenzene, the xylene isomers, and the PAHs was steady for the hydraulic columns but was reduced over time in the electrical columns. The measured concentrations for these compounds were not different in the electrical and hydraulic columns at sampling ports further from the point of injection.

6.5.6 Hydrocarbon Extraction Profiles

The hydrocarbon extraction profiles indicate that acetone and toluene were transported faster in the electrical columns than in the hydraulic columns (Fig. 6.15). After 43 days of electrokinetic treatment with a surfactant, the peak acetone concentration was 9 cm further in the electrical column than the hydraulic column. Similarly, the peak concentration for toluene was 3 cm further in the electrical columns. The peak concentrations were similar in the hydraulic and electrical columns for the other model diesel fuel compounds. The less water-soluble compounds remained at the injection port. The lack of movement of the more hydrophobic contaminants indicates that the surfactant did not permeate into the soil and enhance transport.

6.5.7 pH Profile

The pH profiles of the soil columns in experiment No.4 were similar to experiment No.3 where the anode became acidic and the cathode became alkaline (Fig. 6.16). In the electrical columns, the average pH of the soil was 2.15 and 12.73 at the anode and cathode respectively after 43 days of electrokinetic treatment. The pH profile in the hydraulic columns was always close to 7 with the outflow end being more acidic similar to experiment No.3.

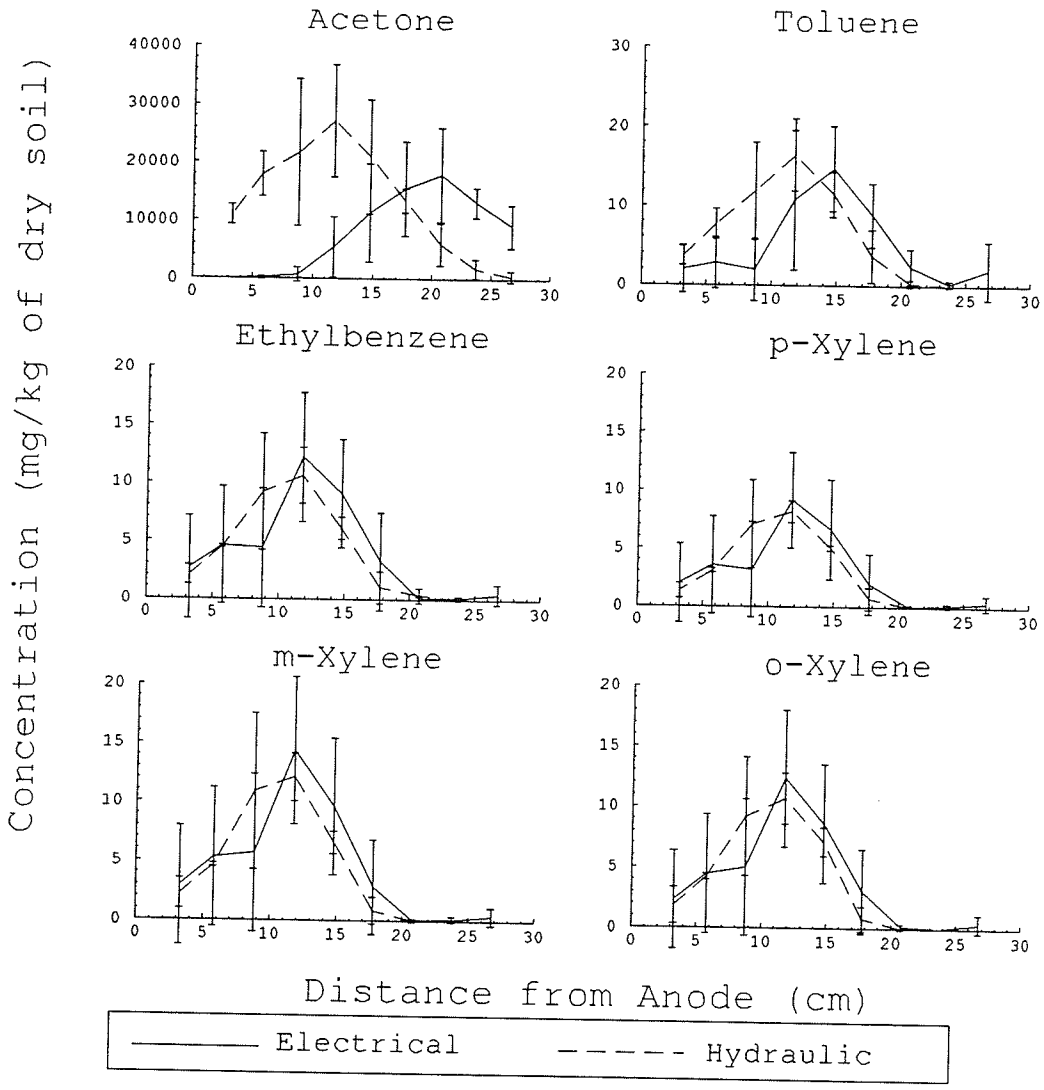

Figure 6.15 (a) Hydrocarbon concentration extraction profiles for acetone, benzene, toluene, ethylbenzene, and the xylene isomers at the end of experiment No.4 with the 95% confidence limits indicated by error bars.

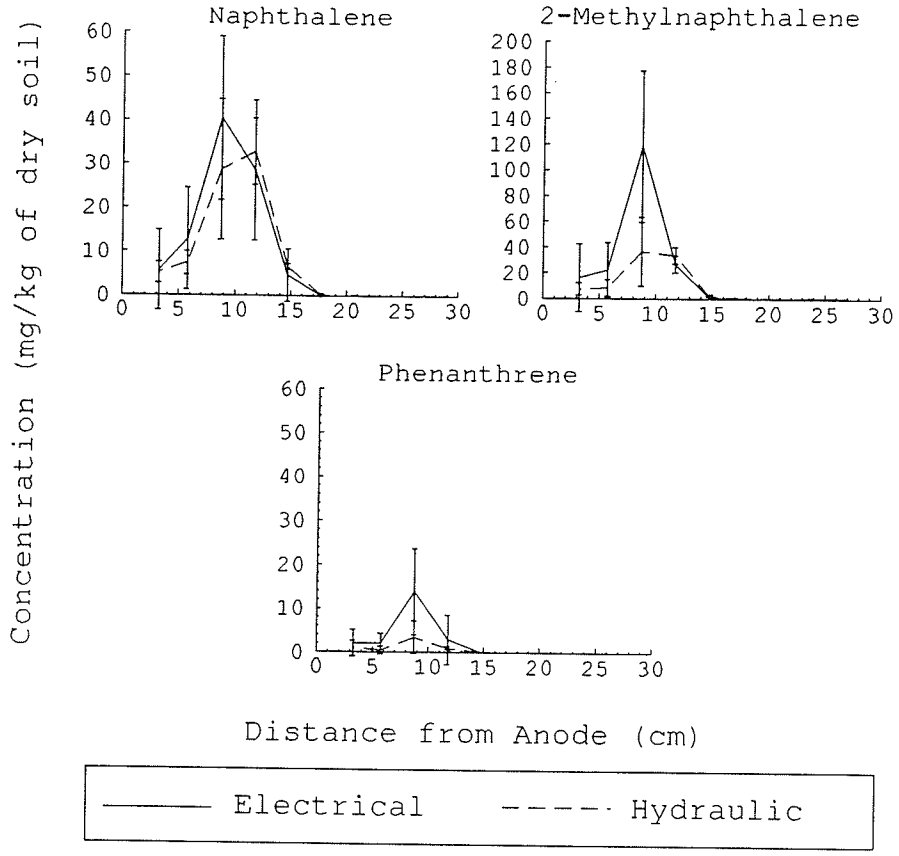

Figure 6.15 (b) Hydrocarbon concentration extraction profiles for naphthalene, 2-methylnaphthalene, and phenanthrene at the end of experiment No.4 with the 95% confidence limits indicated by error bars.

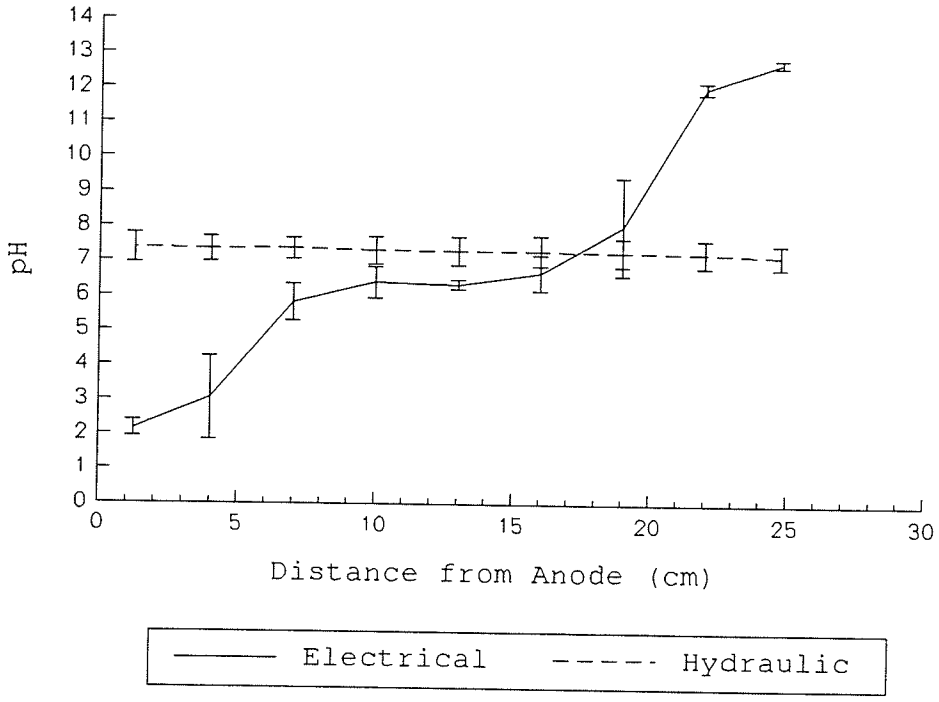

Figure 6.16 pH profiles in the electrical and hydraulic columns after 43 days of surfactant-enhanced electrokinetic remediation with the 95% confidence interval indicated by error bars.

6.5.8 Water Content Profile

The gravimetric water content profile indicated that the electrical columns were significantly drier than the hydraulic columns (Fig. 6.17). The gravimetric water content profile in the electrical columns indicates that electroosmotic flow led to draining of pore fluid from within the clay faster than could be replaced at the anode under the given treatment conditions.

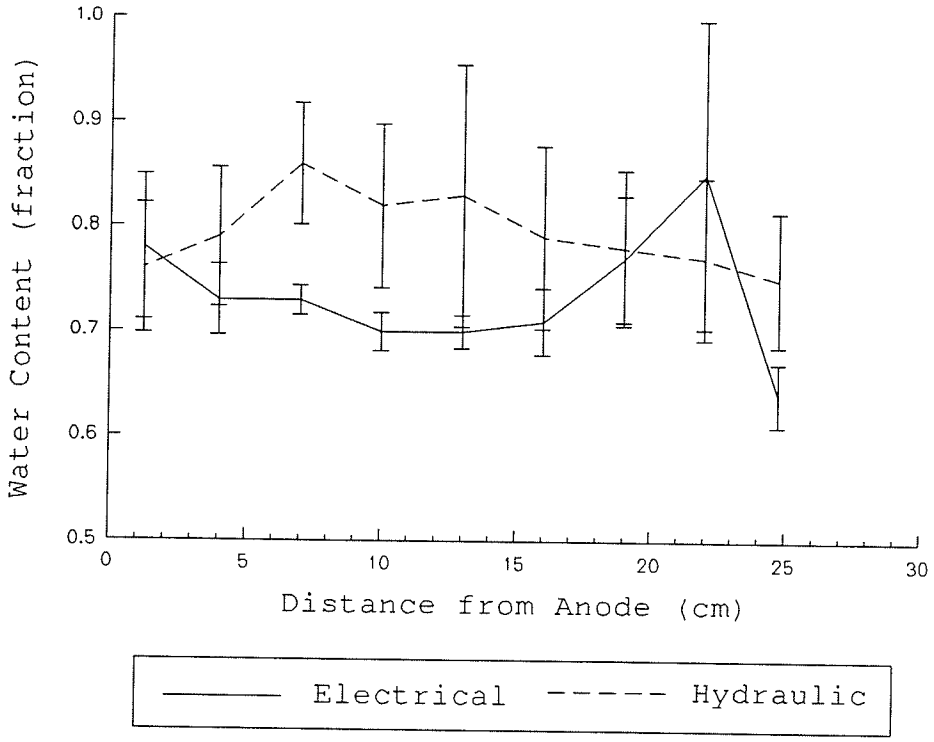

Figure 6.17 Gravimetric water content profiles for the electrical and hydraulic columns at the end of experiment No.4 with the 95% confidence interval indicated by error bars.

6.5.9 Dry Bulk Density Profile

The dry bulk density of the hydraulic and electrical columns were not significantly different (Fig. 6.18). The dry bulk density ranged from 0.76 to 0.87 g/cm^3 for the electrical columns and 0.62 and 0.77 in the hydraulic columns.

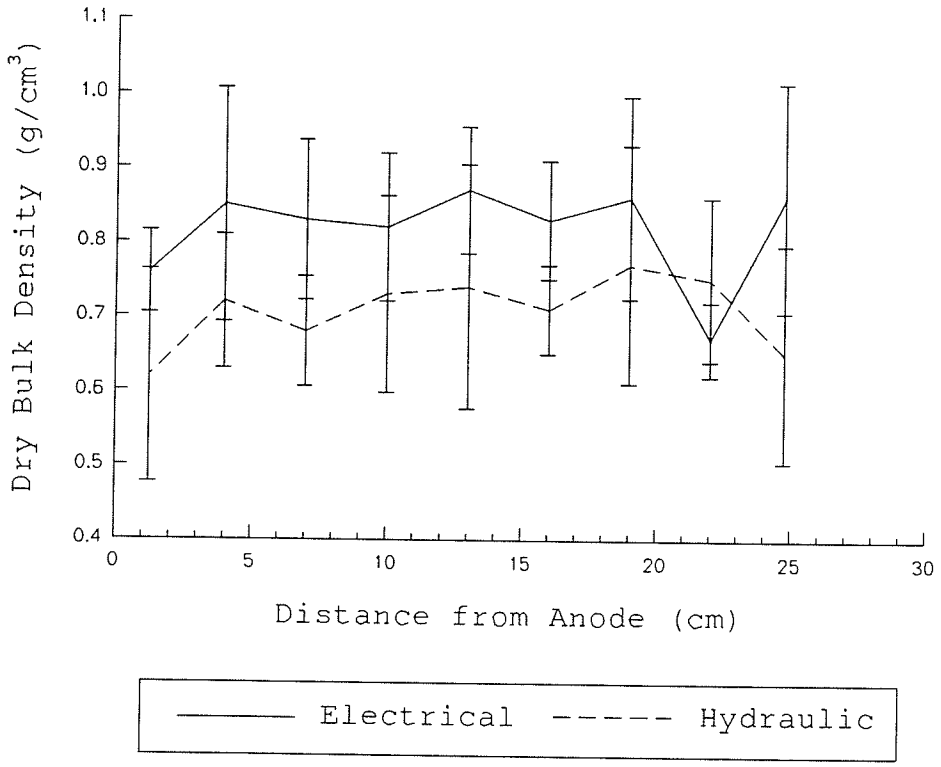

Figure 6.18 Dry bulk density profiles in the electrical and hydraulic columns at the end of experiment No.4 with the 95% confidence interval indicated by error bars.

6.6 Comparison of Results to Model

6.6.1 Introduction

Preliminary experiment No.1 on sand was not modelled because of problems in the flow rate measurement due to air clogging of the soil pores and inaccuracy in measured hydrocarbon concentration profiles. Part A of preliminary experiment No.2 on sand with water flushing and voltage

potential difference application was modelled using the ADRE equation. Although part A of experiment No.2 imposed two voltage potential differences, the measured concentration profiles indicated that most of the BTEX compounds were flushed quickly through the columns with the conditions of a constant voltage of the same magnitude. Therefore, the model, which assumes a constant voltage potential difference of the same magnitude, could be used to model the contaminant transport. Part B of experiment No.2 could not be modelled since the contaminants were already dispersed before the application of a surfactant. Therefore, experimental conditions violated the model assumption of a constant point source of contamination. Part C of experiment No.2 could not be modelled since the voltage potential difference was applied intermittently and the model assumes a constant voltage potential difference throughout the experiment.

Concentration profiles were predicted in part A of experiment No.3 and experiment No.4 using the ADRE equation. Part B of experiment No.3 was not predicted since the model assumes constant treatment conditions and an instantaneous point source of contamination. Since the contaminants were dispersed prior to the application of a surfactant, part B of experiment No.3 could not be predicted using the model.

6.6.2 Experiment No.2

Part A in experiment No.2 was modelled using the applied experimental conditions and a range of plausible modelling parameters determined from literature along with measured experimental values (Table 6.4). The predicted range of the benzene concentration profile in the effluent indicates that the time of peak concentration ranges between 8 hours and 4.5 days (Fig. 6.19). The large range of plausible concentration profiles indicates that the model is sensitive to the chosen values of the modelling parameters. Care must be taken to accurately determine model input parameters to achieve a confident prediction of concentration profiles. The magnitude of the predicted peak concentration is greater than 200 000 mg/L. Modelling of the other BTEX compounds indicate that the time of peak concentration increases as the hydrophobicity of the compound increases. The time range of the predicted benzene concentration peak corresponds well with the measured data where the maximum concentration in the effluent was determined at the first sampling period at 1 day after injection (Fig. 6.19). The peaks of the predicted concentration profiles are not shown in figure 6.19 since the magnitude of the predicted peaks are beyond the scale of the measured concentrations. The tailing in the measured

concentration profile is related to trapped free-phase benzene which forms a long term source of contamination. Note that the predicted and measured concentration profiles for both the electrical and hydraulic columns are not shown in Figure 6.19 since they were found to be similar.

Table 6.4 Plausible Range of Modelling Parameters

Modelling Parameter	Plausible Range	
	Experiment No.2	Experiment No.4
	Sand	Clay
α_L (cm)	0.01 - 0.1	0.0.1 - 1.0
ρ_b (g/cm^3)	1.55 - 1.65	0.8 - 0.9
f_{oc}	0.01 - 0.0001	0.01 - 0.05
D_x (cm^2/sec)	1×10^{-5} - 1×10^{-6}	1×10^{-5} - 1×10^{-6}
K_h (cm/sec)	1×10^{-3} - 5×10^{-3}	1×10^{-6} - 5×10^{-8}
K_{eo} (cm/sec)/(V/cm)	1×10^{-4} - 5×10^{-5}	1×10^{-4} - 5×10^{-5}
dE/dx (V/cm)	0.1 - 0.2	0.05 - 0.2

Discrepancy between the predicted and modelled data occurs since the maximum concentration measured in the experiments was much less than the predicted maximum concentration. The largest experimentally measured concentration was 300 mg/L for benzene. The main reason attributed to the higher predicted concentrations compared to the measured concentrations was lack of samples early in

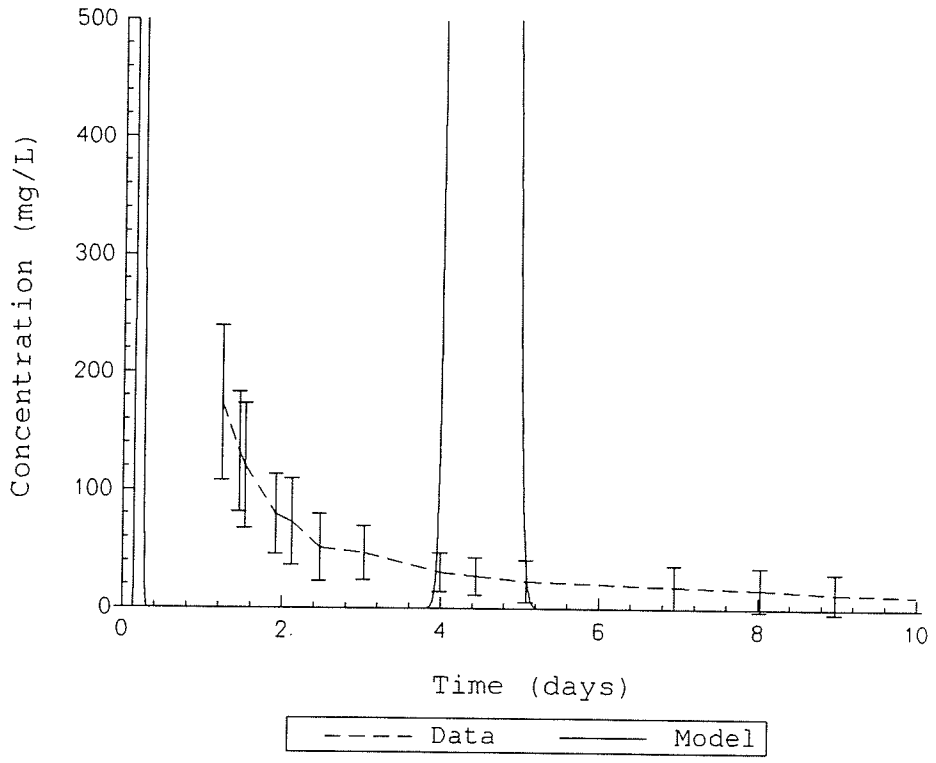

Figure 6.19 Comparison of experimental measured concentration profile to plausible predicted concentration profiles for benzene in the effluent in experiment No.2.

the experiment which resulted in missing the peak in the concentration profile. It is believed that if samples were taken early in the experiment using the new dilution protocol, the high concentration BTEX-profile predicted by the model would have been determined. The discrepancy between the predicted and measured peak concentration can also be partially attributed to loss of BTEX back into the

influent reservoir. Since the BTEX compounds are soluble in water and the influent reservoir has a large volume which forms high concentration gradients, some of the BTEX compounds could have been lost by back diffusion. There may also have been some loss of the volatile compounds due to a time lag between sampling and analysis caused by GC down time. Another reason attributed to the discrepancy between the measured and predicted results is the formation of free-phase. The formation of free-phase leads to errors in predicted concentration since free-phase is not taken into account in the model. The concentration values predicted by the model, assuming that all compounds are in solution, are much higher than the aqueous solubilities of the compounds. It is believed that the model would better predict results if a lower amount of compound were injected into the columns to avoid the formation of free-phase and if care was also taken to prevent contaminant loss due to back diffusion.

6.6.3 Experiment No.3

The contaminant concentration profiles with water flushing in part A of experiment No.3 were predicted by the ADRE model using estimated modelling parameters. The predicted concentration profiles were in correspondence with experimental results where only the more water-soluble

acetone, benzene, and toluene compounds were transported to the middle sampling port (10.5 cm from the point of injection). The more hydrophobic compounds were predicted to remain at the injection point similar to the measured experimental concentration profiles and extraction results. No figure is shown due to the lack of measured samples in part A caused by the clogging of the sampling syringe with clay particles.

6.6.4 Experiment No.4

The modelling of treatment conditions in experiment No.4 with surfactant flushing indicated that the compounds did not move into the electrical columns. The electrophoretic flow was modelled to be much greater than the electroosmotic flow which prevented contaminant transport into the columns toward the cathode and the sampling ports. Therefore, the predicted concentration profiles were not shown to develop within the column. However, the measured concentrations in the test indicated that the contaminants were transported within the column and that the electrical columns had greater contaminant transport. The discrepancy between the model and experiment results can be explained by the fact that the surfactant did not infiltrate into the soil. Flow rate and current

measurements also indicate that the surfactant did not permeate into the soil. Without the influence of a surfactant there is no electrophoretic transport and, therefore, no retardation of the electroosmotic transport. Since the surfactant was believed not to enter the soil, experiment No.4 was modelled assuming water flushing conditions. Assuming no surfactant infiltration and water flushing conditions, predicted concentration profiles were much closer to the measured concentration profiles.

The modelling of experiment No.4 with water flushing and plausible range of modelling parameters given in Table 6.3 indicate a large variation in the predicted concentration profiles (Fig. 6.20). The concentration profile for benzene at 6.5 cm from the point of injection has the low range plausible concentraton profile ploting directly along the x-axis at a concentration of zero. The slow concentration profile predicted for benzene only starts to increase near the end of the experiment. The predicted concentration profiles in the electrical columns using the modelling parameter causing fast contaminant transport shows benzene being transported entirely past the point located 6.5 cm from the point of injection. The benzene concentration predicted for the hydraulic columns is slower than the electrical columns which indicate enhanced transport in the electrical columns over the hydraulic

columns. The large range in the predicted concentration profiles with the plausible range of modeling parameters indicate that modelling parameters must be accurately determined.

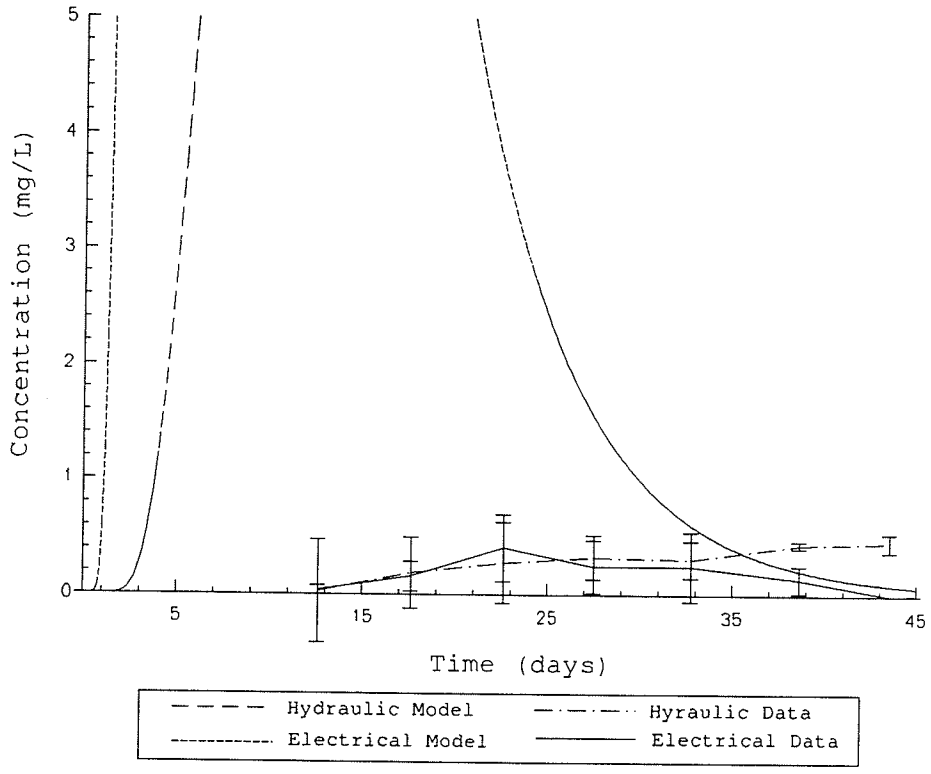

Figure 6.20 Comparison of experimental results for benzene 6.5 cm from point of injection in experiment No.4 to plausible predicted concentration profiles.

Predicted concentration profiles for other model diesel fuel compounds indicate that only the more water-soluble compounds of acetone, benzene, and toluene were predicted to be transported to the middle sampling port (6.5 cm from

point of injection) during the 43-day test. The measured concentration profiles indicate that the hydrophobic compounds were not detected at the concentration port 6.5 cm from the point of injection. The lack of movement for the more hydrophobic compounds was also shown in the measured concentration profiles and in the hydrocarbon extraction profiles.

As with the possible errors discussed in section 6.6.2, errors in the prediction of the experimental results could occur due to the formation of free-phase and precipitation of the PAHs.

6.7 Sensitivity Analysis

6.7.1 Introduction

A sensitivity analysis was performed on the model fitted to the experimental data to identify the importance of various physical and chemical factors on electrokinetic remediation. Various parameters were individually changed systematically and the change in concentration was determined. The magnitude of the change in concentration resulting from the change in the parameter indicates the sensitivity of that parameter (Anderson and Woessner 1992).

6.7.2 Sensitivity Analysis of Experiment No.4 - Water Flushing

The sensitivity of the parameters used in modelling experiment No.4 under water flushing conditions were evaluated. It was found that with the low voltage potential gradient applied in the experiment, the coefficient of electroosmotic permeability was not the dominant factor. The most sensitive parameter was dry bulk density (Fig. 6.21). A 25% increase in dry bulk density leads to an approximate 75% decrease in concentration and vice versa. Since bulk density affects porosity, tortuosity, and hydrodynamic dispersion, the high sensitivity during water flushing with low voltage potential gradient can be expected. Since the range of bulk density is small and since bulk density can be measured accurately in the experiments, the influence of bulk density on the uncertainty of the modelling results is minimal.

The fraction of organic carbon (f_{oc}) was also shown to be a highly sensitive factor. Since the fraction of organic carbon controls the retardation factor during water flushing, the time of peak concentration is control by the value of the fraction of organic carbon. The amount of organic carbon was not measured in the test and, due to the influence on concentration profiles, should be evaluated in other experiments with water flushing treatment.

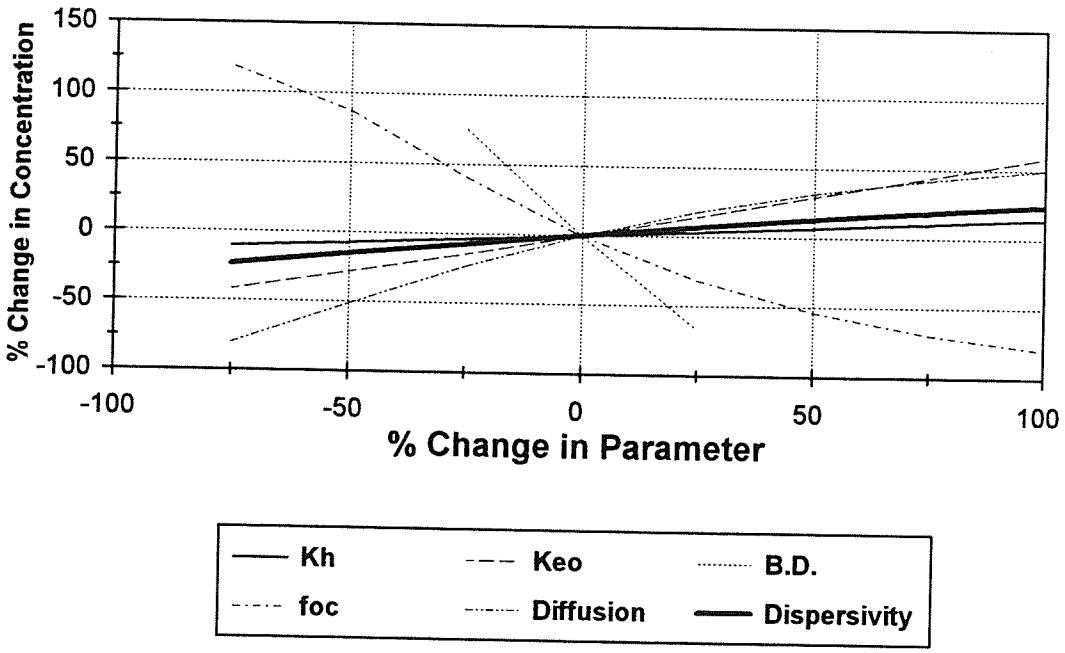

Figure 6.21 Sensitivity analysis of water flushing in experiment No.4.

The coefficient of electroosmotic permeability and the coefficient of diffusion were the next most sensitive parameters. A 75% change in the coefficient of electroosmotic permeability lead to a 50% change in concentration. It is expected that with increased voltage potential gradients the sensitivity of electrokinetic parameters such as the coefficient of electroosmotic permeability will increase. Since the 0.2 V/cm voltage potential gradient applied in experiment No.4 was relatively small, the effects of electrokinetics were minimal as indicated by the sensitivity analysis.

The hydraulic conductivity was found to be the least sensitive parameter in modelling experiment No.4. The low permeability of clay soils causes other transport parameters such as diffusion to become more dominant.

6.7.3 Sensitivity Analysis of Experiment No.4 - Water Flushing with Increased Voltage Gradient

The sensitivity of the modelling parameters was also evaluated with the increase in the electrical gradient to 1 V/cm (Fig. 6.22). This value was chosen since an electrical gradient of 1 V/cm is preferred in applying electrokinetic remediation (Acar and Hamed 1991). The results of the sensitivity analysis show that the coefficient of electroosmotic permeability was now the predominant factor in the electrokinetic treatment. Therefore, in order to fully utilize the effects of the increase in flow due to electroosmosis, the applied voltage potential gradient should be a minimum of 1 V/cm.

6.7.4 Sensitivity Analysis of Experiment No.4 - SDS Flushing

The sensitivity of the modelling parameters was also evaluated with the treatment condition in experiment No.4 with surfactant flushing (Fig. 6.23). With the application

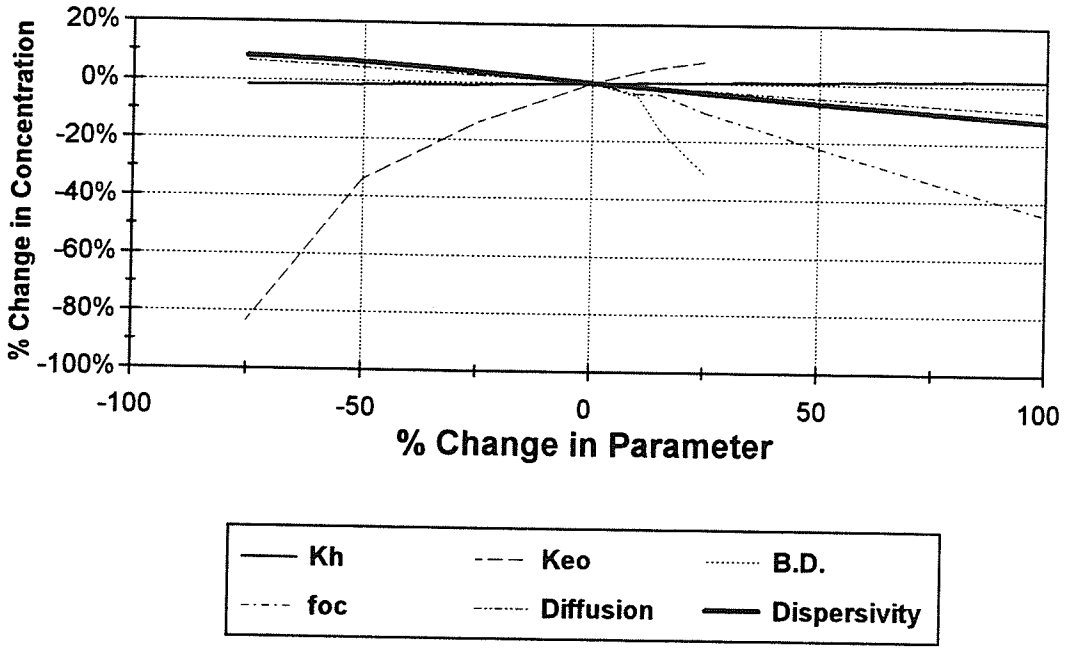

Figure 6.22 Sensitivity analysis of water flushing in experiment No.4 with voltage gradient increased to 1.0 V/cm.

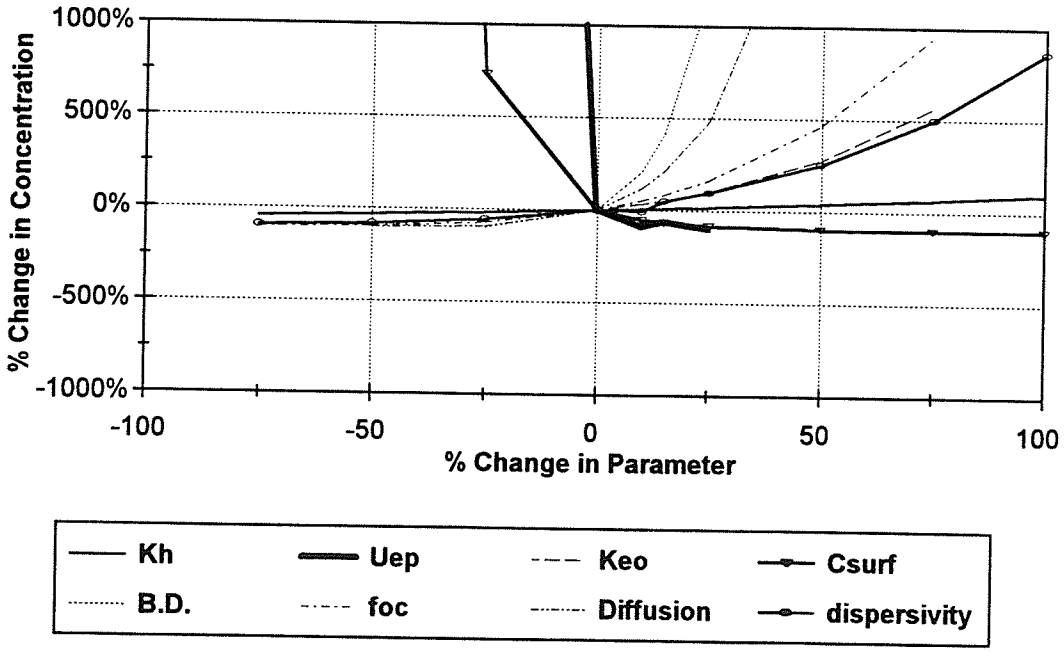

Figure 6.23 Sensitivity analysis of SDS flushing in experiment No.4.

of an electrical gradient and surfactant flushing, the electrophoretic mobility of the SDS micelles was found to be the most dominant factor. The electrophoretic mobility of the SDS micelles are not shown in Figure 6.23 since the sensitivity is much higher than the other model parameters. Since the electrophoretic mobility of the SDS micelles is approximately one order of magnitude greater than the coefficient of electroosmotic permeability, the electrophoretic mobility controls the contaminant transport with surfactant addition.

Surfactant concentration was the second most sensitive parameter. The surfactant concentration effects the amount of contaminants being transport in micelles. Therefore, surfactant concentration should be a dominant factor.

The dry bulk density and fraction of organic carbon were again shown to be sensitive modelling parameters which affected the predicted concentration. Similar to water flushing with the same voltage potential gradient, the bulk density and fraction of organic carbon were more sensitive than the coefficient of electroosmotic permeability. The hydraulic conductivity had the least influence on predicted concentration.

6.8 Modelling Various Treatment Conditions

The model was used to predict the effects of various treatments conditions. Concentration profiles for ethylbenzene 8 cm from the point of contaminant injection in part A of experiment No.2 in sand were predicted with water and SDS flushing (1.5% w/w). Three voltage conditions were modelled: (1) no voltage potential applied, (2) voltage potential gradients of 0.2 V/cm, and (3) voltage potential gradient of 2.0 V/cm. The modelling results indicate that surfactant application enhanced the transport with no voltage applied and at the 0.2 V/cm voltage gradients (Fig. 6.24). However, with the application of a voltage gradient of 2.0 V/cm, contaminant transport with surfactant flushing was significantly reduced and was lower than compared to water flushing. This is a result of electrophoretic transport retarding the transport of the contaminant in the pore fluid. The water flushing concentration profiles with the different voltage applications were all similar since the hydraulic flow dominates in the high permeability sand. Electrical effects were more prominent with a voltage gradient of 2 V/cm.

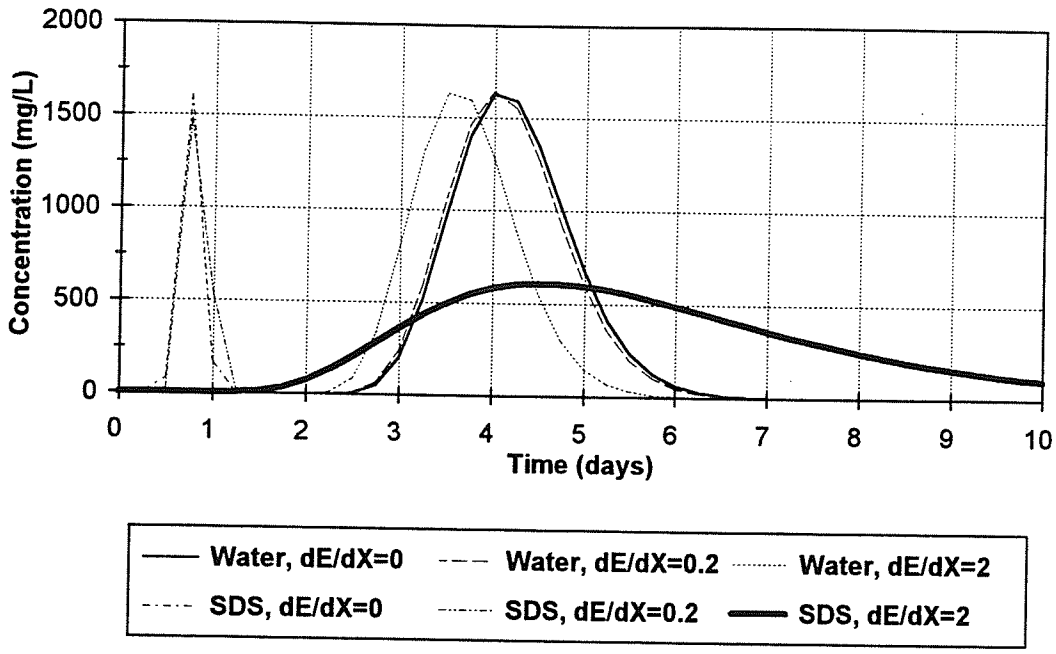

Figure 6.24 Modelling of ethylbenzene concentration profiles 8 cm from point of injection with various treatment conditions in sand.

The treatment conditions were applied with the parameters in experiment No.4 with clay to model the concentration profile of ethylbenzene 2 cm from the point of contaminant injection (Fig. 6.25). The application of SDS without a voltage potential gradient enhanced contaminant transport. However, with the application of a voltage potential gradient with surfactant flushing, there was no movement of ethylbenzene toward the outflow end. The electrophoretic transport of the contaminants in the opposite direction of electroosmotic and hydraulic flow

results in no movement of the contaminants toward the cathode with SDS and voltage application. The application of water flushing with the various voltage gradients show that the contaminant transport is increased in clay with increasing voltage gradient.

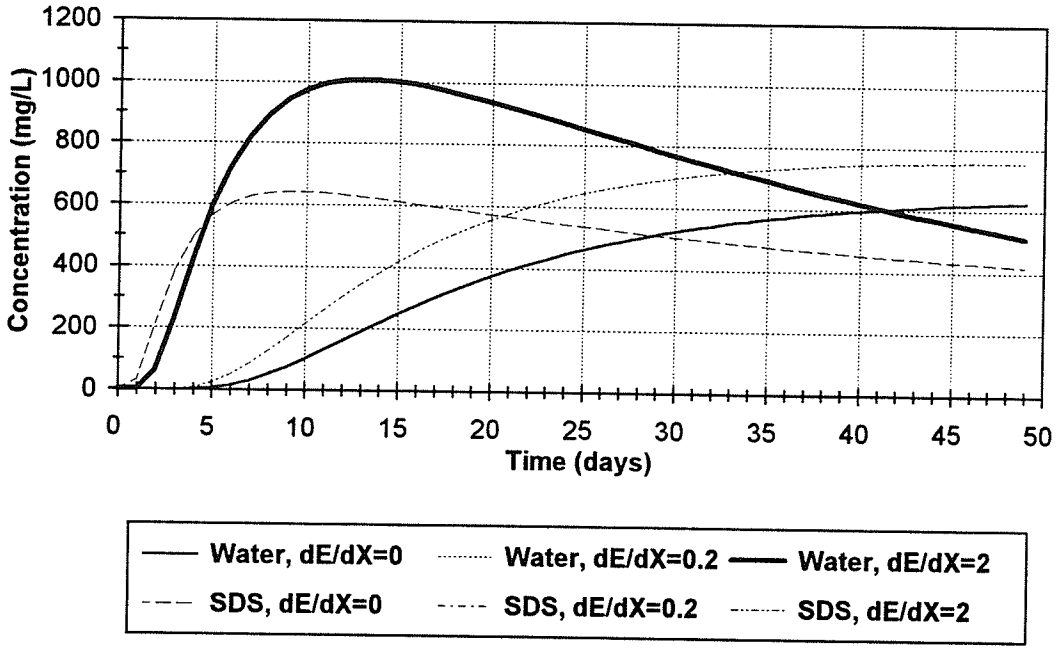

Figure 6.25 Modelling of ethylbenzene concentration profiles 2 cm from point of injection with various treatment conditions in clay.

7.0 Conclusions

Surfactant-enhanced aquifer remediation and electrokinetic remediation are still emerging technologies and a greater understanding of the factors involved is needed before decontamination can be confidently applied in the field. However, the research results significantly adds to the knowledge of surfactant-enhanced electrokinetic remediation. A number of new conclusions were drawn which adds to the known information on the performance of surfactant-enhanced electrokinetic remediation.

One of the three main goals of the research was to evaluate the performance of surfactant-enhanced electrokinetic remediation in removing hydrocarbons from contaminated soils. The following conclusions were made from this objective.

- Application of an electrical gradient to contaminated sand had no effect on the flow rate with water or SDS (0.25% w/w) as the processing fluid with an hydraulic gradient of 0.333.
- Flow rate and contaminant transport was enhanced in clay with the application of a voltage potential gradient with water flushing when the cathode was located at the outflow.
- A minimum voltage potential gradient of 1.0 V/cm is recommended to utilize electroosmotic contaminant transport in water flushing.

• Application of a surfactant increased the current which led to increased gas production and hydrogen and hydroxyl ion production.

• The coefficient of electroosmotic permeability remained relatively constant under the treatment conditions even after prolonged periods of electrokinetic remediation. This was attributed to the higher hydraulic gradient, lower voltage potential gradient, and uniform pH of the soil in the electrokinetic treatment.

• The anionic surfactant SDS does not permeate into clay soil when the positively charged anode is located at the inflow end.

The second main goal of the research was to identify the effect of various physical and chemical factors on the performance of surfactant-enhanced electrokinetic remediation. The following conclusions were made related to this objective:

• Concentrations of SDS greater than 2% (w/w) leads to no further reduction in the modified retardation factor. Therefore, the optimum SDS concentration that should be used in surfactant-enhanced remediation is below 2% (w/w).

• SDS micelle-water partition coefficients were determined as 3.19, 3.42, 3.45, 3.39, and 3.36 for toluene, ethylbenzene, and the xylene isomers respectively.

• The apparent solubility increased at the SDS CMC for a factor of 1.6 for *m*-xylene up to 3.2 for ethylbenzene. The increase in hydrocarbon solubility of SDS at the CMC has not been considered in other determinations of the micelle-water partition coefficient.

• A new relationship between log K_{ow} and log K_{mm} values was determined. Therefore, values of log K_{ow} can be used to predict the SDS micelle-water partition coefficients and electrophoretic transport in micelles for other hydrocarbon compounds.

• The CMC is reduced by 33% in the presence of saturated toluene, ethylbenzene, and xylene isomer compounds.

• Electroosmotic consolidation was observed in the electrical columns at the cathode.

• The pH profiles in the clay columns under prolonged electrokinetic remediation indicated the anode region became highly acidic with a pH between 2 and 3 and the cathode region became highly alkaline with a pH between 11 and 13. An acid front did not develop over the entire soil column with the pH of the interior of the clay remaining close to initial neutral pH values.

The third main goal of the research was to develop equations that can be used to predict contaminant transport during surfactant-enhanced electrokinetic remediation. The following conclusions were drawn from this objetive.

• A modified retardation factor coupled with classical advection dispersion transport equations and electrokinetic effects is a preliminary model that can be used to evaluate and predict various surfactant-enhanced electrokinetic remediation treatments. However, since the model was sensitive to the input parameters, accurate measurements of the modelling parameters are needed for better predictions. A more complete model taking into account transient effects, multi-phase flow, and mass transfer should be used for more accurate predictions.

• At the preferred electrical gradient of approximately 1 V/cm in electrokinetic remediation, the coefficient of electroosmotic permeability is the most important factor in water flushing.

• With the application of surfactant-enhanced electrokinetic remediation with SDS, the most dominant factor was the electrophoretic mobility of the SDS micelles.

• Electrophoretic transport was an order of magnitude greater in the opposite direction than electroosmotic transport with the anionic surfactant SDS.

• Modelling theory indicates electrophoretic transport in SDS micelles will be greater than electroosmotic transport for the majority of hydrocarbons under typical treatment conditions.

A number of other new results and new information was found in this study:

- A model diesel fuel greatly simplifies experiments involving diesel fuel contamination and allows for results of individual compounds to be distinguished.
- A dilution is necessary to reduce the concentration of hydrocarbons below the aqueous solubilities indicated by Raoult's Law to determine high concentrations of hydrocarbons in water using the SPME-GC-FID analysis method.
- The developed dilution protocol is a new analytical technique which allows the fast, simple, inexpensive, and solvent-free SPME method to be used for evironmental investigations encountering free-phase or high concentrations of hydrocarbons.
- Vibration-enhanced SPME increases the amount of analyte sorbed over a given period of time prior to equilibrium between the compound and the fibre. Therefore, sample agitation provided by the new sample carousel agitation device reduces equilibration time and improves limits of detection, especially for compounds with higher distribution constants.

8.0 Recommendations

The following recommendations can be made from this research:

- Future research should concentrate on the effect of electrophoretic transport in micelles when applying an anionic surfactant.
- A lower amount of hydrocarbon should be injected further into the soil columns to avoid contaminant loss due to back diffusion.
- A more complex numerical model including transient effects, mass transfer, and multi-phase flow is needed to confidently predicted contaminant transport during surfactant-enhanced electrokinetic remediation.
- Application of a nonionic surfactant should be attempted to avoid contaminant transport from electrophoretic flow moving in the opposite direction of electroosmotic flow. Since nonionic surfactants have a higher solubilization capacity than anionic surfactants, they may be more suited to surfactant-enhanced electrokinetic remediation.
- An anionic surfactant should be applied using a reversed electrode configuration with the cathode being located at the inflow end and the anode at the outflow end.
- Temperature effects for applying a surfactant should be evaluated before field use in Manitoba.

• Secondary temperature effects have been shown to decrease the efficiency of electroosmotic flow when the current density is greater than 5 mA/cm^2 (Hamed et al. 1991). Therefore, electrode area should be increased in future work to decrease current density. Relatively inexpensive graphite electrodes could be employed for this purpose.

• Thicker glass columns should be used in further experiment to reduce chance of leakage and to increase durability.

• Duration of experiments should be reduced to allow greater amount of data collection on various conditions to be obtained. In addition, shorter tests allow the short term effects of electrokinetics to be evaluated.

• Current and voltage drop measurements need only to be taken every half an hour to avoid large data files which are difficult to work with.

References

Abdul, A.S., Gibson, T.L., Ang, C.C., Smith, J.C. and Sobczynski, R.E., 1992. "In Situ Surfactant Washing of Polychlorinated Biphenyls and Oils from a Contaminated Site." *Ground Water* **30**(2):219-231.

Abdul, A.S., Gibson, T.L. and Rai, D.N., 1990. "Selection of Surfactants for the Removal of Petroleum Products from Shallow Sandy Aquifers." *Ground Water* **28**(6):920-926.

Abdul, S.A. and Gibson, T.L., 1991. "Laboratory Studies of Surfactant-Enhanced Washing of Polycholorinated Biphenyl from Sandy Material." *Environmental Science and Technology* **25**(4):665-670.

Abriola, L.M., Dekker, T.J. and Pennell, K.D., 1993. "Surfactant-Enhanced Solubilization of Residual Dodecane In Soil Columns. 2. Mathematical Modeling." *Environmental Science Technology* **27**(12):2341-2351.

Acar, Y.B. and Alshawabkeh, A.N., 1993a. "Principles of Electrokinetic Remediation." *Environmental Science and Technology* **27**(13):2638-2647.

Acar, Y.B., Alshawabkeh, A.N. and Gale, R.J., 1993b. "Fundamentals of Extracting Species from Soils by Electrokinetics." *Waste Management* **13**:141-151.

Acar, Y.B., Li, H. and Gale, R.J., 1992. "Phenol Removal from Kaolinite by Electrokinetics." *Journal of Geotechnical Engineering* **118**(11):1837-1852.

Acar, Y.B. and Hamed, J., 1991. "Electrokinetic Soil Processing in Waste Remediation and Treatment: Synthesis of Available Data." *Bulletin of Transportation Research, Record No. 1312, "Energy and Environmental Issues"* p.153-161.

Acar, Y.B., Gale, R.J., Hamed, J. and Putnam, G., 1990a. "Acid/Base Distributions in Electrokinetic Soil Processing." *Bulletin of Transportation Research, Record No.1288, "Soils, Geology, and Foundations"* p.23-34.

Acar, Y.B., Gale, R.J., Putnam, G.A., Hamed, J. and Wong, R.L., 1990b. "Electrochemical Processing of Soils: Theory of pH Gradient Development by Diffusion, Migration, and Linear Convection." *Journal of Environmental Science and Health, Part (a): Environmental Science and Engineering* **25**(6):687-714.

Almgren, M., Grieser, F. and Thomas, J.K., 1979. "Dynamic and Static Aspects of Solubilization of Neutral Arenes in Ionic Micellar Solutions." *Journal of the American Chemical Society* **101(2)**:279-291.

Alshawabkeh, A.N. and Acar, Y.B., 1992. "Removal of Contaminants from Soils by Electrokinetics: A Theoretical Treatise." *Journal of Environmental Science and Health, Part (a): Environmental Science and Engineering* **27**(7):1835-1861.

Anderson, M.P. and Woessner, W.W., 1992. *Applied Groundwater Modeling - Simulation of Flow and Advective Transport.* Academic Press, Inc., San Diego, California.

Aronstein, B.N., Calvillo, Y.M. and Alexander, M., 1991. "Effect of Surfactants at Low Concentrations on the Desorption and Biodegradation of Sorbed Aromatic Compounds in Soil." *Environmental Science and Technology* **25**(10):1728-1731.

Arthur, C.L., Killam, L.M., Buchholz, K.D., Pawliszyn, J. and Berg, J.R., 1992a. "Automation and Optimization of Solid-Phase Microextraction." *Analytical Chemistry* **64**:1960-1966.

Arthur, C.L., Killam, L.M., Motlagh, S., Lim, M., Potter, D.W., et al., 1992b. "Analysis of Substituted Benzene Compounds in Groundwater Using Solid-Phase Microextraction." *Environmental Science and Technology* **26**(5):979-983.

Arthur, C.L., Pratt, K., Motlagh, S. and Pawliszyn, J., 1992c. "Environmental Analysis of Organic Compounds in Water Using Solid Phase Micro Extraction." *Journal of High Resolution Chromatography* **15**:741-744.

Arthur, C.L. and Pawliszyn, J., 1990. "Solid Phase Microextraction with Thermal Desorption Using Fused Silica Optical Fibers." *Analytical Chemistry* **62**(19):2145-2148.

Baetsle, L.H., 1969. Migration of Radionuclides in Porous Media. *Progress in Nuclear Energy, Series XII, Health Physics.* Pergamon Press Ltd., London, U.K., p.707-730.

Banjaree, S., Horng, J.J. and Ferguson, J.F., 1991. "Field Experience with Electrokinetics at a Superfund Site." *Bulletin of Transportation Research, Record No. 1312, "Energy and Environmental Issues"* p.167-174.

Block, R.N., Allworth, N. and Bishop, M., 1991. Assessment of Diesel Contamination in Soil. *Hydrocarbon Contaminated Soils*. Lewis Publishers, Inc., Chelsea, MI, p.135-148.

Borden, R.C. and Kao, C.M., 1989. *Water Flushing of Trapped Residual Hydrocarbon: Mathematical Model Development and Laboratory Validation*. Proceedings of the Conference on Petroleum Hydrocarbons and Organic Chemicals in Groundwater: Prevention, Detection, and Restoration, National Water Well Association, November 15-17, Houston, Texas, p.473-486.

Brown, C.L. and Pope, G.A., 1994. "Simulation of surfactant-enhanced aquifer remediation." *Water Resources Research* **30**(11):2959-2977.

Bruell, C.J., Segall, B.A. and Walsh, M.T., 1992. "Electroosmotic Removal of Gasoline Hydrocarbons and TCE from Clay." *Journal of Environmental Engineering* **118**(1):68-83.

Buchholz, K.D. and Pawliszyn, J., 1993. "Determination of Phenols by Solid-Phase Microextraction and Gas Chromatographic Analysis." *Environmental Science and Technology* **27**(13):2844-2848.

Bury, S.J. and Miller, C.A., 1993. "Effect of Micellar Solubilization on Biodegradation Rates of Hydrocarbons." *Environmental Science and Technology* **27**(1):104-110.

Chai, M.C., Arthur, C.L., Pawliszyn, J., Belardi, R.P. and Pratt, K.F., 1993. "Determination of Volatile Chlorinated Hydrocarbons in Air and Water With Solid-phase Microextraction." *Analyst* **118**:1501-1505.

Clarke, A.N., Oma, K.H., Megehee, M.M. and Wilson, D.J., 1993. "Soil Clean-Up by Surfactant Washing II. Design and Evaluation of the Components of the Pilot-Scale Surfactant Recycle System." *Separation Science and Technology* **28**(13-14):2103-2135.

Clarke, A.N., Plumb, P.D. and Wilson, D.J., 1991. "Soil Clean-Up by Surfactant Washing. I. Laboratory Results and Mathematical Modeling." *Separation Science and Technology* **26**(3):301-343.

Datla, S., 1994. *A Unified Theory on Electro-Kinetic Extraction of Contaminants*. M.Sc. Thesis in Civil Engineering, Texas A & M University, College Station, Texas.

Dineen, D., 1991. Remediation Options for Diesel-Contaminated Soil. *Hydrocarbon Contaminated Soils*. Lewis Publishers, Inc., New York, NY, p.181-191.

Domenico, P.A. and Schwartz, F.W., 1990. *Physical and Chemical Hydrogeology*. John Wiley & Sons, Inc., New York, NY.

Draper, N.R. and Smith, H., 1981. *Applied Regression Analysis*. John Wiley & Sons, Inc., New York, NY.

Edwards, D.A., Lui, Z. and Luthy, R.G., 1991a. "Surfactant Solubilization of Organic Compounds in Soil/Aqueous Systems." *Journal of Environmental Engineering* **120**(1):5-22.

Edwards, D.A., Lui, Z. and Luthy, R.G., 1991b. "Experimental Data and Modeling For Surfactant Micelles, HOCs, and Soil." *Journal of Environmental Engineering* **120**(1):22-41.

Edwards, D.A., Luthy, R.G. and Zhongbao, L., 1991c. "Solubilization of Polycyclic Aromatic Hydrocarbons in Micellar Nonionic Surfactant Solutions." *Environmental Science and Technology* **25(1)**:127-133.

Eykholt, G.R. and Daniel, D.E., 1994. "Impact of System Chemistry of Electroosmosis in Contaminated Soil." *Journal of Geotechnical Engineering* **120**(5):797-815.

Fletcher, C.L. and Kaufman, D.D., 1980. "Effect of Sterilization Methods on 3-Chloroaniline Behavior in Soil." *Journal of Agricultural Food Chemistry* **28**(3):667-671.

Foreman, W.T., Zaugg, S.D., Faires, L.M., Werner, M.G., Leiker, T.J., et al., 1992. "Analytical Interferences of Mercuric Chloride Preservative in Environmental Water Samples: Determination of Organic Compounds Isolated by Continuous Liquid-Liquid Extraction or Closed- Loop Stripping." *Environmetal Science and Technology* **26**(7):1307-1312.

Fountain, J.C., Klimek, A., Beikirch, M.G. and Middleton, T.M., 1991. "The use of surfactants for *in situ* extraction of organic pollutants from a contaminated aquifer." *Journal of Hazardous Materials* **28**:295-311.

Frankenburger, W.T., Jr., 1992. The Need for a Laboratory Feasibility Study in Bioremediation of Petroleum Hydrocarbons. *Hydrocarbon Contaminated Soils and Groundwater*. Lewis Publishers, Inc., Chelsea, Michigan, p.558.

Freeze, R.A. and Cherry, J.A., 1979. *Groundwater*. Prentice-Hall Inc., Englewood Cliffs, N.J.

Fu, J.K. and Luthy, R.G., 1986. "Aromatic Compound Solubility in Solvent/Water Mixtures." *Journal of Environmental Engineering* **112**(2):328-345.

Gannon, O.K., Bibring, P., Raney, K., Ward, J.A. and Wilson, D.J., 1989. "Soil Clean Up by *in-situ* Surfactant Flushing. III. Laboratory Results." *Separation Science and Technology* **24**(14):1073-1094.

Gillespie, R.J., Humphreys, D.A., Baird, N.C. and Robinson, E.A., 1989. *Chemistry*. Allyn and Bacon, Inc., Needham Heights, Massachuetts.

Gopinath, S., 1994. *A Laboratory Study of Electro-Kinetic Remediation of Fine-Grained Soil Contaminated with Organic Compounds*. M.Sc. Thesis in Civil Engineering, Texas A & M University, College Station, Texas.

Hachisu, S., 1984. Electrokinetics. *from Electrical Phenomena at Interfaces - Fundamentals, Measurments, and Applications*. Marcel Dekker, Inc., New York, NY. p.99-117.

Hamed, J., Acar, Y.B. and Gale, R.J., 1991. "Pb(II) Removal from Kaolinite by Electrokinetics." *Journal of Geotechnical Engineering* **117**(2):241-271.

Hoag, G.E. and Marley, M.C., 1986. "Gasoline Residual Saturation in Unsaturated Uniform Aquifer Materials." *Journal of Environmental Engineering* **112**(3):586-606.

Jafvert, C.T., 1991. "Sediment- and Saturated-Soil-Associated Reactions Involving an Anionic Surfactant (Dodecylsulfate). 2. Partition of PAH Compounds among Phases." *Environmental Science and Technology* **25(6)**:1039-1045.

Kan, A.T. and Tomson, M.B., 1986. *Facilitated Transport of Naphthalene and Phenanthrene in a Sandy Soil Column with Dissolved Organic Matter - Macromolecules and Micelles*. Proceedings of the NWWA/API Conference on Petroleum Hydrocarbons and Organic Chemicals in Groundwater - Prevention, Detection and Restoration, National Water Well Association, November 12-14, Houston, Texas, p.93-105.

Kile, D.E. and Chiou, C.T., 1989. "Water Solubility Enhancements of DDT and Trichlorobenzene by Some Surfactants Below and Above the Critical Micelle Concentration." *Environmental Science and Technology* **23(7)**:832-836.

Knox, R.C., Sabatini, D.A. and Canter, L.W., 1993. *Subsurface Transport and Fate Processes*, Lewis Publishers, Boca Raton, Florida.

Lageman, R., 1993. "Electroreclamation." *Environmental Science and Technology* **27**(13):2648-2651.

Lageman, R., Pool, W. and Seffinga, G., 1989. *Electro-Reclamation: Theory and Practice*. Chemistry & Industry, p.585-590.

Laha, S. and Luthy, R.G., 1991. "Inhibition of Phenanthrene Mineralization by Nonionic Surfactants in Soil-Water Systems." *Environmental Science and Technology* **25**(11):1920-1930.

Lane, W.F. and Loehr, R.C., 1992. "Estimating the Equilibrium Aqueous Concentrations of Polynuclear Aromatic Hydrocarbons in Complex Mixtures." *Environmental Science and Technology* **26**(5):983-990.

Lo, K.Y. and Ho, K.S., 1991. "The effects of electroosmotic field treatment on the soil properties of a soft sensitive clay." *Canadian Geotechnical Journal* **28**(6):763-770.

Louch, D., Motlagh, S. and Pawliszyn, J., 1992. "Dynamics of Organic Compound Extraction from Water Using Liquid-Coated Fused Silica Fibers." *Analytical Chemistry* **64**:1187-1199.

Lui, Z., Jacobson, A.M. and Luthy, R.G., 1995. "Biodegradation of Naphthalene in Aqueous Nonionic Surfactant Systems." *Applied Environmental Microbiology* **61**(1):145-151.

Lui, Z., Laha, S. and Luthy, R.G., 1991. "Surfactant Solubilization of Polycyclic Aromatic Hydrocarbon Compounds in Soil-Water Suspensions." *Water Science Technology* **23**:475-485.

Lymann, W.J., Reidy, P.J. and Levy, B., 1992. *Mobility and Degradation of Organic Contaminants in Subsurface Environments*. C.K. Smoley, Inc., Chelsea, MI.

MacGillvray, B. and Pawliszyn, J., 1994. "Headspace Solid-Phase Microextraction versus Purge and Trap for the Determination of Substituted Benzene Compounds in Water." *Journal of Chromatographic Science* **32**:317-322.

Mattson, E.D. and Lindgren, E.R., 1994. *Electrokinetics: An Innovative Technology for In-Situ Remediation of Heavy Metals*. Proceedings of the Eighth National Outdoor Action Conference and Exposition, Aquifer Remediation/ Ground Water Monitoring/ Geophysical Methods, National Ground Water Association, May 23-25, Minneapolis, MN, p.235-245.

Milner, G.C., James, R.C. and Nye, A.C., 1992. "Human Health-Based Soil Cleanup Guidelines for Diesel Fuel No. 2." *Journal of Soil Contamination* **1**(2):103-157.

Mitchell, J.K., 1976. *Fundamentals of Soil Behaviour*. John Wiley & Sons, Inc, New York, NY.

Mitchell, J.K. and Yeung, A.T., 1990. "Electro-Kinetic Flow Barriers in Compacted Clay." *Bulletin of Transportation Research, Record No. 1288, "Soils, Geology, and Foundations"* p.1-9.

Morris, D.V. and Caldwell, S.F., 1985. "Improvement of sensitive silty clay by electroosmosis." *Canadian Geotechnical Journal* **22**:17-24.

Mukerjee, P. and Mysels, K.J., 1971. *Critical Micelle Concentrations of Aqueous Surfactant Systems*. National Bureau of Standards, Washington, D.C..

Myers, D., 1992. *Surfactant Science and Technology*. VCH Publishers, Inc., New York, NY.

Neter, J., Wasserman, W. and Kutner, M.H., 1985. *Applied Linear Statistical Models - Regression, Analysis of Variance, and Experimental Designs*. Irwin, Inc., Homewood, IL.

Pamucku, S., Khan, L.I. and Fang, H., 1990. "Zinc Detoxification of Soils by Electro-Osmosis." *Bulletin of Transportation Research, Record No. 1288, "Soils, Geology, and Foundations"*, p.41-46.

Pamucku, S. and Wittle, J.K., 1992. "Electrokinetic Removal of Selected Heavy Metals from Soil." *Environmental Progress* **11**(3):241-250.

Pennel, K.D., Abriola, L.M. and Weber, W.J., Jr., 1993. "Surfactant-Enhanced Solubilization of Residual Dodecane in Soil Columns. I. Experimental Investigation." *Environmental Science and Technology* **27**(12):2332-2340.

Pennel, K.D., Jin, M., Abriola, L.M. and Pope, G.A., 1994. "Surfactant enhanced remediation of soil columns contaminated by residual tetrachloroethylene." *Journal of Contaminant Hydrology* **16**:35-53.

Peters, R.W., Montemagno, C.D. and Shem, L., 1992. "Surfactant Screening of Diesel-Contaminated Soil." *Hazardous Waste & Hazardous Materials* **9**(2):113-136.

Potter, D.W. and Pawliszyn, J., 1992. "Detection of substituted benzenes in water at the pg/ml level using solid-phase microextraction and gas chromatography-ion trap mass spectrometry." *Journal of Chromatography* **625**:247-255.

Potter, D.W. and Pawliszyn, J., 1994. "Rapid Determination of Polyaromatic Hydrocarbons and Polychlorinated Biphenyls in Water Using Solid-Phase Microextraction and GC/MS." *Environmental Science and Technology* **28**(2):298-305.

Putnam, G.A., 1988. *Determination of pH Gradients in the Electrochemical Processing of Koalinite*. M.Sc. Thesis in Civil Engineering, Louisiana State University, Baton Rouge, Louisiana.

Rixey, W.G., Johnson, P.C., Deeley, G.M., Byers, D.L. and Dortch, I.J., 1991. Mechanisms for the Removal of Residual Hydrocarbons from Soils by Water, Solvent, and Surfactant Flushing. *from Hydrocarbon Contaminated Soils,* Lewis Publishers, Inc., New York, NY, p.387-409.

Rouse, J.D., Sabatini, D.A. and Harwell, J.H., 1993. "Minimizing Surfactant Losses Using Twin-Head Anionic Surfacants in Subsurface Remediation." *Environmental Science and Technology* **27(10)**:2072-2078.

Roy, D., Liu, M. and Wang, G., 1994. "Modeling of Anthracene Removal from Soil Columns by Surfactant." *Journal of Environmental Science and Health, Part A* **29**(1):197-213.

Runnells, D.D. and Larson, J.L., 1986. *A Laboratory Study of Electromigration as a Possible Field Technique for the Removal of Contaminants from Ground Water.* Ground Water Monitoring Review, p.81-91.

Runnells, D.D. and Wahli, C., 1993. "In Situ Electromigration as a Method for Removing Sulfate, Metals, and Other Contaminants from Ground Water." *Ground Water Monitoring and Review* **Winter**, p.121-129.

Sale, K. and Pitts, M., 1989. *Chemically Enhanced In Situ Soil Washing.* Proceedings of the Conference on Petroleum Hydrocarbons and Organic Chemicals in Groundwater: Prevention, Detection, and Restoration, National Ground Water Association, November 15-17, Houston, TX, p.487-503.

Sanemasa, I., Miyazaki, Y., Arakawa, S., Kumamaru, M. and Deguchi, T., 1987. "The Solubility of Benzene-Hydrocarbon Binary Mixtures in Water." *Bulletin of the Chemical Society of Japan* **60**:517-523.

Sarna, L.P., Webster, G.R.B., Friesen-Fischer, M.R. and Sri Ranjan, R., 1994. "Analysis of petroleum components benzene, toluene, ethyl benzene, and the xylenes in water by commericially available solid-phase microextraction and carbon-layer open tubular capillary column gas chromatography." *Journal of Chromatography A* **677**:201-205.

Segall, B.A. and Bruell, C.J., 1992. "Electroomostic Contaminant-Removal Processes." *Journal of Environmental Engineering* **118**(1):84-100.

Shapiro, A.P. and Probstein, R.F., 1993. "Removal of Contaminants from Saturated Clay by Electroosmosis." *Environmental Science and Technology* **27**(2):283-291.

Shapiro, A.P., Renaud, P.C. and Probstein, R.F., 1989. "Preliminary Studies on the Removal of Chemical Species from Saturated Porous Media by Electrosmosis." *PhysicoChemical Hydrodynamics* **11**(5/6):785-802.

Shirey, R.E., Wachob, G.D. and Pawliszyn, J., 1993. "Solventless Sample Preparation for Extracting Organic Compounds in Water." *Supelco Reporter* **XII**(4):8-11.

Spiegler, K.S., 1958. "Transport Processes in Ionic Membranes." *Transactions of the Faraday Society* **54**:1408-1428.

Stigter, D. and Mysels, K.J., 1955. "Tracer Electrophoresis. II. The Mobility and the Micelle of Sodium Lauryl Sulfate and its Interpretation in Terms of Zeta Potential and Charge." *Journal of Physical Chemistry* **59**:45-51.

Stone, W.A., Jr., 1991. Assessing Health Risks Associated with Diesel Contaminated Soils and Groundwater. *Hydrocarbon Contaminated Soils*. Lewis Publishers, Inc., Chelsea, MI, p.167-179.

Stumm, M. and Morgan, J.M., 1981. *Aquatic Chemistry: An Introduction Emphasizing Chemical Equilibria in Natural Waters*. John Wiley & Sons, New York, NY.

Trombly, J., 1994. "Electrochemical Remediation Takes to the Field." *Environmental Science and Technology* **28**(6):289-291.

Underwood, J.L., Debelak, K.A. and Wilson, D.J., 1993. "Soil Clean Up by *in-situ* Surfactant Flushing. VI. Reclamation of Surfactant for Recycle." *Separation Science and Technology* **29**(9):1647-1669.

Valsaraj, K.T., Gupta, A., Thibodeaux, L.J. and Harrison, D.P., 1988. "Partitioning of Chloromethanes Between Aqueous and Surfactant Micellar Phases." *Water Research* **22(9)**:1173-1183.

Valsaraj, K.T. and Thibodeaux, L.J., 1989. "Relationships Between Micelle-Water and Octanol-Water Partition Constants for Hydrophobic Organics of Environmental Interest." *Water Research* **23(2)**:183-189.

Vigon, B.W. and Rubin, A.J., 1989. "Practical Considerations in the Surfactant-Aided Mobilization of Contaminants in Aquifers." *Journal of the Water Pollution Control Federation* **61**(7):1233-1240.

Vold, R.D. and Vold, M.J., 1983. *Colloid and Interface Chemistry*. Addison-Wesley Publishing Company, Inc., San Diego, California.

Volkering, F., Breure, A.M., van Andel, J.G. and Rulkens, W.H., 1995. "Influence of Nonionic Surfactants on Bioavailability and Biodegradation of Polycyclic Aromatic Hydrocarbons." *Applied Environmental Microbiology* **61**(5):1699-1705.

West, C.C. and Harwell, J.H., 1992. "Surfactants and Subsurface Remediation." *Environmental Science and Technology* **26**(12):2324-2330.

Wolf, D.C., Dao, T.H., Scott, H.D. and Lavy, T.L., 1989. "Influence of Sterilization Methods on Selected Soil Microbiological, Physical, and Chemical Properties." *Journal of Environmental Quality* **18**:39-44.

Wunderlich, R.W., Fountain, J.C. and Jackson, R.E., 1992. In Situ Remediation of Aquifers Contaminated with Dense Nonaqueous Phase Liquids by Chemically Enhanced Solubilization. *Hydrocarbon Contaminated Soils and Groundwater*. Lewis Publishers, Inc., Chelsea, MI, p.261-278.

Yaws, C.L., Pan, X. and Lin, X., 1993a. "Water Solubility Data for 151 Hydrocarbons." *Chemical Engineering* **100**(2):108-111.

Yaws, C.L., Haur-Chung, Y., Hopper, J.R. and Hansen, K.C., 1993b. "Organic Chemicals: 168 Water Solubility Data." *Chemical Engineering* **100**(2):24-25.

Zhang, Z. and Pawliszyn, J., 1993. "Headspace Solid-Phase Microextraction." *Analytical Chemistry* **65**:1843-1852.

Appendix A:

Data Acquisition Control Program

```
/*************************************************************/
/* CURRENT2.C  Written July  94  Updated Dec 95              */
/* Program controls the 24 channel multiplexer used for data*/
/* measurment in the electrokinetic remediation laboratory  */
/* experiments.  Program sets duration of applied voltage    */
/* and time for voltage drop and current measurements.  Data*/
/* is written to 4 output files, one for the applied voltage*/
/* and current for all three columns and three files for the*/
/* measured voltage drops across each soil column.           */
/*                                                           */
/* Variables :                                               */
/*  t_on  = how long voltage is on (min)                     */
/*  t_off = how long voltage is off (min)                    */
/*  t_drop= how long between voltage drop measurements (min)*/
/*  t_max = total time length of test (min)                  */
/*  t_change = increment/decrement in on/off time (min)      */
/*  v_rs = voltage drop across the resistor                  */
/*  v_ps = voltage supplied by the power supply              */
/*  v_sample = voltage drop across sample = (v_ps)-(v_rs)    */
/*  current = current through the sample                     */
/*  S1,S2,S3= file name extensions for sample column data    */
/*            1,2,3, respectively                            */
/*  PS1,PS2,PS3 = power supply for columns 1,2, and 3.       */
/*  resistance = resistance of the resistor                  */
#include <stdio.h>
#include <stdlib.h>
#include <conio.h>
#include <process.h>
#include <math.h>
#include <dos.h>
#include <string.h>
#include <time.h>

#define N 21
#define PS1 1
#define PS2 9
#define PS3 17
/* channels 1,9,17 control power supply */
#define DROP1 2
#define DROP2 3
#define DROP3 4
#define DROP4 5
#define DROP5 6
#define DROP6 7
#define C1 8
#define DROP7 10
#define DROP8 11
#define DROP9 12
#define DROP10 13
#define DROP11 14
#define DROP12 15
#define C2 16
#define DROP13 18
#define DROP14 19
#define DROP15 20
```

```
#define DROP16 21
#define DROP17 22
#define DROP18 23
#define C3 24
/* assign data to appropriate channel above */

#define DATA      0x378          /* Printer Port I/O address. Data
register*/
/* set for IBM computer */
#define STATUS    0x379          /* Status register */
#define CONTROL   0x37A          /* Control register*/

#define ON    0;
#define OFF   1;

struct bits
   {
   unsigned bit0:   1;
   unsigned bit1:   1;
   unsigned bit2:   1;
   unsigned bit3:   1;
   unsigned bit4:   1;
   unsigned bit5:   1;
   unsigned bit6:   1;
   unsigned bit7:   1;
   };

union data
   {
   struct bits databits;
   int          dataint;
   };

union data databyte0, databyte1, databyte2;
union data *byte0p, *byte1p, *byte2p;

union status
   {
   struct bits statusbits;
   int          statusint;
   } statusunion;

union control
   {
   struct bits controlbits;
   int          controlint;
   } controlunion;


/* declare global functions */
/* these functions written by Matt McDonald */
void PSOnOff(int num, char *state);
void ChOn(int num);
void DataSwitch(union data *dataunion, div_t chnum);
void PSSwitch(union data *dataunion, char *state);
```

```
void ChDsp(int num);
float ReadVm(void);
void Init(void);

/* declare functions, need prototype if main before functions */
/* void declared when function does not return a value */
void intro(void);


void main(void)
{
 FILE *f1,*f2,*f3,*f4,*f5;
 /* declare variables */
 int test1,test2,test3;
 char name1[N],name2[N],name3[N],name4[N],name5[N],*p,re_enter[N];
 float vm_reading;
 double
v_ps,v_rs1,v_rs2,v_rs3,v_sample1,v_sample2,v_sample3,current1,curr
ent2,current3;
 double resistance,zero,onea,twoa,threea,foura,fivea,sixa;
 double onec,twoc,threec,fourc,fivec,sixc;
 double onee,twoe,threee,foure,fivee,sixe;
 double avg1,avg2,avg3,avg4,avg5,avg6,curravg;
 double t_on,t_off,t_change,t_max,t_drop,t_on1,t_drop1;
 time_t t,t_start;

 /* start of program */

 byte0p = &databyte0;
 byte1p = &databyte1;
 byte2p = &databyte2;
 databyte0.dataint = databyte1.dataint = databyte2.dataint = 255;

 Init();   /* function connects channels to the voltmeter */
 clrscr();
 intro();  /* introscreen */

    /* input set-up data */
    do {
     clrscr();
     printf("\n\n\n\t\Input file name to store data: ");
     scanf("%s",name1);
     printf("\n\tEnter the voltage on and off time (min): ");
     scanf("%lf%lf",&t_on,&t_off);
     printf("\n\tEnter the magnitude of applied voltage (volt):
");
     scanf("%lf",&v_ps);
     printf("\n\tEnter the duration of experiment (min): ");
     scanf("%lf",&t_max);    /* &t indicates address of t_max */
     printf("\n\tEnter the increment/decrement of on/off time
(min): ");
     scanf("%lf", &t_change);
     printf("\n\tEnter time interval between voltage drop
measurements (min): ");
     scanf("%lf",&t_drop);
```

```
      printf("\n\tWould you like to change this data? (Y/N): ");
      scanf("%s",re_enter);
      printf("\n\n\n");
     }
     while ((re_enter[0] != 'N')); /* do until N is entered */

     t_on = t_on *60; /* convert to seconds */
     t_off = t_off * 60;
     t_max = t_max*60;
     t_change = t_change*60;
     t_drop=t_drop*60;

     /* create other file names */
     strcpy(name2,name1); /* name2.S1 will store voltage drop data
for */
     strcpy(name3,name1); /* S1, etc..  Name1 with no extension
gives */
     strcpy(name4,name1); /* applied voltage data for three columns
*/
     strcpy(name5,name1);
     p=".S1";
     strcat(name2,p);      /* concentrates two strings */
     p=".S2";
     strcat(name3,p);
     p=".S3";
     strcat(name4,p);
     p=".avg";
     strcat(name5,p);
      /* open files */
      f1=fopen(name1,"a");
      f2=fopen(name2,"a");
      f3=fopen(name3,"a");
      f4=fopen(name4,"a");
      f5=fopen(name5,"a");

      /* check that files can be opened */
      if((f1=fopen(name1,"a")) ==NULL) {
      printf("\nFile %s cannot be opened.",name1);
      exit(1);
      }
      /* "a" = Open for append */
      /*  and create if the file does not exist. */
      if((f2=fopen(name2,"a"))==NULL) {
      printf("\nFile %s cannot be opened.",name2);
      exit(1);
      }
      if((f3=fopen(name3,"a"))==NULL) {
      printf("\nFile %s cannot be opened.",name3);
      exit(1);
      }
      if((f4=fopen(name4,"a"))==NULL) {
      printf("\nFile %s cannot be opened.",name4);
      exit(1);
      }
      if((f5=fopen(name5,"a"))==NULL) {
```

```
      printf("\nFile %s cannot be opened.",name5);
      exit(1);
      }

   t_drop1= t_drop;
   t_drop=0;      /* record voltage drops before test starts */
   t_on1 = t_on;

   test1=0; /* test to see that "if's" only get executed once */
   test2=0;
   test3=0;

    /* echo input to file */
    fprintf(f1,"\n\n Voltage on time is %-7.0f minutes.",t_on/60);
    fprintf(f1,"\n Voltage off time is %-7.0f minutes.",t_off/60);
    fprintf(f1,"\n Time between voltage drop measurments is %-7.0f
minutes.",t_drop1/60);
   fprintf(f1,"\n Increment/decrement in on/off time is %-7.0f
minutes.",t_change/60);
   fprintf(f1,"\n Voltage supplied by the power supply is %-8.2f
volts.",v_ps);
   /* write headings to files */
   fprintf(f1,"\n\nTIME (MIN), VOLT.1, CURR.1, VOLT.2, CURR.2,
VOLT.3, CURR.3");
   fprintf(f2,"\n Voltage drop given in Volts ");
   fprintf(f3,"\n Voltage drop given in Volts ");
   fprintf(f4,"\n Voltage drop given in Volts ");

   fprintf(f2,"\n\nTIME
(MIN),DROP1,DROP2,DROP3,DROP4,DROP5,DROP6");
   fprintf(f3,"\n\nTIME
(MIN),DROP7,DROP8,DROP9,DROP10,DROP11,DROP12");
   fprintf(f4,"\n\nTIME
(MIN),DROP13,DROP14,DROP15,DROP16,DROP17,DROP18");
   fprintf(f5,"\n\nTIME
(MIN),AvgCURR,AVG1,AVG2,AVG3,AVG4,AVG5,AVG6");

   fclose(f1);
   fclose(f2);
   fclose(f3);
   fclose(f4);
   fclose(f5);

  t_start = time(NULL);     /* Initialize time values to start of
test from 1972 */
  t = time(NULL);

  /* loop */
  while((t-t_start)<=t_max) {
   t = time(NULL);    /*time in seconds since 1972 */
    if((t-t_start)==t_drop){
     printf("\n\nMeasure voltage drop and current.");
     printf("\nTime (min) from start of test is
%ld",(t-t_start)/60);
```

```
      zero= (t-t_start)/60;  /* time in minutes */

      /* measure voltage drop */
      ChOn(DROP1);  /* connect channel to voltmeter */
      ChDsp(DROP1); /* display channel on front of voltmeter */
      vm_reading = ReadVm(); /* take voltage measurment */
      onea = vm_reading;

      ChOn(DROP2);
      ChDsp(DROP2);
      vm_reading = ReadVm();
      twoa = vm_reading;

      ChOn(DROP3);
      ChDsp(DROP3);
      vm_reading = ReadVm();
      threea = vm_reading;

      ChOn(DROP4);
      ChDsp(DROP4);
      vm_reading = ReadVm();
      foura = vm_reading;

      ChOn(DROP5);
      ChDsp(DROP5);
      vm_reading = ReadVm();
      fivea = vm_reading;

      ChOn(DROP6);
      ChDsp(DROP6);
      vm_reading = ReadVm();
      sixa = vm_reading;

      ChOn(C1);
      ChDsp(C1);
      vm_reading = ReadVm();
      v_rs1 = vm_reading;

      /* output to screen */
      printf("\n\nTIME (MIN)    DROP1     DROP2     DROP3     DROP4
DROP5     DROP6");
      printf("\n%7.3f      % 4.3f    % 4.3f    % 4.3f    % 4.3f    %
4.3f    % 4.3f",zero,onea,twoa,threea,foura,
      fivea,sixa);

      f2=fopen(name2,"a");
      fprintf(f2,"\n%7.3f,% 4.4f,% 4.4f,% 4.4f,% 4.4f,% 4.4f,%
4.4f",zero,onea,twoa,threea,foura,
      fivea,sixa);

      zero = (t-t_start)/60;

      ChOn(DROP7);
      ChDsp(DROP7);
      vm_reading = ReadVm();
```

```
      onec = vm_reading;

      ChOn(DROP8);
      ChDsp(DROP8);
      vm_reading = ReadVm();
      twoc = vm_reading;

      ChOn(DROP9);
      ChDsp(DROP9);
      vm_reading = ReadVm();
      threec = vm_reading;

      ChOn(DROP10);
      ChDsp(DROP10);
      vm_reading = ReadVm();
      fourc = vm_reading;

      ChOn(DROP11);
      ChDsp(DROP11);
      vm_reading = ReadVm();
      fivec = vm_reading;

      ChOn(DROP12);
      ChDsp(DROP12);
      vm_reading = ReadVm();
      sixc = vm_reading;

      ChOn(C2);
      ChDsp(C2);
      vm_reading = ReadVm();
      v_rs2 = vm_reading;

      /* output to screen */
      printf("\n\nTIME (MIN)    DROP7     DROP8     DROP9     DROP10
DROP11    DROP12");
      printf("\n%7.3f      % 4.3f    % 4.3f    % 4.3f     % 4.3f    %
4.3f    % 4.3f",zero,onec,twoc,threec,fourc,
      fivec,sixc);

      f3=fopen(name3,"a");
      fprintf(f3,"\n%7.3f,% 4.4f,% 4.4f,% 4.4f,% 4.4f,% 4.4f,%
4.4f",zero,onec,twoc,threec,fourc,
      fivec,sixc);

      zero =(t-t_start)/60;

      ChOn(DROP13);
      ChDsp(DROP13);
      vm_reading = ReadVm();
      onee = vm_reading;

      ChOn(DROP14);
      ChDsp(DROP14);
      vm_reading = ReadVm();
      twoe = vm_reading;
```

```
      ChOn(DROP15);
      ChDsp(DROP15);
      vm_reading = ReadVm();
      threee = vm_reading;

      ChOn(DROP16);
      ChDsp(DROP16);
      vm_reading = ReadVm();
      foure = vm_reading;

      ChOn(DROP17);
      ChDsp(DROP17);
      vm_reading = ReadVm();
      fivee = vm_reading;

      ChOn(DROP18);
      ChDsp(DROP18);
      vm_reading = ReadVm();
      sixe = vm_reading;

      ChOn(C3);
      ChDsp(C3);
      vm_reading = ReadVm();
      v_rs3 = vm_reading;

      /* output to screen */
      printf("\n\nTIME (MIN)    DROP13    DROP14    DROP15    DROP16
DROP17    DROP18");
      printf("\n%7.3f      % 4.3f    % 4.3f    % 4.3f    % 4.3f    %
4.3f    % 4.3f",zero,onee,twoe,threee,foure,
      fivee,sixe);

      /* output voltage drop measurments to files */
      f4=fopen(name4,"a");
      fprintf(f4,"\n%7.3f,% 4.4f,% 4.4f,% 4.4f,% 4.4f,% 4.4f,%
4.4f",zero,onee,twoe,threee,foure,
      fivee,sixe);
      /* Voltage measured in volts */
      /* compute current and voltage drop across samples */
      resistance = 1; /* resistors have resistance of 1000 ohms */
      current1 = v_rs1/resistance; /* units of milliamps */
      current2 = v_rs2/resistance;
      current3 = v_rs3/resistance;
      v_sample1 = v_ps-v_rs1;
      v_sample2 = v_ps-v_rs2;
      v_sample3 = v_ps-v_rs3;

      /* output to screen */
      printf("\n\nTIME (MIN)    VOLT.1    CURR.1    VOLT.2    CURR.2
VOLT.3    CURR.3");
      printf("\n%7.3f      % 5.3f  % 5.3f    % 5.3f  % 5.3f    % 5.3f
% 5.3f",(t_drop/60),v_sample1,current1,
      v_sample2,current2,v_sample3,current3);

      /* output to file */
```

```
      f1=fopen(name1,"a");
      fprintf(f1,"\n%7.3f,% 5.3f,% 5.3f,% 5.3f,% 5.3f,% 5.3f,%
 5.3f",(t_drop/60),v_sample1,current1,
      v_sample2,current2,v_sample3,current3);

      curravg=(current1+current2+current3)/3;
      avg1=(onea+onec+onee)/3;
      avg2=(twoa+twoc+twoe)/3;
      avg3=(threea+threec+threee)/3;
      avg4=(foura+fourc+foure)/3;
      avg5=(fivea+fivec+fivee)/3;
      avg6=(sixa+sixc+sixe)/3;


      /* output average to file */
      f5=fopen(name5,"a");
      fprintf(f5,"\n%7.3f,% 5.3f,% 5.3f,% 5.3f,% 5.3f,% 5.3f,%
 5.3f,% 5.3f",(t_drop/60),curravg,avg1,
      avg2,avg3,avg4,avg5,avg6);


      fclose(f1);
      fclose(f2);
      fclose(f3);
      fclose(f4);
      fclose(f5);
      t_drop = t_drop + t_drop1;
     }

     /* voltage on/off control */
     if ((t-t_start)<(t_on) && (test1==0)) {
      /*printf("\n\n  Time (min) from start of test is
%ld",(t-t_start)/60);*/
      /*printf("\n  Voltage is turned ON "); */

      /* turn power supply on */
      PSOnOff(PS1,"on");
      PSOnOff(PS2,"on");
      PSOnOff(PS3,"on");

      /* output to file */
      /*f1=fopen(name1,"a"); */
      /*fprintf(f1,"\n Voltage is ON."); */
      /*fclose(f1); */

      test1++;

     }

    if ((t-t_start)==(t_on) && (test2==0)) {
      /*printf("\n\n   Time (min) from start of test is
%ld",(t-t_start)/60);*/
      /*printf("\n   Voltage is ON (t=ton)");*/

       /* check and see if voltage is on all the time */
```

```
        if(t_off==0){
         t_on = t_on +(t_on1+t_change);
         test2=0;
        }
        else {
         test2++;
        }

       test1=0;
      }

     if ((t-t_start)>t_on && (t-t_start)<(t_on+t_off) &&
 (test3==0)) {
      /*printf("\n\n   Time (min) from start of test is
 %ld",(t-t_start)/60);*/
      /*printf("\n   Voltage is turned OFF "); */

      /* turn power supply off */
      PSOnOff(PS1,"off");
      PSOnOff(PS2,"off");
      PSOnOff(PS3,"off");

      /* output to file */
      /*f1=fopen(name1,"a");  */
      /*fprintf(f1,"\n Voltage is OFF.");*/
      /*fclose(f1); */

      test2=0;
      test3++;

     }

     if ((t-t_start)==(t_on+t_off)) {
      /*printf("\n\n   Time (min) from start of test is
 %ld",(t-t_start)/60);*/
      /*printf("\n   Voltage is OFF (t=(ton+toff))"); */

      t_on = t_on + (t_on1+t_change) + t_off;
      t_off = t_off + t_change;
      test3=0;
     }
    }

   /* turn power off at  end of test */
   PSOnOff(PS1,"off");
   PSOnOff(PS2,"off");
   PSOnOff(PS3,"off");

   Init(); /* disconnects all channels from the voltmeter */

   printf("\n\n  Power is off and all channels are disconnected
from voltmeter ");

printf("\n\n\t\t            ********* ");
  printf("\n\t\t          **         ** ");
```

```
   printf("\n\t\t          **  0      0  **");
   printf("\n\t\t           **     v    **");
   printf("\n\t\t---ooO----------------------Ooo---");
   printf("\n\t\t-                                -");
   printf("\n\t\t-         END OF TEST !!!        -");
   printf("\n\t\t-                                -");
   printf("\n\t\t---------------------------------");
   printf("\n\t\t              ||    ||              ");
   printf("\n\t\t              ||    ||              ");
   printf("\n\t\t             oooO   Oooo            ");

} /* end of main program */

 void intro()
 {
  printf("\n\n\n\tThis program controls the applied voltage and
");
  printf("\n\tvoltage drop measurements of the electrokinetic ");
  printf("\n\tremediation laboratory experiments.  The duration");
  printf("\n\tof the applied voltage can be varied along with ");
  printf("\n\tthe length of time between voltage drop and ");
  printf("\n\tcurrent measurments. ");
  printf("\n\n\n\tOutput is stored in four files, one file for "
);
  printf("\n\tapplied voltage and current for all three columns,
");
  printf("\n\tand three files for voltage drop measurments for
each");
  printf("\n\tseperate column with the extensions S1, S2, and
S3.");
  printf("\n\n\n\tPress any key to proceed:");
  getch();
  printf("\a");
  return;
 }

void PSOnOff(int num, char *state)
{
  int dummy = 0;

  switch (num)
    {
    case 1:
      {
      PSSwitch(byte0p, state);
      break;
      }
    case 9:
      {
      PSSwitch(byte1p, state);
      break;
      }
    case 17:
      {
```

```
        PSSwitch(byte2p, state);
        break;
        }
      }

   controlunion.controlbits.bit1 = 1;
   controlunion.controlbits.bit2 = 0;
   dummy = outp(CONTROL, controlunion.controlint);
   dummy = outp(DATA, databyte0.dataint);
   controlunion.controlbits.bit1 = 0;
   controlunion.controlbits.bit2 = 1;
   dummy = outp(CONTROL, controlunion.controlint);

   controlunion.controlbits.bit1 = 0;
   controlunion.controlbits.bit2 = 0;
   dummy = outp(CONTROL, controlunion.controlint);
   dummy = outp(DATA, databyte1.dataint);
   controlunion.controlbits.bit1 = 0;
   controlunion.controlbits.bit2 = 1;
   dummy = outp(CONTROL, controlunion.controlint);

   controlunion.controlbits.bit1 = 1;
   controlunion.controlbits.bit2 = 1;
   dummy = outp(CONTROL, controlunion.controlint);
   dummy = outp(DATA, databyte2.dataint);
   controlunion.controlbits.bit1 = 0;
   controlunion.controlbits.bit2 = 1;
   dummy = outp(CONTROL, controlunion.controlint);
   if(!dummy);
   return;
}


void ChOn(int num)
{
  div_t chnum;
  int denom = 8;
  int dummy = 0;

  chnum = div((num - 1), denom);

  switch (chnum.quot)
    {
    case 0:
      {
      DataSwitch(byte0p, chnum);
      break;
      }
    case 1:
      {
      DataSwitch(byte1p, chnum);
      break;
      }
    case 2:
      {
```

```
        DataSwitch(byte2p, chnum);
        break;
        }
      }

    controlunion.controlbits.bit1 = 1;
    controlunion.controlbits.bit2 = 0;
    dummy = outp(CONTROL, controlunion.controlint);
    dummy = outp(DATA, databyte0.dataint);
    controlunion.controlbits.bit1 = 0;
    controlunion.controlbits.bit2 = 1;
    dummy = outp(CONTROL, controlunion.controlint);

    controlunion.controlbits.bit1 = 0;
    controlunion.controlbits.bit2 = 0;
    dummy = outp(CONTROL, controlunion.controlint);
    dummy = outp(DATA, databyte1.dataint);
    controlunion.controlbits.bit1 = 0;
    controlunion.controlbits.bit2 = 1;
    dummy = outp(CONTROL, controlunion.controlint);

    controlunion.controlbits.bit1 = 1;
    controlunion.controlbits.bit2 = 1;
    dummy = outp(CONTROL, controlunion.controlint);
    dummy = outp(DATA, databyte2.dataint);
    controlunion.controlbits.bit1 = 0;
    controlunion.controlbits.bit2 = 1;
    dummy = outp(CONTROL, controlunion.controlint);

    if (dummy);
    return;
}

void DataSwitch(union data *dataunion, div_t chnum)
{
    int dummy = 0;

    /* clear all channels(except power supply channels) */

    databyte0.dataint |= 254;
    databyte1.dataint |= 254;
    databyte2.dataint |= 254;

    switch (chnum.rem)
      {
      case 1:
        {
        dataunion->databits.bit1 = 0;
        break;
        }
      case 2:
        {
        dataunion->databits.bit2 = 0;
        break;
        }
```

```
      case 3:
        {
        dataunion->databits.bit3 = 0;
        break;
        }
      case 4:
        {
        dataunion->databits.bit4 = 0;
        break;
        }
      case 5:
        {
        dataunion->databits.bit5 = 0;
        break;
        }
      case 6:
        {
        dataunion->databits.bit6 = 0;
        break;
        }
      case 7:
        {
        dataunion->databits.bit7 = 0;
        break;
        }
      default:
        {
        dataunion->dataint = 255;
        dummy = outp(DATA,dataunion->dataint);
        controlunion.controlbits.bit1 = 1;
        controlunion.controlbits.bit2 = 0;
        dummy = outp(CONTROL, controlunion.controlint);
        controlunion.controlbits.bit1 = 0;
        controlunion.controlbits.bit2 = 0;
        dummy = outp(CONTROL, controlunion.controlint);
        controlunion.controlbits.bit1 = 1;
        controlunion.controlbits.bit2 = 1;
        dummy = outp(CONTROL, controlunion.controlint);
        controlunion.controlbits.bit1 = 0;
        controlunion.controlbits.bit2 = 1;
        dummy = outp(CONTROL, controlunion.controlint);
        break;
        }
    }
  if (!dummy);
  return;
}

void PSSwitch(union data *dataunion, char *state)
{
  int dummy = 0;

  if (*(state + 1) == 'n')
    dataunion->databits.bit0 = 0;
  else
```

```
    dataunion->databits.bit0 = 1;
   if(dummy);
   return;
 }

 void ChDsp(int num)
 {
   int dummy = 0;

   int i, j;

   controlunion.controlbits.bit0 = 0;
   dummy = outp(CONTROL, controlunion.controlint);
   controlunion.controlbits.bit0 = 1;
   dummy = outp(CONTROL, controlunion.controlint);
   for (i = 0; i < num; i++)
     {
     controlunion.controlbits.bit3 = OFF;
     dummy = outp(CONTROL, controlunion.controlint);
     controlunion.controlbits.bit3 = ON;
     dummy = outp(CONTROL, controlunion.controlint);
     }
   if(dummy);
   return;
 }

 float ReadVm(void)
 {
   int chrs = 80;
   char rdg[80];
   FILE *filep1;
   float vmr;
   system("readvm1.exe");
   filep1 = fopen("rdg.out","r");
   fgets(rdg,chrs,filep1);
   fclose(filep1);
   vmr = (float) atof(rdg);

   return vmr;
 }

 void Init()
 {
   int dummy = 0;

   union data dataunion;

   controlunion.controlbits.bit0 = 0;
   dummy = outp(CONTROL, controlunion.controlint);
   controlunion.controlbits.bit0 = 1;
   dummy = outp(CONTROL, controlunion.controlint);
   dataunion.dataint = 0xff;
   dummy = outp(DATA,dataunion.dataint);
   controlunion.controlint = 3;
   dummy = outp(CONTROL, controlunion.controlint);
```

```
    controlunion.controlint = 1;
    dummy = outp(CONTROL, controlunion.controlint);
    controlunion.controlint = 7;
    dummy = outp(CONTROL, controlunion.controlint);
    controlunion.controlint = 5;
    dummy = outp(CONTROL, controlunion.controlint);

    if(!dummy);
    return;
}
```

Appendix B:

Model Program

```
/*************************************************************/
/*  The advection-dispersion-electrokinetic analytical       */
/* contaminat transport equation is modeled using this       */
/* program.  Various input parameters are requested and      */
/* then the concentration at a specified point in time is    */
/*  given.                                                   */


/*  Variables:                                               */
/*  Kh  = hydraulic conductivity (cm/sec)                    */
/*  Keo = coefficient of electroosmotic permeability         */
/* (cm/sec)/(V/cm)                                           */
/*  Uep = electrophoretic mobility (cm/sec)/(V/cm)           */
/*  dhgrad = hydraulic gradient  (dimensionless)             */
/*  dEgrad = electrical gradient (V/cm)                      */
/*  veo = electroosmotic velocity (cm/sec)                   */
/*  vh  = hydraulic velocity (cm/sec)                        */
/*  veo = electroosmotic velocity (cm/sec)                   */
/*  vw = vh + veo                                            */
/*  x   = distance travelled in the x direction (cm)         */
/*  t   = elapsed time (sec)                                 */
/*  SolCMC = solubility of the compound at the CMC (mg/L)    */
/*  foc = fraction of organic carbon                         */
/*  C   = contaminant concentration in solution (mg/L        */
/* CMC = critical micelle concentration  (mol/L)             */
/* Csurf = surfacant concentration (mol/L)                   */
/* M = mass of contaminant added to the system (ug)          */
/* Km = micelle-water partition coeffecient                  */
/* (mole fraction units)                                     */
/* logKm = log micelle-water partition coefficient           */
/* (mole fraction units)                                     */
/* logKow = log octanol-water partition coefficient          */
/* logKoc = log organic carbon-soil partion coefficient      */
/* occ = mean occupancy number                               */
/* Rf = modified retardation factor (dimensionless)          */
/* Df = diffusion coeffecient (cm squared)/(sec)             */
/* Dx = hydrodynamic disperision                             */
/* alpha = dispersivity (cm)                                 */
/* n = porosity                                              */
/* rho = bulk density g/cc                                   */
/* rhop = particle density (g/cc)                            */
```

```
#include <stdio.h>
#include <stdlib.h>
#include <math.h>
#include <dos.h>
#include <string.h>
#include <conio.h>

/* start of program */
void main(void)
{
  FILE *f1;
 /* declare variables */
  char re_enter[1],name1[8];
  double
Kh,Keo,Uep,veo,vep,vh,vw,x,t,C,CMC,Csurf,M,Km,Koc,Kow,logKoc
,occ,Rf,Dx,Df,n;
  double
alpha,area,outflow,rho,rhos,zetas,zetam,dhgrad,dEgrad,SolCMC
,foc,logKm,logKow,Volw,Xmod;
  double outflow1,C1,prmd,check1,check2;
  void intro(void);

  intro();

 /* input variables */
  Kh=1.00e-06;
  Keo=1.00e-04;
  Uep=4.1e-04;
  Csurf=0.008;
  CMC=0.008;
  logKow=2.12;
  occ=35.0;
  foc=0.01;
  dhgrad=2.12;
  dEgrad=0.0;
  rho=0.80;
  Df=1.0e-05;
  M=500.0;
  alpha=1.0;
  t=48399660.0;
  x=6.5;

do {
  clrscr();
  printf("\n\n\nInput filename to store output: ");
  scanf("%s",name1);   /*
  printf("\nInput the hydraulic conductivity (cm/sec): ");
  scanf("%lf",&Kh);
  printf("\nInput the coefficient of electroosmotic
```

```
permeability (cm/sec)/(V/cm): ");
   scanf("%lf",&Keo);
   printf("\nInput the electrophoretic mobility
(cm/sec)/(V/cm): ");
   scanf("%lf",&Uep);
   printf("\nInput the hydraulic gradient (dimensionless):
");
   scanf("%lf",&dhgrad);
   printf("\nInput the electrical gradient (V/cm): ");
   scanf("%lf",&dEgrad);
   printf("\nInput the distance travelled in the x direction
(cm): ");
   scanf("%lf",&x);
   printf("\nInput the elapsed time (sec): ");
   scanf("%lf",&t);
   printf("\nInput the logKow of the compound: ");
   scanf("%lf",&logKow);
   printf("\nInput the fraction of organic carbon: ");
   scanf("%lf",&foc);
   printf("\nInput the surfacant concentration (mol/L): ");
   scanf("%lf",&Csurf);
   printf("\nInput the mass of contaminant added to the
system (ug): ");
   scanf("%lf",&M);
   printf("\nInput the mean occupency number: ");
   scanf("%lf",&occ);
   printf("\nInput the diffusion coeffecient (cm
squared)/(sec): ");
   scanf("%lf",&Df);
   printf("\nInput the bulk density (g/cc): ");
   scanf("%lf",&rho);     */
   printf("\n\n\nWould you like to change this data? (Y/N):
");
   scanf("%s",re_enter);
   }
   while ((re_enter[0] != 'N')); /*Do until N is entered */

  /* open file */
  f1=fopen(name1,"a");
  if((f1=fopen(name1,"a"))==NULL) {
  printf("\nFile %s cannot be opened.",name1);
  exit(1);
  }

   /*calculations */

   /* calculate porosity */
   area=17.8; /*cross sectional area of soil */
   rhos = 2.65;   /* use particle density of 2.65 g/cc */
```

```
    n = 1 - rho/rhos;

    if ((Csurf-CMC) <0.00001)
      {logKoc=0.4047*logKow+1.059;
      printf("\nWater flusing Koc");
      }
      else
      {logKoc=0.52228*logKow+0.5353;}
      Koc=pow(10,logKoc);

   /* calculate logKm (mole fraction units) from relationship
*/
      logKm=0.948*logKow+0.843;
      Km=pow (10,logKm);
      Volw=0.01805;

   /* find modified retardation coefficient */

Rf=1+(rho*Koc*foc)/(n*(1+(Km*Volw*(Csurf-CMC)*(62+occ)/62)))
;
    printf("\nRf is %8.5f:",Rf);

    /* compute concentration versus time or versus distance
*/
    /*x=0.0; */
    t=0.0;
    C=0.0;
    C1=0.0;
    outflow1=0.0;
    prmd=0.0;

    /* calculate velocites */
    vh = Kh*dhgrad;
    veo = Keo*dEgrad;
    vep = Uep*dEgrad;
    vw = vh + veo;
    outflow=vw*t*area; /*outflow in mL */

    /* compute hydrodynamic dispersion */
    Dx=alpha*vw+Df;

    fprintf(f1,"Concentration (mg/L), Time (days), Outflow
(mL) , %RMD");

fprintf(f1,"\n%8.5f,%8.3f,%8.5f,%8.5f",C,t/24/60/60,outflow,
prmd);

    t=t+86400/100;
```

```
    do {
    if ((Csurf-CMC) <0.00001)
    {
    Xmod = x-vw*t/Rf;
    printf("\nWater Flushing");
    }
    else
    {
    Xmod =
x-vw*t/Rf+vep*t/(Rf*(1+1/(Km*Volw*(Csurf-CMC)*(62+occ)/62)))
;
    printf("\nSurfactant Flushing");
    }
    printf("\nXmod is %8.5f:",Xmod);


C=(M/(2.0*sqrt(3.1415926*Dx*t/Rf)))*exp(-(Xmod*Xmod)/(4.0*Dx
*t/Rf));
    check1=exp(-(Xmod*Xmod)/(4.0*Dx*t/Rf));
    check2=(M/(2.0*sqrt(3.1415926*Dx*t/Rf)));
    printf("\ncheck1 is: %8.5f",check1);
    printf("\ncheck2 is: %8.5f",check2);

    outflow=vw*t*area;      /* outlfow in mL */

    /* Compute % Removed */
    prmd=((C+C1)/2*(outflow/area-outflow1/area))/M+prmd;

    /* output results */
    printf("\nTime (sec) is: %12.2f",t);
    /*printf("\nDistance (cm) is: %8.3f",x);*/
    printf("\nConcentration (mg/L) is: %8.8f",C);
    /*printf("\nConcentration 1 is: %8.8f",C1);
    printf("\nOutflow (mL) is: %8.5f",outflow);
    printf("\nOutflow1(mL) is: %8.5f",outflow1); */

fprintf(f1,"\n%8.5f,%8.3f,%8.5f,%8.5f",C,t/24/60/60,outflow,
prmd);

    C1=C;
    outflow1=outflow;

    t=t+86400/8; /* compute 1/8 every day */
    /*x=x+1.0; */
    /*getch(); */
    }
    while (t<3888000);

    /* Echo input and display results */
```

```
   printf("\n\n\nThe hydraulic conductivity (cm/sec) is:
%8.8f ",Kh);
   printf("\nThe coefficient of electroosmotic permeability
(cm/sec)/(V/cm) is: %8.8f",Keo);
   printf("\nThe electrophoretic mobility (cm/sec)/(V/cm):
%8.8f ",Uep);
   printf("\nThe hydraulic gradient (dimensionless) is:
%8.8f ",dhgrad);
   printf("\nThe electrical gradient (V/cm) is:
%8.3f",dEgrad);
   printf("\nThe distance travelled in the x direction (cm)
is: %8.3f ",x);
   printf("\nThe elapsed time (sec) is: %8.3f ",t);
   printf("\nThe fraction of organic carbon is: %8.3f
",foc);
   printf("\nThe critical micelle concentration (mol/L) is:
%8.5f ",CMC);
   printf("\nThe surfactant concentration (mol/L) is: %8.5f
",Csurf);
   printf("\nThe mass of contaminant added to the system
(ug) is: %8.3f",M);
   printf("\nThe mean occupency number is: %8.3f ",occ);
   printf("\nThe effective diffusion coeffecient (cm
squared)/(sec) is: %8.6f ",Dx);
   printf("\nThe bulk density (g/cc) is: %8.3f",rho);
   printf("\n\nCalculated values are:");
   printf("\nThe porosity is: %8.3f ",n);
   printf("\nThe hydrodynamic dispersion is: %8.8f",Dx);
   printf("\nThe logKm value (mole fraction units) is: %8.5f
",logKm);
   printf("\nThe logKoc value is: %8.5f ",logKoc);
   printf("\nThe modified retardation factor is: %8.5f
",Rf);
   printf("\nThe hydraulic velocity (cm/sec) is: %8.8f
",vh);
   printf("\nThe electroosmotic velocity (cm/sec) is:  %8.8f
",veo);
   printf("\nThe pore fluid velocity (cm/sec) is:
%8.8f",vw);
   printf("\nThe electrophoretic velocity (cm/sec) is:
%8.8f ",vep);
   printf("\nThe volume of outflow (mL) is: %8.3f
",outflow);
   printf("\nThe contaminant concentration (mg/L) is: %8.5f
",C);
   /* Find relationship between Rf and Kow */
   /*  logKow=0;
     fprintf(f1,"\nlogKoc, logKow");
     do{
```

```
      if ((Csurf-CMC) <0.00001)
      {logKoc=0.4047*logKow+1.059;}
      else
      {logKoc=0.52228*logKow+0.5353;}
      Koc=pow(10,logKoc);
      /* calculate logKm (mole fraction units) from
relationship */
      /*
      logKm=0.948*logKow+0.843;
      Km=pow (10,logKm);

Rf=1+(rho*Koc*foc)/(n*(1+(Km*Volw*(Csurf-CMC)*(62+occ)/62)))
;
      printf("\n%8.5f , %8.5f",logKow,log10(Rf));
      fprintf(f1,"\n%8.5f , %8.5f",logKow,log10(Rf));
      logKow = logKow + 0.25;
      getch();
     }
     while (logKow < 7.1);
     */
}

   void intro() /* introscreen */
  {
   clrscr();
   printf("\n\n\n\tThis program models electrokinetic
remediation with a surfactant");
   printf("\nusing the advection-dispersion-electrokinetic
equation with the modified");
   printf("\nretardation factor.  Water flushing can modeled
by inputting the");
   printf("\nsurfactant concentration equal to the CMC.");
   printf("\n\n\n\nPress any key to proceed:");
   getch();
   /*printf("\a"); */ /* beep */
   return;
  }
```